DESIGN AND MODELING OF A COMPLIANT MECHANISM

By
MERVE ACER

Submitted to the Graduate School of Engineering and Natural Sciences
in partial fulfillment of
the requirements for the degree of
Master of Science

SABANCI UNIVERSITY
Spring 2007

DESIGN AND MODELING OF A
COMPLIANT MECHANISM

APPROVED BY:

ASIF ŞABANOVİÇ .....
(Dissertation Advisor)

MAHMUT F. AKŞİT .....
(Dissertation Co-Advisor)

ATA MUGAN .....

KEMALETTİN ERBATUR .....

MUSTAFA ÜNEL .....

DATE OF APPROVAL: .....

DESIGN AND MODELING OF A COMPLIANT MECHANISM

Merve ACER

Electronics Engineering and Computer Science, M.S. Thesis, 2007

Thesis Supervisor: Prof. Dr. Asif ŞABANOVİÇ

Thesis Co-advisor: Doç. Dr. Mahmut F. AKŞİT

Keywords: Compliant Mechanisms, Flexure Based Mechanisms, Beam Dynamics, Distributed Parameter Systems

ABSTRACT

Compliant mechanisms are widely used in high precision systems, because they provide high resolution, frictionless, smooth and continuous motion. These kinds of mechanisms are also cheaper than the other types of high precision mechanisms. The main idea of this kind of mechanism is that no additional joints are used for creating the motion, the deflection of the flexible elements are used to create the desired motion.

In this thesis, a planar parallel compliant mechanism is designed. The mechanism is actuated from three ends by using piezo mike micromotors to create motion in XY plane. The mathematical model of the mechanism is derived by using Euler Bernoulli dynamic equation for the three beams on the mechanism. The separation of variables technique is used to solve the dynamic equations. Necessary transformations are calculated for defining the center position of the stage in terms of the deflections of the beam. The mathematical model is represented in state space form and it is simulated in MATLAB Simulink. The position results are compared with another simulation called COMET. The mathematical model is reduced to two input and two output system in order to make the XY position control of the mechanism by using PID control. Finally, the mechanism is manufactured by using laser cutting and water jet cutting techniques, open loop experiments of the mechanism are verified by actuating the piezo motors manually and by giving voltage signal.

ESNEK BAĞLANTILI BİR MEKANİZMANIN TASARIMI VE MODELLENMESİ

Merve ACER

Elektronik Mühendisliği ve Bilgisayar Bilimi, Yüksek Lisans Tezi, 2007

Tez Danışmanı: Prof. Dr. Asif ŞABANOVİÇ

Tez Yardımcı Danışmanı: Doç. Dr. Mahmut F. AKŞİT

Anahtar Kelimeler: Esnek Bağlantılı Mekanizmalar, Paralel Mekanizmalar, Kiriş Dinamiği, Dağınık Parametreli Sistemler

ÖZET

Esnek bağlantılı mekanizmalar yüksek hassaslık gerektiren sistemlerde çok yaygın olarak kullanılmaktadır. Çünkü bu tip mekanizmalar yüksek çözünürlülük, sürtünmesiz, düzgün ve sürekli hareket sağlar. Bu tip mekanizmalar aynı zamanda diğer yüksek hassasiyet kazandıran mekanizmalardan maliyeti daha düşük olan sistemlerdir. Bu tip mekanizmaların temel fikri hareketi sağlamak için ilave bağlantı elemanları kullanmamaları, istenilen hareketi esnek elemanların eğilmesiyle sağlamalarıdır.

Bu tezde, paralel ve düzlemsel olan esnek bağlantılı bir mekanizmanın tasarımı yapılmıştır. Mekanizma XY düzleminde hareket edecek şekilde üç noktasından piezomike mikro motorlar kullanılarak tahriki sağlanmıştır. Mekanizmanın matematiksel modeli, mekanizmada bulunan üç kirişin Euler Bernoulli dinamik denklemleri kullanılarak oluşturulmuştur. Değişkenleri ayırma metodu kullanılarak da bu denklemler çözülmüştür. Mekanizmanın merkezinin pozisyonu kirişlerin eğilmeleri cinsinden yazılabilmesi için gerekli transformasyonlar hesaplanmıştır. Matematiksel model durum denklemlerine çevrilmiş ve MATLAB Simulink kullanılarak benzetimi yapılmıştır. Benzetimden çıkan konum sonuçları COMET adı verilen başka bir benzetimle karşılaştırılmıştır. Daha sonra sistemin matematiksel modeli, XY düzleminde pozisyon kontrolü PID kullanılarak yapılabilmesi için iki girişli iki çıkışlı sisteme indirgenmiştir. Son olarak da, mekanizma lazer kesme ve su jeti kesme

yöntemleriyle üretilmiş, piezo motorlar elle ve voltaj sinyali vererek harekete geçirilerek sistemin açık döngülü deneyleri gerçekleştirilmiştir.

“To my parents”

ACKNOWLEDGEMENTS

Firstly, I would like to express my gratitude to my advisor, Professor Asif Şabanoviç. I would like to thank him not for only completion of this thesis but also his support in my education, his patience and encouragement.

I would like to thank to my dissertation committee; Ata Mugan, Mustafa Ünel, Kemalettin Erbatur and Mahmut F. Akşit for their interest and valuable suggestions. I also want to thank especially Volkan Patoğlu for helping me in this thesis.

I also would like to thank all my friends at Mehcatronics, especially, Meltem Elitaş, Erhan Demirok, A. Teoman Naskali and Emrah Deniz Kunt for their great friendship and sharing all they know. And thanks to Muhammet A. Hocaoğlu and Hakan Bilen for their support in the experiments and not being bored of my questions. I also want to thank my best friend Erinç Karatoprak for his existence since my undergraduate years and his valuable suggestions and ideas in every aspect of life. And also thanks to Volkan Aydınol for being there when I need.

Finally, I would like to express my gratitude to my parents Selma and Kadri Acer for their unlimited support.

TABLE OF CONTENTS

LIST OF FIGURES

TABLE OF SYMBOLS

F_A	Actuating force on beam A
F_B	Actuating force on beam B
F_C	Actuating force on beam C
w_A	Transverse deflection on beam A
w_B	Transverse deflection on beam B
w_C	Transverse deflection on beam C
$T_{forcetransverse}$	Transformation matrix between the actuating forces and the transverse forces
E	Young's modulus or modulus of elasticity
I	Inertia
t	Time
L	Length of the beam
w(x,t)	Transverse motion of the beam
$Y(x)$	Shape function
$f(t)$	Function depends on time
ρ	Density of the material
A	Cross section area
ω	Frequency
n	Mode number
m	Mode number
β	Frequency
$\eta(t)$	Transverse displacement function depending on time
m_n	Modal mass
k_n	Modal stiffness
R_n	Modal damp
ζ	Damping mode ratio

x_α	Displacement on α axis
x_β	Displacement on β axis
T_T	Transformation matrix between the transverse deflections and the center coordinates
x_A	Longitudinal deflection on bar A
x_B	Longitudinal deflection on bar B
x_C	Longitudinal deflection on bar C
$T_{forcelongitudinal}$	Transformation matrix between the actuating forces and the longitudinal forces
$\xi(x,t)$	Longitudinal motion of the bar
μ(t)	Longitudinal displacement function depending on time
m_m	Modal mass
k_m	Modal stiffness
R_m	Modal damp
T_L	Transformation matrix between the longitudinal deflections and the center coordinates
A	State matrix
B	Input matrix
C	Output matrix
D	Feed forward matrix
$x_{\alpha ref}$	Desired displacement on α axis
$x_{\beta ref}$	Desired displacement on β axis
K_P	Proportional gain
K_I	Integral gain
K_D	Derivative gain

TABLE OF ABBREVIATIONS

COMET	The Compliant Mechanism Tool
FEA	Finite Element Analysis
DOF	Degree of freedom
WJC	Water jet cutting
LC	Laser cutting
PRB	Pseudo rigid body

1 INTRODUCTION

1.1 Flexures and Compliant Mechanisms

1.1.1 Definitions

Mechanisms are mechanical devices that are used to transfer motion, force or energy in a mechanical system. Most of the mechanisms consist of rigid links that connected to each other by using proper joints to give the desired motion or to transfer the desired force or energy. Especially rotational joints are used to transfer motion. In the high precision mechanisms, these joints begin to make troubles to the system like backlash, friction etc. So, another type of joint is developed for these high precision mechanisms. These joints are called flexure hinges. Flexures are the thin members that give the relative rotation between two rigid links through bending of the elastic materials as shown in Figure 1-1. They can also be considered as bearings with limited rotation capability [1]. Although a standard revolute joint is based upon the sliding and rolling, the flexure joints are based upon the bending deflection of cantilever beams [3]. So material's young's modulus or modulus of elasticity is the basic tool to create desired motion.

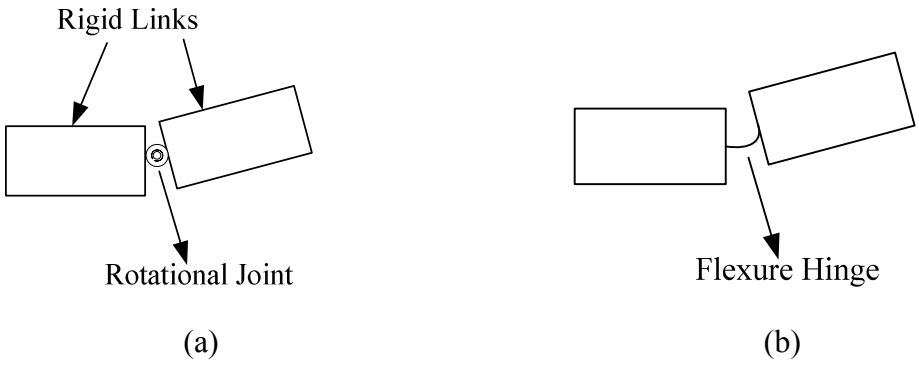

Figure 1.1 Joints used in mechanisms. (a) bearing joint; (b) flexure hinge

Compliant mechanisms are mechanisms that use flexures. They are also called flexible mechanisms or flexure based mechanisms [1]. Deflection in mechanisms has been used and relied on to create motion throughout history. The first compliant mechanisms that are used are bows and catapults. Flexible materials are used to construct bows so that the strain energy of the flexible material transform to kinetic energy. Catapults, shown in Figure 1-2, are also an ancient mechanism that used by the Greeks at the 4th century B.C. [2]. They are used in ancient wars to propel the missiles across long distances. Early catapults are made of flexible wooden members to store energy and when it is released, the missiles are propelled.

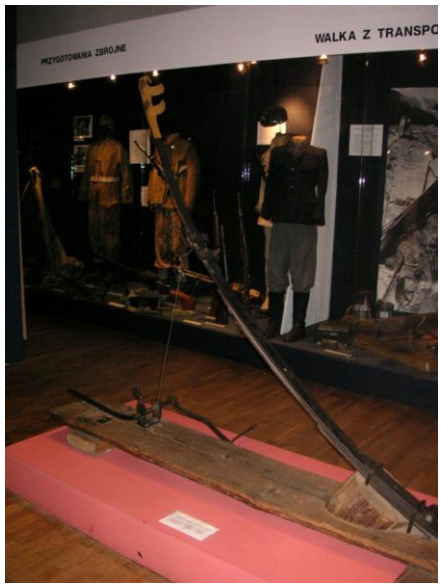

Figure 1.2 Catapult [wikipedia]

When we look around there are many simple devices that we use are compliant mechanisms. Common compliant devices that are around us can be seen in Figure 1-3. Tweezers are used to grasp small objects by using two flexible beams, paper clips are used to attach papers together by using the flexibility of the materials, nail scissors is also a compliant mechanism because the given force deflects the upper beam and closes the gap and cuts the nail and safety belt tools are also used to lock the belt by the help of the deflection of the beams.

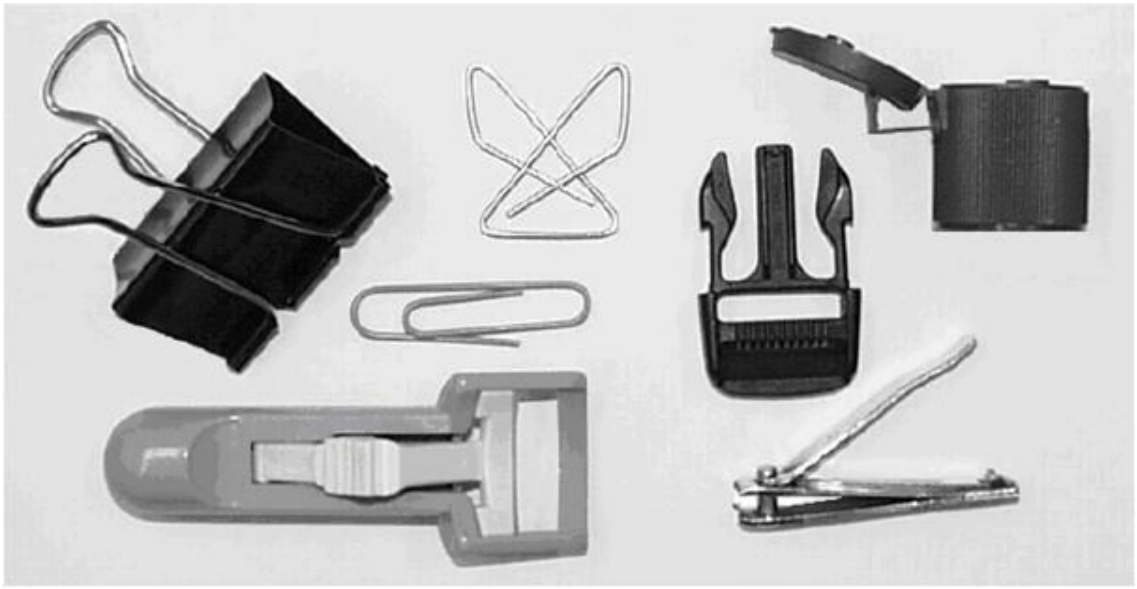

Figure 1.3 Simple Compliant Mechanisms

In Figure 1-4 there is an example of compliant mechanism which is a crimping mechanism. By using hand grips the input force is taken and transferred to the output port through the flexible members of the mechanism which stores strain energy. There are types of flexures used in the mechanism which are compound flexures and simple flexures to provide the minimum closing at the output port with a human force. The detail discussion about flexure types will be in the following subsection [2].

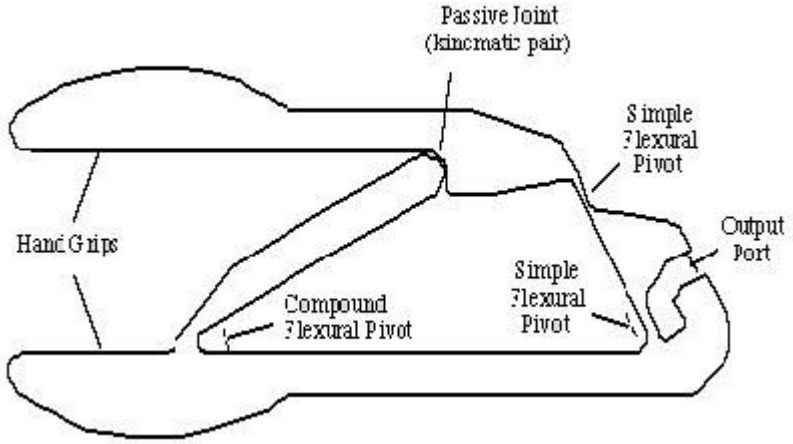

Figure 1.4 Crimping Mechanism [2]

1.1.2 Types of Flexures and Flexure Mechanisms

Basically, flexures have three main types as shown in Figure 1-5. The single-axis flexures provide only linear or only angular motion whereas, the multiple-axis flexures and the two axis flexures provide both linear and angular motion. [1]

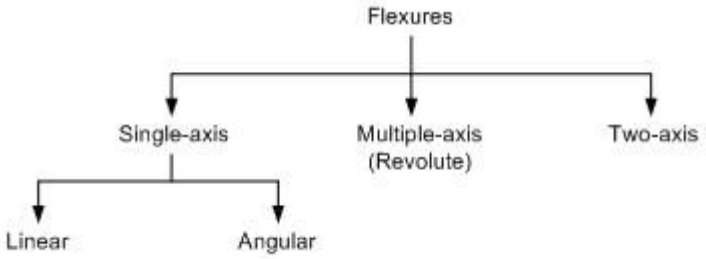

Figure 1.5 Types of Flexures

Single-axis flexures: They are the flexures which are supposed to be compliant in one axis which is called compliant or sensitive axis as shown in Figure 1-6. They are used in two dimensional (planar) mechanisms.

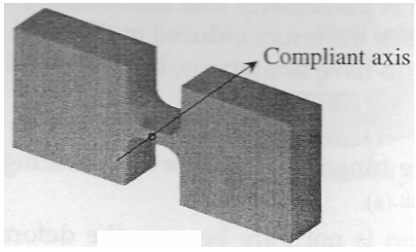

Figure 1.6 Single-axis flexure [1]

Single-axis flexures are also divided into two groups. Linear flexures that only provide linear motions and angular flexures that only provide angular motion.

Linear flexures: The simplest linear flexure mechanism that uses single axis flexure is cantilever beam shown in Figure 1-7. The main problem of this type of mechanisms is that the end of the beam is free of rotation. The force should be applied to the beam midway between the cantilever and its end and this prevents the rotation of the end of the beam. But it is not very stable because the beam can have buckling and twisting. Misalignment of the actuation force or any other unexpected sources can cause large unwanted parasitic deflections. To prevent these parasitic errors, new types of flexure mechanisms are designed [5].

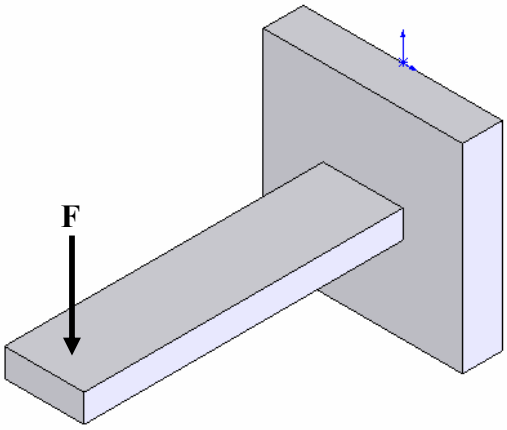

Figure 1.7 Simple Cantilever Beam [5]

The mechanisms which have leaf-spring flexures have more resistance to torsional deflection because it is improved by attaching two or more flexures together as in Figure 1-8a. The main advantages of leaf type of linear mechanisms are that they are stiffer in torsion and they provide larger area on which to mount specimens. The main disadvantage of these mechanisms is that in directions except the drive axis they have low stiffness which causes the mechanism to have parasitic errors (deflections in unwanted directions). Especially the rotation about z axis is the weakest part of the mechanism [5]. Compound leaf spring mechanisms are designed to cancel the parasitic errors. The main idea is to attach a simple linear spring mechanism to the underside of another simple linear spring mechanism as shown in Figure 1-8b. The parasitic errors in platform B is cancelled out by the parasitic errors in platform A so more precise linear motion is produced. The deflection of this mechanism under the same amount of force is twice the deflection of simple linear spring mechanism [5].

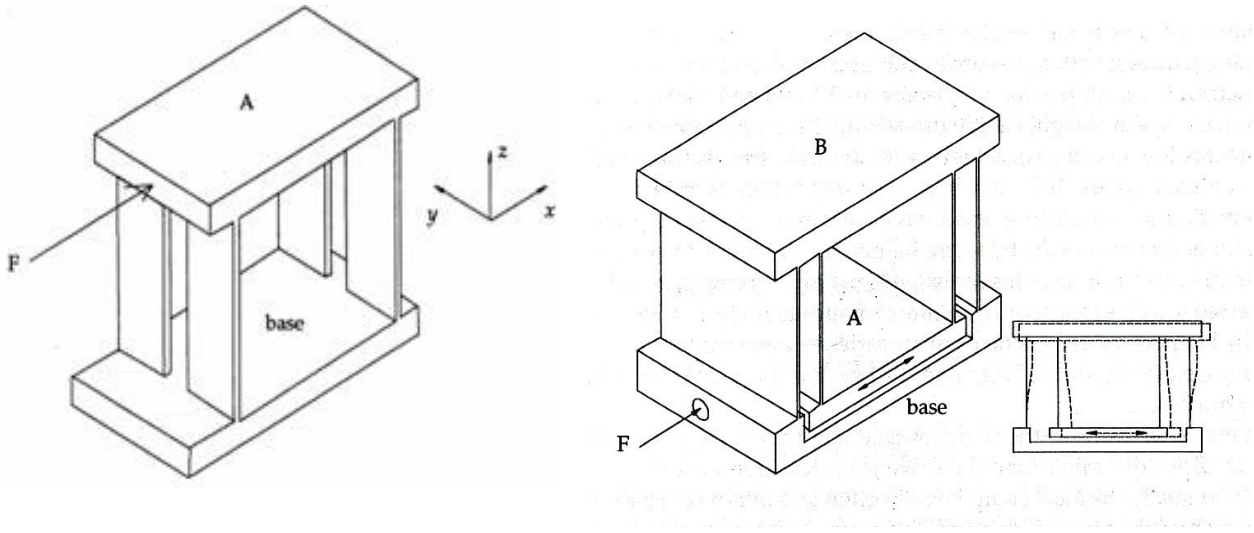

(a) (b)

Figure 1.8 (a) Simple Linear Leaf Type Mechanism , (b) Compound Linear Spring Mechanism [5]

There is an S shaped deflection in leaf spring mechanisms which cause parasitic deflections. To overcome this, the centers of the beams can be done straight or reinforcements can be added to the center of the beams but this solution increases both buckling resistance and drive stiffness which cause the mechanism to fail in high precision applications. So another type of flexure was designed called “notch hinges” [5]. Notch hinges are the flexures with two holes are drilled close together as in Figure 1-9. They act like elastic rotary bearings.

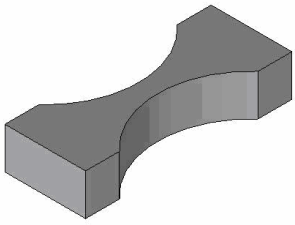

Figure 1.9 Notch Type Flexure

In Figure 1-10a the simple spring mechanism is composed of notch hinge flexures. The bending is restricted by the tensile stress in the notch hinge sections which cause the bending to be highly localized so it can be easily estimated by work-energy methods. Although the load capacity of leaf type of flexures are limited by the Euler buckling, notch type flexures undergo this by changing its stiffness due to the loading [5]. Notch type compound spring mechanism in Figure 1-10b is developed to increase

the torsional stiffness of notch type mechanisms. As the linear type compound mechanisms, the notch type compound mechanism has also half the stiffness of the simple stage, so the same stress applied to the compound mechanism gives twice deflection of simple mechanism [5].

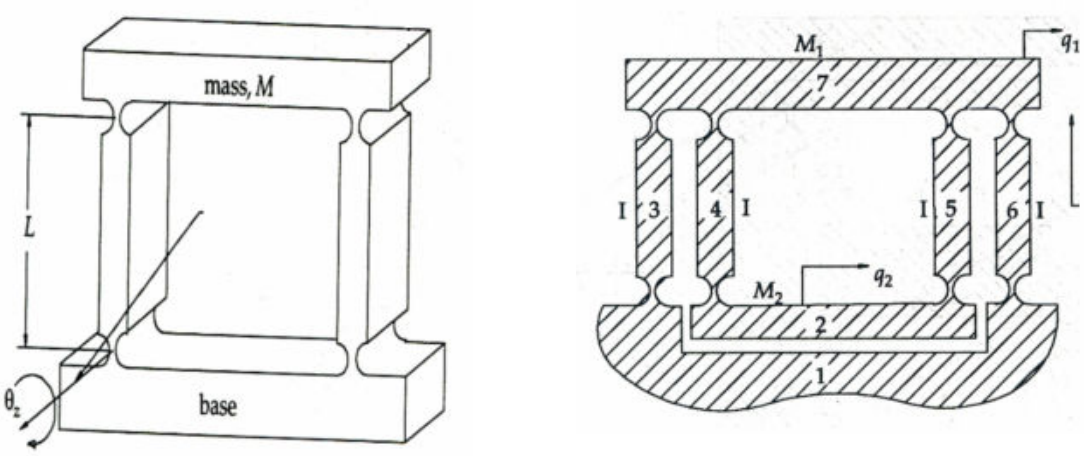

(a) (b)

Figure 1.10 (a)Simple Notch Type Spring Mechanism, (b) Notch Type Compound Spring Mechanism [5]

Double compound spring mechanisms are designed to have the superior rectilinear performance. In Figure 1-11a there is a leaf type double compound mechanism and in Figure 1-11b there is a notch type double compound mechanism. These types of mechanisms also provide low errors from thermal expansion due to their symmetry [5].

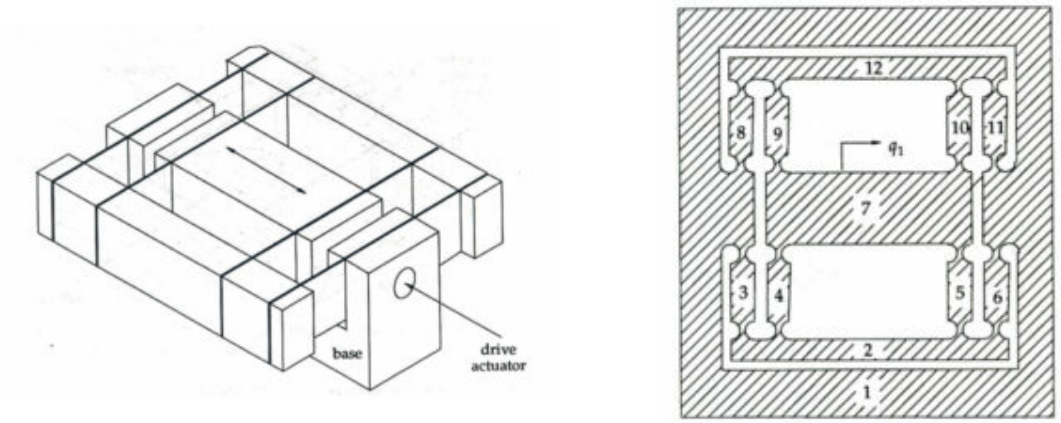

(a) (b)

Figure 1.11 Double Compound Spring Mechanisms [5]

Angular flexures: They are used in applications where a small range of angular rotation motion is needed. The simplest flexure is the short cantilever beam in Figure

1.12 used by Eastman 1937. Greater range of angular motions can be achieved due to the longer and wider cantilever flexures. The basic drawback of simple cantilevers is that the center of rotation moves with the angle of rotation.

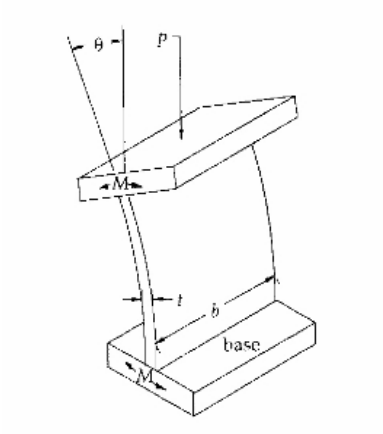

Figure 1.12 Cantilever Beam

The other types of angular flexures are in Figure 1-13. The crossed strip flexures are developed by Haringx in 1949. He also developed a formula for the shift of the axis with the angular displacement. Monolithic flexures are more resistant to parasitic errors which are developed by Young in 1989. Also Jones, 1955, designed the twisting beams about their longitudinal axis called the cruciform angle flexures.

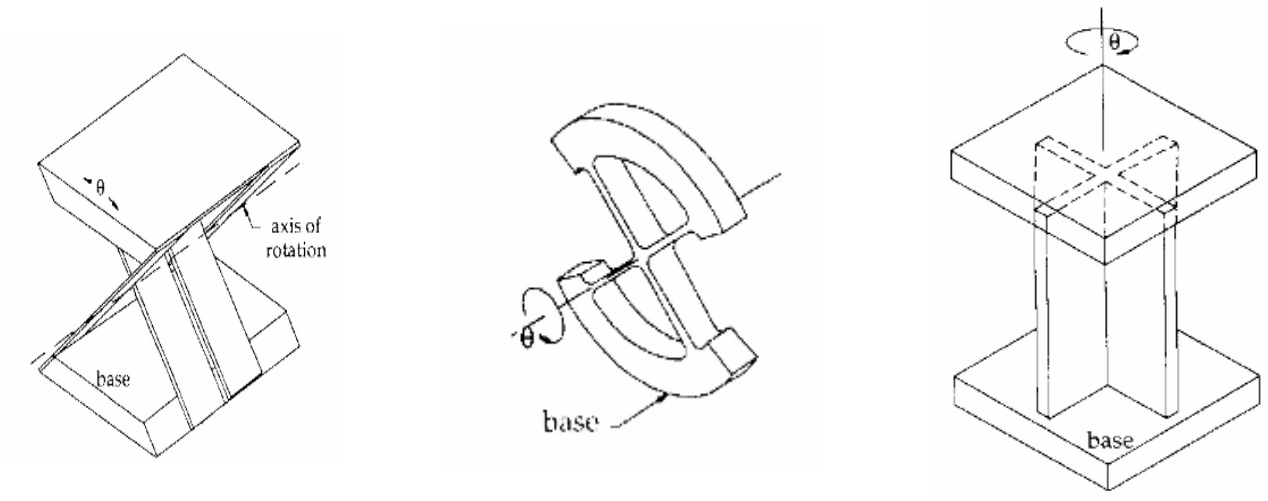

(a) (b) (c)

Figure 1.13 (a) crossed strip flexure, (b) monolithic flexure, (c) cruciform angle flexure

Multi axis flexures: These flexures have multiple compliant axes. They have a revolute geometry as shown in Figure 1-14. The compliant axis is still on the cross-section of the minimum thickness but it doesn't have any specific orientation. So they

can be used in three dimensional applications where the direction of the rotation is not important.

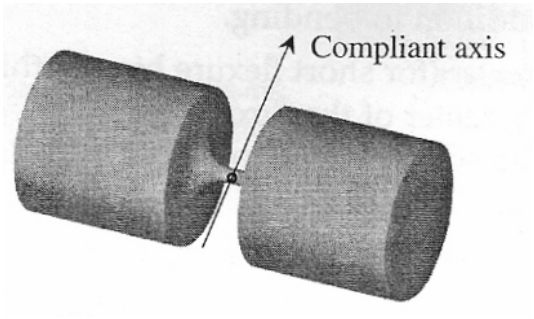

Figure 1.14 Multi-axis flexure

Two-axis flexures: They are designed to give the mechanism two dimensional action and used in three-dimensional (spatial) applications. They have two compliant axes as shown in Figure 1-15. The compliance of secondary axis is slightly smaller than the primary compliant axis.

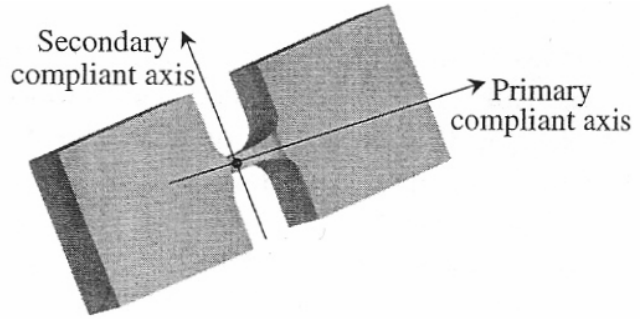

Figure 1.15 Two axis flexure

Paros and Weisbord have designed two axis flexures by putting single axis flexures in a serial configuration. But these types of flexures require extra length of space to locate the flexures in serials. In Figure 1-16a two notch hinge flexures are combined to be perpendicular to each other to provide two axis motion. In Figure 1-16b a universal circular flexure is developed for the same purpose.

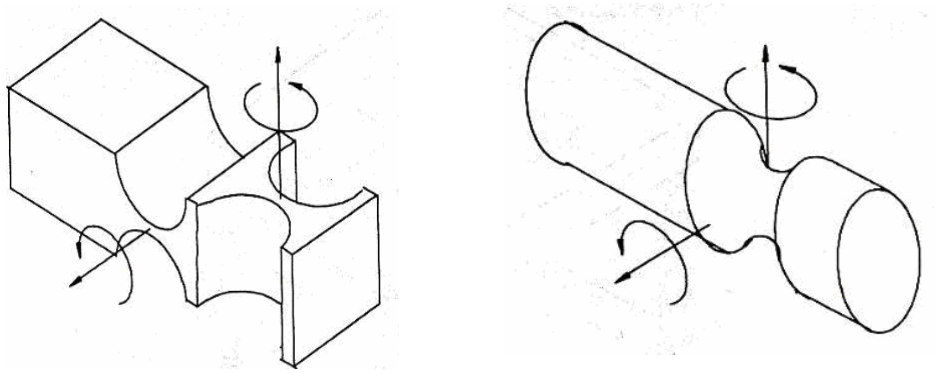

(a) (b)

Figure 1.16 Two degree of freedom flexures

1.2 Advantages and Disadvantages

Advantages:

Compliant mechanisms have many advantages to be used in a variety of applications especially applications where high precision is needed.

- They can be manufactured from a single piece of material which means that compliant mechanisms are monolithic mechanisms. In other words they have fewer movable joints so this reduces the high clamping stiffness, creep of joints and wear. This also reduces the weight which is an important factor of compliant mechanisms to be used in aerospace and other applications that need light weight systems [5].
- Using compliant mechanisms reduces the number of parts required to achieve a specific task. This reduction causes the reduction of manufacturing, assembly and cost. For example as shown in Figure 1-17a fewer parts are required for the assembly of compliant running clutch mechanism than the rigid body mechanism shown in Figure 1-17b [2].

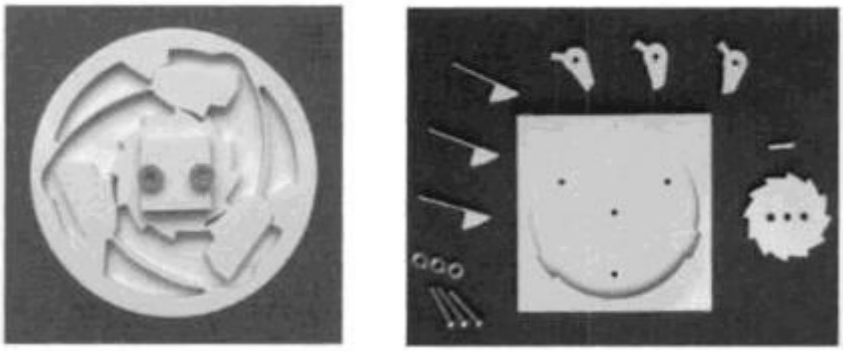

(a) (b)

Figure 1.17 (a) Compliant running clutch (b) Disassembled rigid body mechanism [2]

– There is no backlash between joints and no need of lubrication because no additional joint is used for creating motion.

– Displacements are smooth and continuous at all levels and flexures can provide small rotations which are the main reasons of using compliant mechanisms in high precision motions [2].

– By using the symmetry it is possible to be insensitive to temperature changes.

– If they are designed correctly, they can be controlled easily. The motion of the mechanism can be accurately predicted for known forces. Because the bending of flexures can be modeled as springs which have constant proportion between force and displacement characteristics. So, motion control of these mechanisms can be achieved easily by using these relations [5].

– The compliant mechanisms can be miniaturized easily. The reduction of number of parts and joints of a system gives the advantage in fabrication of micro mechanisms. These mechanisms can be fabricated easily by using micro electro mechanical system (MEMS) fabrication techniques [1].

Disadvantages:

Despite of these advantages that are listed above, compliant mechanisms have also some disadvantages that cause challenges when they are used in some applications.

– The main disadvantage of compliant mechanism is that it is difficult to analyze and design compliant mechanism. Knowledge of mechanism analysis, synthesis methods and deflections of flexible elements are required. When flexible elements

are subjected to large deflections, linear beam equations are no longer valid so non linear equations are taken into account because of the geometric nonlinearities caused by the large deflections. Because of this, in the past many compliant mechanisms are designed by trial and error methods. But these methods can be used just for simple systems that will perform simple task and small displacements. However, pseudo-rigid-body model is produced to model the compliant mechanisms which model the compliant parts as two or more rigid bodies connected by a pin joint.

– Another disadvantage is that complaint mechanisms depend on modulus of elasticity of a material which is hard to control and usually calibration is needed after the system is produced. The mechanism also can have hysteresis due to dislocation movements in the material if the stresses are in the plastic deformation range, i.e. if we exceed the yield strength of the material as seen in Figure 1-18 plastic deformation will occur on the mechanism so when the force is cut the mechanism can't go its initial position because the material is distorted. The material must not have any plastic deformation. The stresses must be in the elastic deformation region of the material that is used.

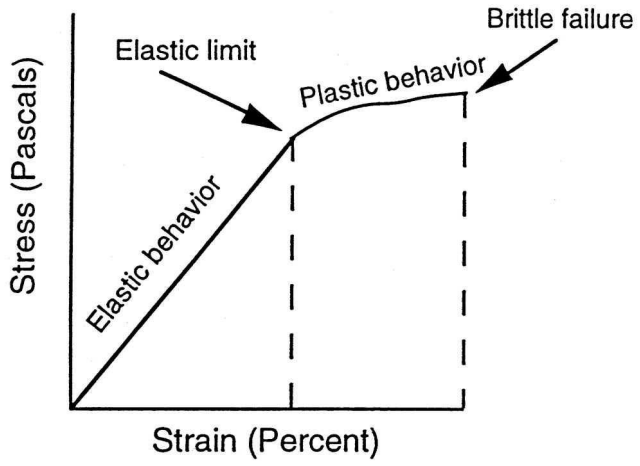

Figure 1.18 Stress-Strain Relationship

– Compliant mechanisms also have weak toleration for large loads because large loads can cause buckling. Accidental overloads can lead to fatigue, catastrophic failures and plastic deformations. Lastly, the drive axis should be collinear with the desired motion because of the reason that the out of plane stiffness is low and drive direction stiffness is high [2, 5].

1.3 Applications

Compliant mechanisms are used in many applications because they can be designed for the purpose of the application. The flexible members can have large deflections or they can create small motions by having small deflections. The material selection, the geometric design and the manufacturing method give the compliant mechanisms opportunity to be used in both macro scale and micro scale applications. This section will give some examples of micro and macro compliant mechanisms.

1.3.1 Micro Compliant Mechanisms

They are a type of micro electro mechanical systems (MEMS) which integrate electrical and mechanical parts together with sizes in range of micrometers. These mechanisms are fabricated by using special fabrication techniques like etching, lithography, surface micromachining etc. They are barely visible with human eye on and the motions of these mechanisms are also can not be seen. Here are some examples of parallel compliant Stages that are used in small scale world:

Bi-stable Mechanisms: They are the mechanisms with two stable positions within its range of motion. When they are actuated, they move from first equilibrium position to the second one [6]. In compliant bi-stable mechanisms this motion is provided by the deflection of flexible elements. These micro bi-stable mechanisms are used as micro valves, micro switches in micro applications. In Figure 1-19 a compliant bi-stable mechanism is presented. Figure 1-19a shows the first stable position, by the thermal actuation and bending of the flexible links, the mechanism moves to its second stable position in Figure 1-19b.

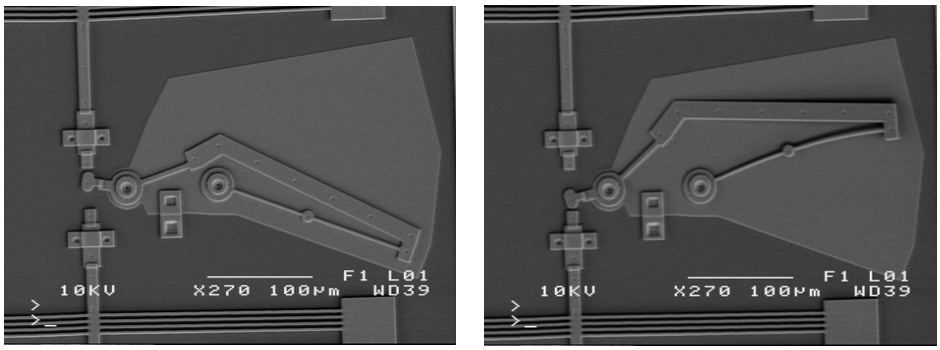

(a) (b)

Figure 1.19 The Young Mechanism [7]

Pin joints: Floating pin joints in Figure 1-20 have been designed by using two layers of polysilicon and manufactured by using Multi layer MEMS processes. They have a rotation as well as a translation capability. They have also used in bi-stable mechanisms as joints. [8]

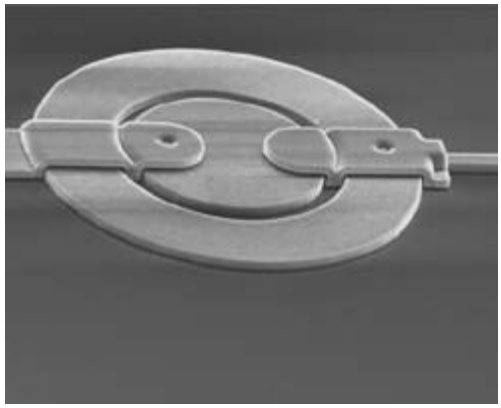

Figure 1.20 Compliant micro pin joint

Micro compliant pantographs: Micro pantographs were built in Brigham Young University laboratories. Some views of these micro pantographs are in Figure 1-21 [9].

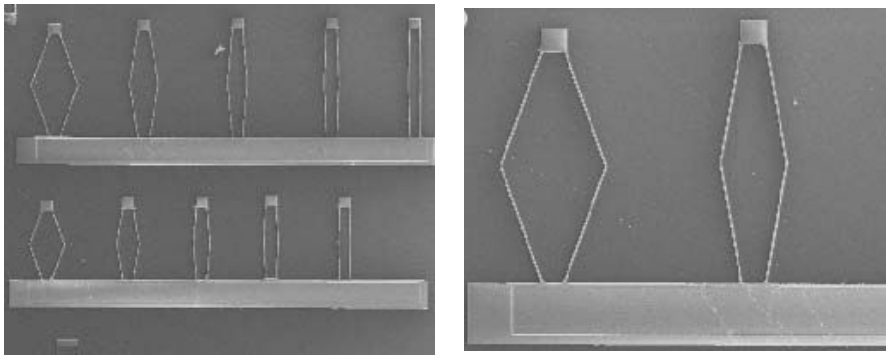

Figure 1.21 Micro compliant pantographs

Microgrippers: Microgrippers are tools in micro systems that pick and place very small particles that are in micro or nano range. They are also compliant mechanisms because no additional joints are used in grippers, the motion is created bye the bending of the beams. In Figure 1-22 there is a silicon based micro gripper [10]. It is fabricated by using etching and lithography processes. The thin arms which are the tips of the micro gripper have 1μm width and 3 μm length.

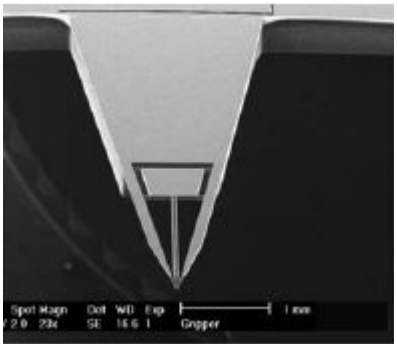

Figure 1.22 A Silicon microgripper [10]

There are also microgrippers that are fabricated by using micro wire electrical discharge machine (EDM) shown in Figure 1-23a. The materials of this micro gripper are aluminum and spring steel because they can be manufactured by using EDM technique. This microgripper is actuated by using piezo motors which can be seen in Figure 1-23b [11].

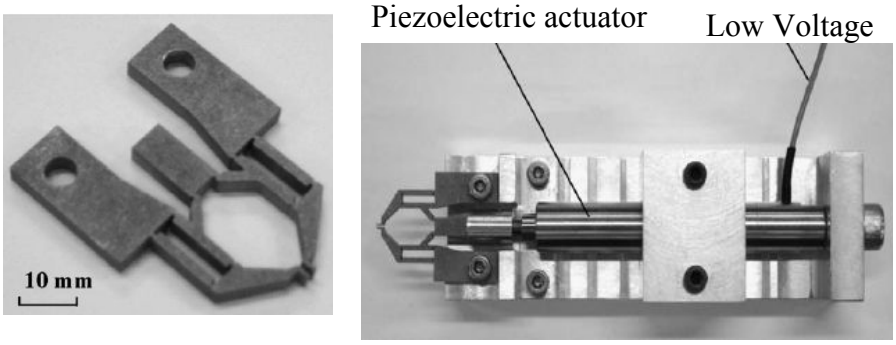

(a) (b)

Figure 1.23 An aluminum microgripper [11]

In Figure 1-24 there is another type of microgripper, which is made by shape memory alloy (SMA) and is holding a piece of optical fiber of 140 μm diameter. The size of that gripper is 2mm x 5.8mm and it is made of TiNi alloy [12]. They are materials that remember their geometry so they are adequate materials for compliant mechanisms. They are metals that, after being strained, at a certain temperature revert back to their original shape. They can recover large strains so they can be used for large movement actuation.

Figure 1.24 SMA microgripper [12]

Micro platforms: Spatial or planar micro platforms are also type of micro compliant mechanisms [13]. In Figure 1-25 there is a spatial and a planar micro platform which is made by micro machining techniques.

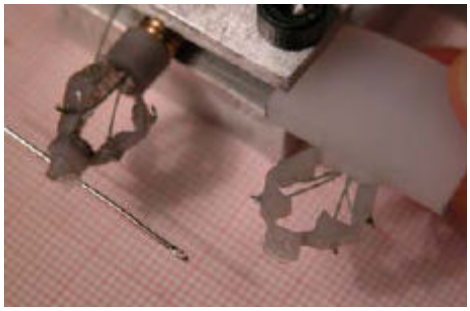

Figure 1.25 Spatial and planar micro platforms [13]

Nano Positioners: Nano positioners are developed for applications in nano technology and optical sensors. The nano positioner shown in Figure 1-26 is composed of a parallel bi lever flexure mechanism and a bent-beam thermal actuator. The flexure mechanism is providing high precision and nano motion. Thermal actuator is used to give the necessary force and displacement [14].

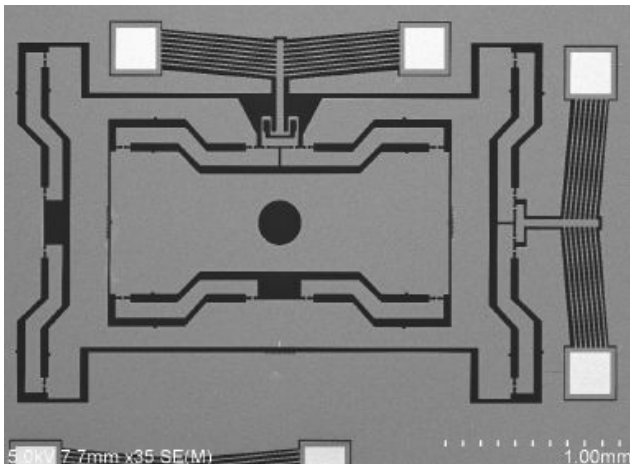

Figure 1.26 2 DOF Nano positioner [14]

Force Gauges: There are also some surface micro machined force gauges that measures the force in micro devices. Suzuki (1996) developed a microgripper that can measure gripping force using the voltage applied and the elasticity of the microgripper. Xiong developed a method in 1998 to calculate the force which is based on the deflection of the beams [15]. So micro force gauges shown in Figure 1-27 were developed to measure the force by using the flexibility of the beams.

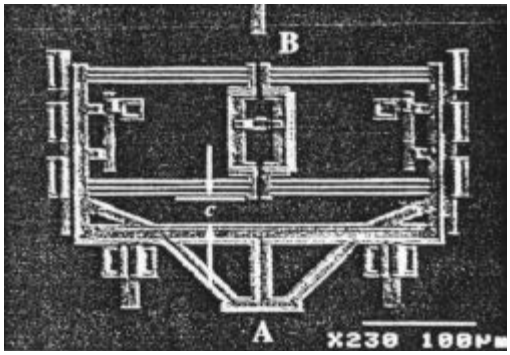

Figure 1.27 Micro force gauge

1.3.2 Macro Compliant Mechanisms

Macro compliant mechanisms are also used where high precision motion is needed. They are visible and usable on a larger scale than the micro compliant mechanisms. Some examples of macro compliant mechanisms will be given in this section.

Compliant Bicycle Brakes: Larry L. Howell and his students did a project about bicycle brakes shown in Figure 1-28. They have replaced the joints of the bicycle brakes with flexible beams. Compliant brakes provide absolute parallel motion; reduce the noise and the wear. It also solves lubrication problem.

Figure 1.28 Bicycle Brake [BYU]

Bi-stable switches: As mention in micro bi-stable mechanisms, there are bi-stable macro compliant mechanisms. They are used as switches, breakers, clamps, snap hinges, closures, positioning devices etc. In Figure 1-29 there is an example of compliant switch. Though they require external force to move from their fist equilibrium position to their second equilibrium position, no holding energy is required to remain in either position .They have also advantages like they are cheap and their fabrication is easy [16].

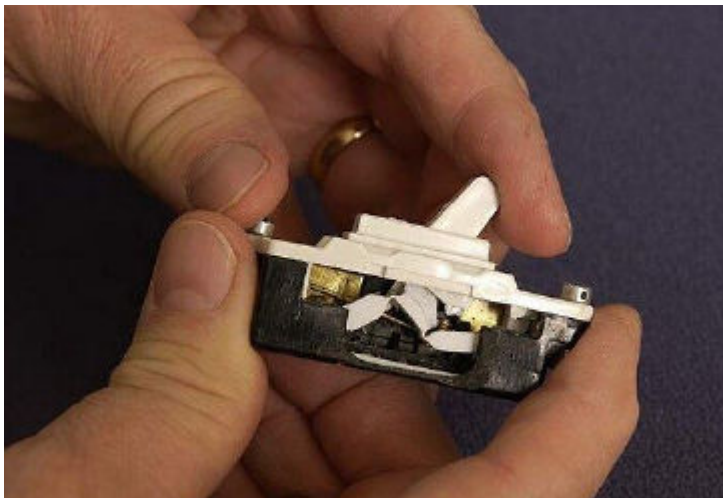

Figure 1.29 A compliant switch [BYU]

Ortho-Planar Flat Springs: They are flat thin circular or polygon shaped platforms which mode up or down orthogonal to the plane. They do not rotate. They can be actuated manually or electromagnets. Ortho-planar flat springs applications are

positioners, damping devices, touch probes, speakers, pneumatic valves, electrical contacts etc. Some examples can be shown in Figure 1-30 [17].

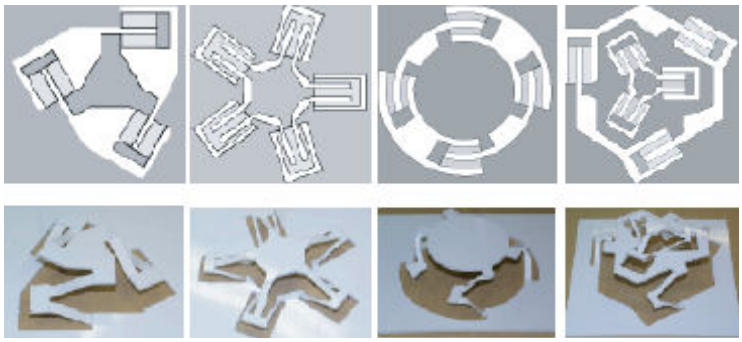

Figure 1.30 Ortho-Planar Flat Springs [BYU]

Centrifugal Clutches: They are used to get rid of rotational motion rather than lateral. When they are made as compliant mechanisms like shown in Figure 1-31, numerous segments, springs, pins etc. are eliminated. Flexible segments are assembled into the moving part. They are simple, have maximum surface friction and torque, eliminate self locking. When compared, their performance is better than the traditional centrifugal clutches [17].

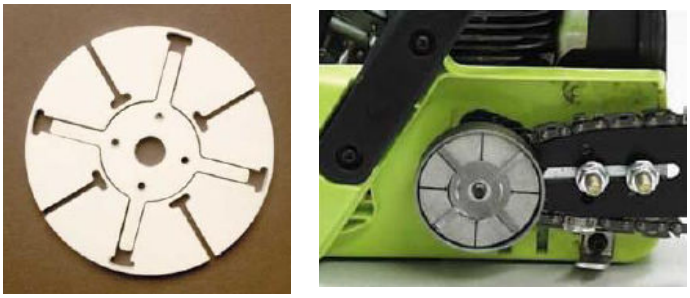

(a) (b)

Figure 1.31(a) Compliant centrifugal clutch, (b) Assembled [17]

Positioning Stages: Compliant mechanisms are also used as high precision positioning stages in micro assembly systems. Because positioning the particles or devices is one of the most important problems in micro assembly. In this thesis, we will be focusing on micro positioning stages so in the following section some positioning stages in the literature will be presented.

1.4 Literature Review of Compliant Positioning Stages

Parallel mechanisms are rigid architectures which are necessary to obtain high accuracy and on the contrary to serial mechanisms they can limit the accumulation of error. That's why in the literature there are many approaches that have been taken to design of high precision micro positioning stages. In the literature some of these micro positioning stages are compliant mechanisms having different kind of flexure types. They have all aimed to design the most precise and controllable mechanism for their purposed applications.

Yao Q.,Dong J.,Ferreira P.M. [18] have built a novel piezo-driven parallel kinematic, micro positioning XY stage shown in Figure 1-32. Their design is composed of four bar linkages and they are connected with flexure hinges. Piezo actuators were used to give motion to the system. Their design has two independent kinematic chains that connect the end effector to a fixed base. They are saying that a viable positioning stage must have independent working actuators, the platform can move along any direction in XY plane and the system should be always kinematically determined. Firstly, they have built an open loop system to see the force-displacement relationship of the stage. Then two fiber optic sensors are used to make a closed loop controlled system.

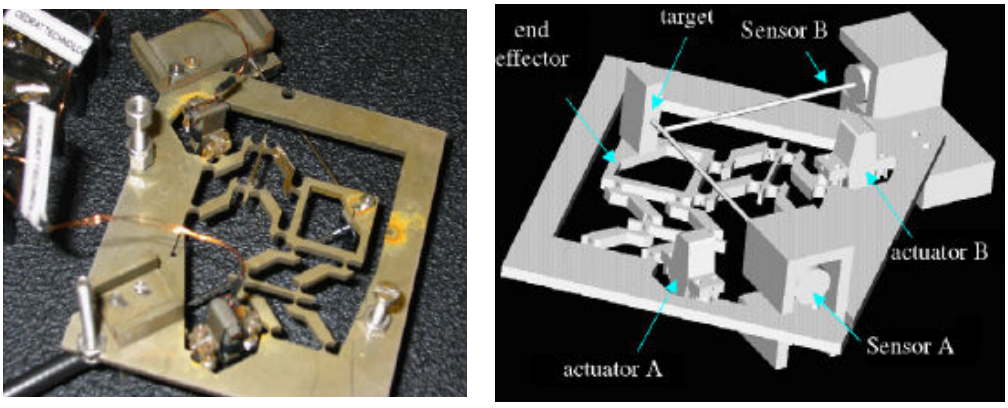

Figure 1.32 Piezo-driven parallel micro positioning XY stage

Lu, Handley, Yong, and Eales [19] developed a three degree of freedom compliant micro motion stage shown in Figure 1-33 which is actuated by three piezo actuators. The three linkages are connected to the end effector platform as illustrated by a triangle. The stage translates along x-y direction and rotates about z axis. It is a compact, light weight, cost effective design. The kinematic model is calculated by

assuming the stage as a 3RRR mechanism. They have also controlled this stage by using simple PI control. But they had problems in modeling. Their modeling accuracy is not good. The kinematic models that are derived by the researchers are inaccurate even after calibration.

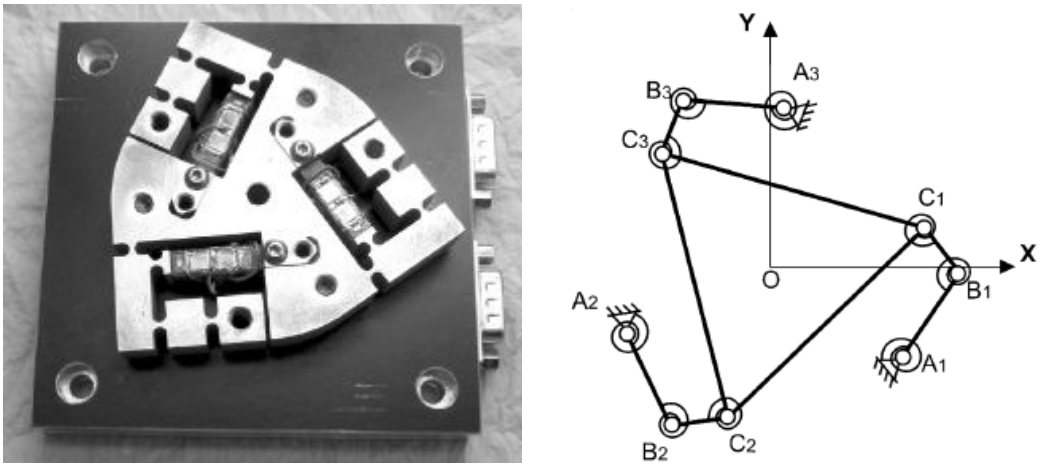

Figure 1.33 3 DOF micro motion stage

Shorya [20] has studied compliant mechanism design in his Phd. Thesis. He has designed 6 different xy positioning stages. The aim of his project is to get rid of the parasitic errors in x and y motions. Finally he has developed the stage shown in Figure 1-34. Two actuators produce motion independent of each other by arranging the planer constraints properly. So a x force produces only x displacement of the motion stage and y force produces only y displacement. He also used piezo actuators for actuation.

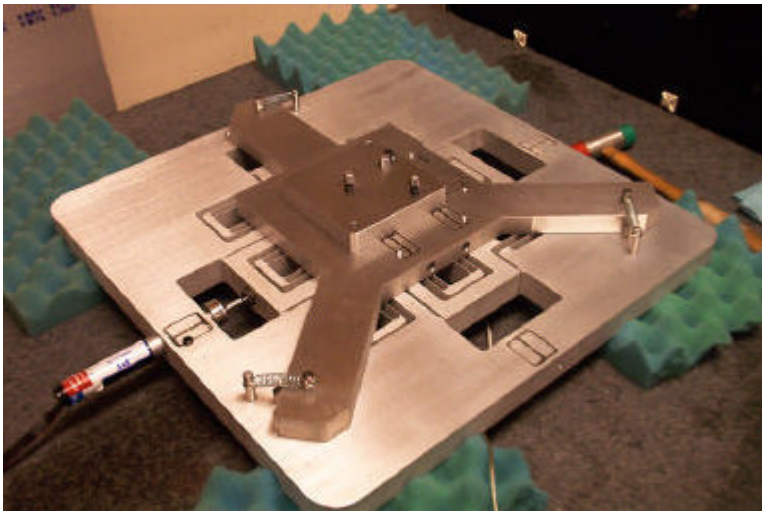

Figure 1.34 XY positioning stage

Another type of XYθ micro motion stage shown in Figure 1-35 which is a monolithic flexure hinge mechanism has been built by Ryu , Gwean and Moant [21]. Firstly, they have made an optimization to find the best parameters for the design then they have built the experimental setup. They have also used piezoelectric actuator for actuation. Their stage have 41,5 μm x 47 μm XY range and the yaw motion range is 1,565 mrad.

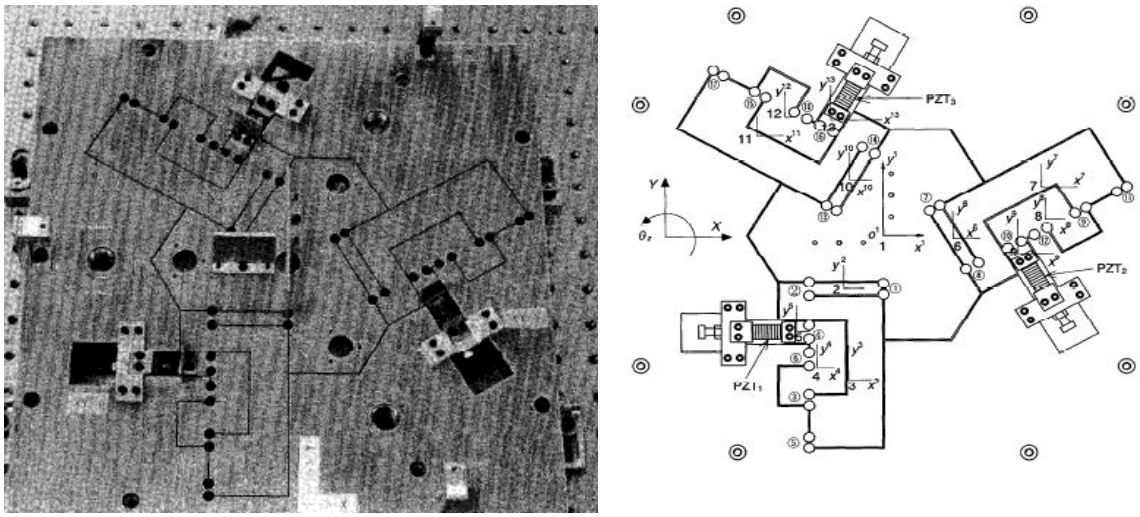

Figure 1.35 XYθ micro motion stage

Kang, Wen, Dagalakis and Gorman have used “Pareto Frontier” optimization criteria to select the best parameters for designing their compliant mechanism shown in Figure 1-36. If a feasible decrease is seen in one of the design metrics which causes at least one other metric design increase, this solution is called “Pareto”. They have also showed that 2 DOF circular notch joint performs better than other types of joints [22].

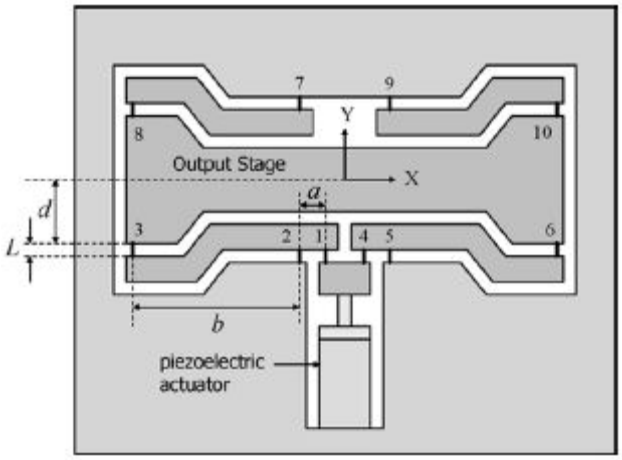

Figure 1.36 2 DOF compliant mechanism

Finally, Culpepper and Anderson have designed a monolithic compliant mechanism called “Hexflex”. Their main aim was to design a low cost nano manipulator. Hexflex have 100 nm x 100 nm x 100 nm work space. Two axis magnet coil actuators were used for actuation of the system. They have also built a MATLAB script tool called COMET™ which is a helping tool for selecting the right parameters for the design of compliant mechanisms [24]. In this thesis, the compliant mechanism design is inspired by their design so in the following chapter their design will be explained.

2 DESIGN OF XY COMPLIANT STAGE

Compact stages are desirable for many micro and nano applications where high precision motion is required. Some of these applications are semiconductor mask, scanning interferometery, atomic force microscopy, micromanipulation, microassembly, MEMS applications, biological experiments and wafer alignment. Since precision and small range of motion is required, flexures are the only choice of bearing joints for the stages. Magnetic and air bearings can be used for large range high precision motion applications [24].

While designing a compact XY stage, there are two main kinds of design configurations which are serial and parallel designs. Serial mechanisms are mechanisms that have only one open kinematic chain. They have poor acceleration and stiffness and the workspace of serial mechanisms is very large. So, serial mechanisms are used where large workspace is important for the application. In fact almost all macro-scale machines that don't need either high dynamic performance nor nanometer resolutions, serial mechanisms are used. Parallel mechanisms are mechanisms that several independent linkages connected to each other and make a closed loop system. The workspace of parallel mechanism is smaller than the serial mechanisms. These mechanisms are also lighter, stronger and faster than the serial mechanisms. They are used in applications that have small workspace and need high precision motion. So because of the advantages of parallel mechanisms to serial mechanism in micro world all stages are designed as parallel mechanisms.

Our XY stage must be designed as it can be used in microassembly work station. The stage must have small work space, high precision motion and must be small enough to be used in the microassembly workstation. So if we look at the literature of micro world and making compressions between the types of stages we can see that a flexure based compliant and parallel XY stage will be compatible for our application.

2.1 Design Requirements of the Parallel Compliant XY Stage

The main design requirements for XY compliant stage are:

- The size of the stage must be compatible with the space of the microassembly workstation. It mustn't be very large.
- The maximum X and Y stroke of the stage must be 1 mm. So the stage material must not be under plastic deformation when the center of the triangle moves in 1x1 mm area.
- The position repeatability must be achieved.
- The stage must have small resolution so that the stage can be precise enough to be used in microassembly workstation.
- The stage must be easily produced. The geometry of the stage must not be complicated.

2.2 Six-axis compliant mechanism, HexFlex

Martin L. Culpepper and his research team in MIT have developed a new planar, six-axis compliant mechanism called HexFlex [23]. The mechanism has x-y-z-θ_x-θ_y-θ_z motion. The main idea of this mechanism is that in Figure 2-1 there is a triangular stage in the middle and the stage is actuated by the deflection of the flexures that is connected to the edges of the triangle.

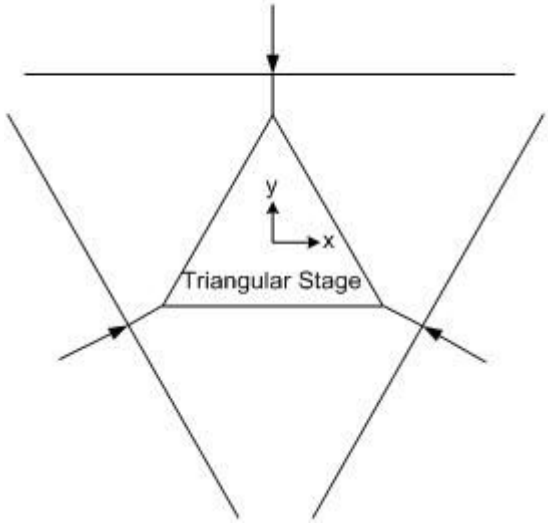

Figure 2.1 Triangular Stage

The main components of HexFlex are shown in Figure 2-2. The Stage is fixed by using the supporting beams. The force should be applied at the edges of the triangular stage so the tabs are designed to create the desired motion of the triangular stage. The flexural hinges are also used as compliant joints to connect the tab and the triangular stage.

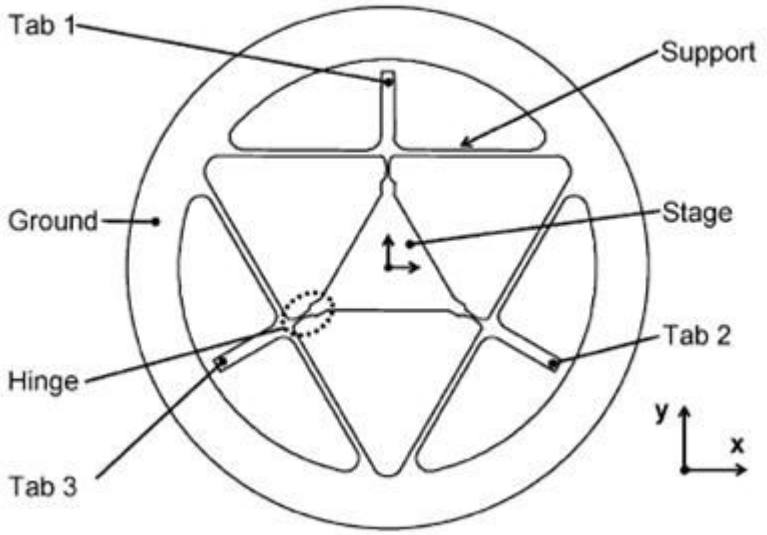

Figure 2.2 The elements of Hexflex [25]

The mechanism is actuated from the tabs by using electro magnetic coil actuators. The forces that are generated by the electro magnetic coil actuators create in-plane and out-of-plane displacements. The examples of combination of actuations and displacements are shown in Figure 2-3.

The x,y, θ_z are the in plane displacements that are generated by F_p forces. In Figure 2-3 A and C situations are the examples of in plane displacements. The z, θ_x and θ_y are the out of plane displacements that are actuated by the F_z forces. In Figure 2-3 B and D situations are the examples of out of plane displacements.

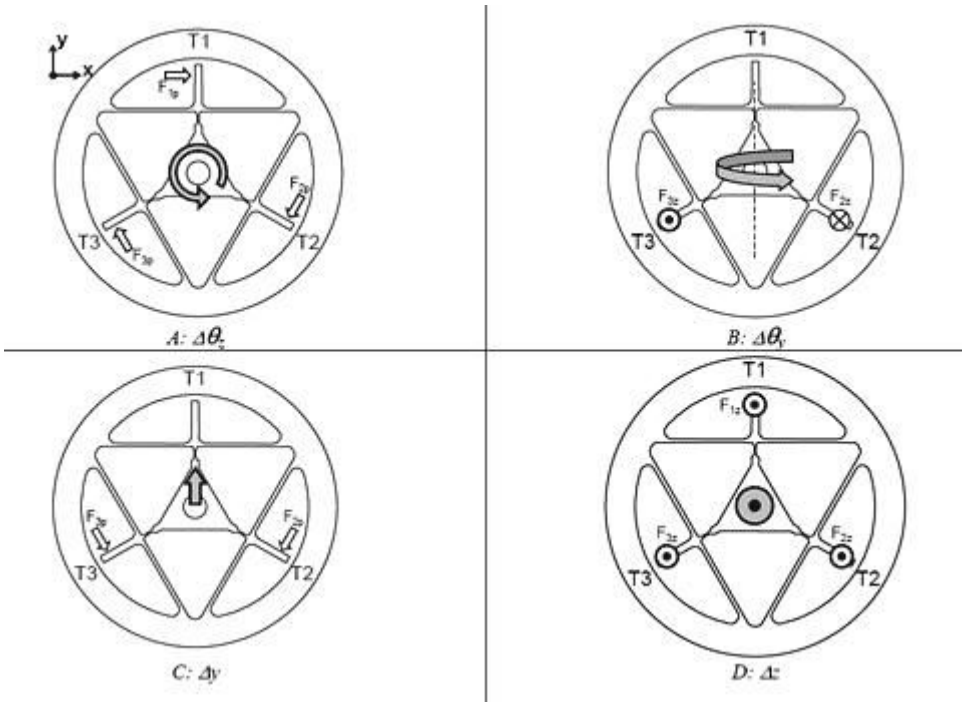

Figure 2.3 Example displacements for combined actuator inputs [25]

Their final compliant Hexflex mechanism design and the stage that is assembled to its actuators and sensors can be seen in Figure2-4.

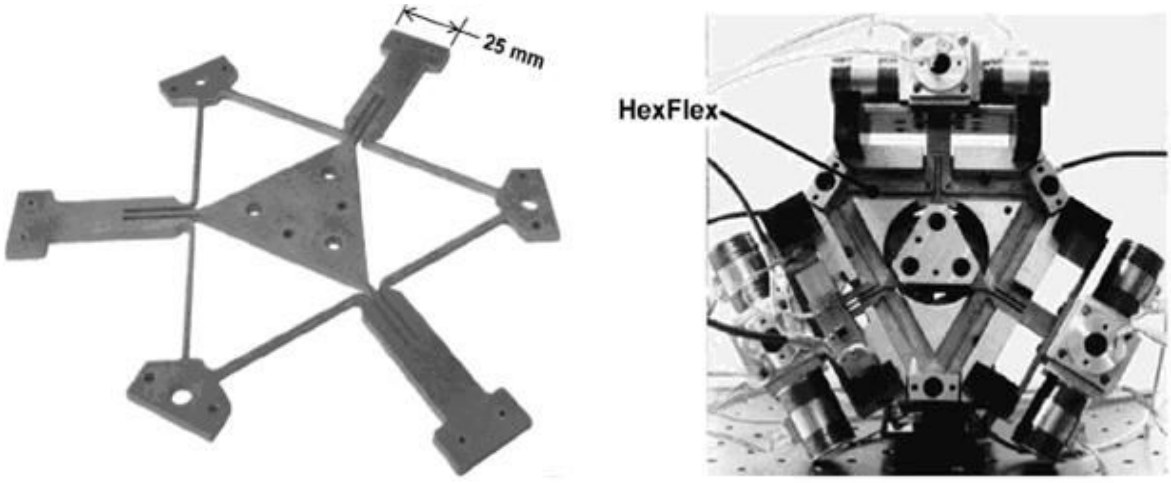

Figure 2.4 The HexFlex mechanism and the assembly of the mechanism [23]

2.3 The Proposed Design

2.3.1 Actuating XY Stage

We have used the Hexflex mechanism which is a spatial compliant mechanism, but we have only used as a planar parallel mechanism which has only two degree of freedom. In their case [23] the tabs of the mechanism shown in Figure 2-2 is not actuated by linear forces which are in the direction of the tabs but in our proposed design three tabs are actuated by these forces which are in the beams direction and create motion for planar triangular stage in x and y directions shown in Figure 2-5. The deflections of the flexural beams due to the forces that are acting on them generate x-y displacements for the triangular stage. The triangle is an equilateral triangle and the angles between the flexural beams are 120˚. This means that the forces acting through these flexural beams are intersecting at the center of the equilateral triangle. This situation causes no rotation in z direction. So the stage moves only in x-y direction.

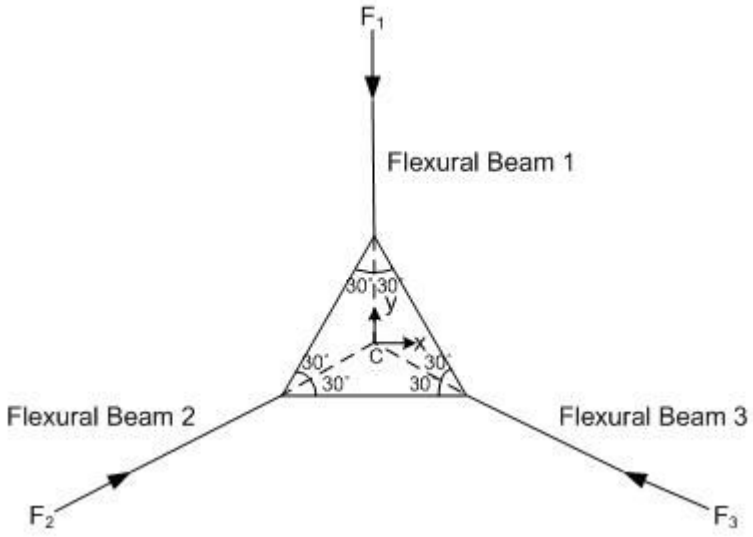

Figure 2.5 The equilateral triangular stage actuation

Figure 2-5 also shows that F_1 creates a motion only in –y direction, F_2 creates a motion in +y and +x directions and F_3 creates a motion in +y and –x direction.

If the stage is actuated only from beam 1, the other two beams will bend and the stage will move in –y direction like shown in Figure 2-6a. To make the stage move in

+y direction shown in Figure 2-6b, only F_2 and F_3 forces should be given to the system and the x component of F_2 and F_3 forces should be equal to each other so that the forces in x direction cancel each other and only the forces in y direction affects the bending of the 2nd and 3rd beams as shown in Figure 2-6b. Beam 1 will not bend in x direction because the sum of the forces.

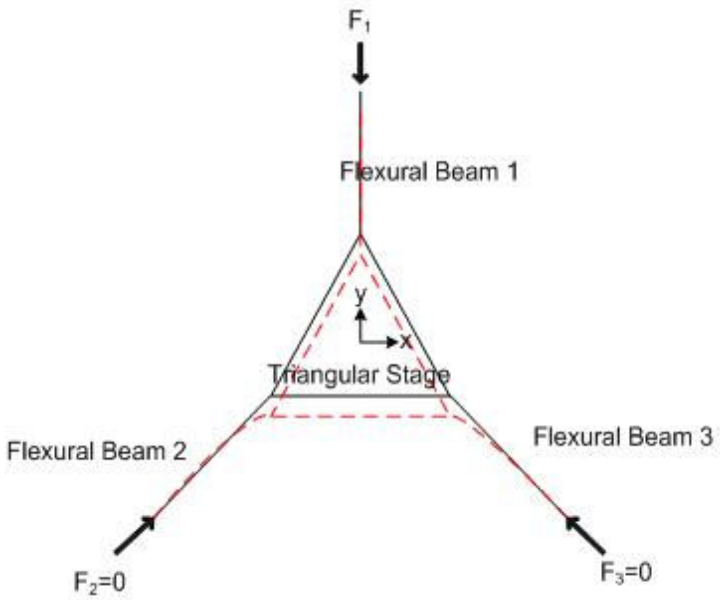

(a)

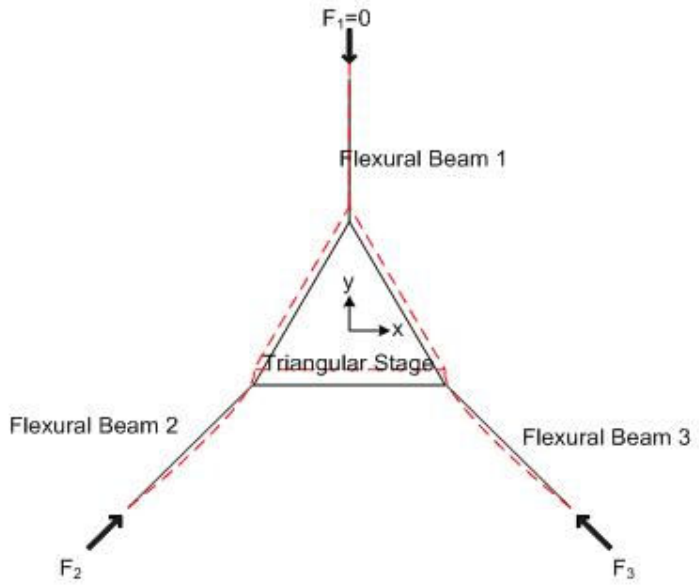

(b)

Figure 2.6 y displacements of the stage fort he given linear forces

In Figure2-7 the stage is moving only in +x and –x direction. To move the stage only in +x direction, F_1 and F_2 forces are used. F_1 cancels the y projection of F_2 so

the stage moves only in +x direction like shown in Figure 2-7a. On the contrary to move the stage only in –x direction F_1 and F_3 forces are used in Figure 2-7b. Same way F_1 is used to cancel the y projection of F_3.

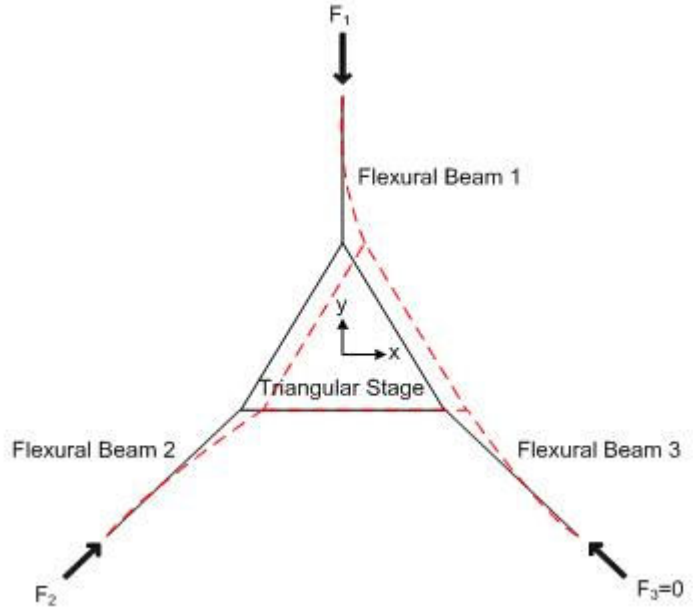

(a)

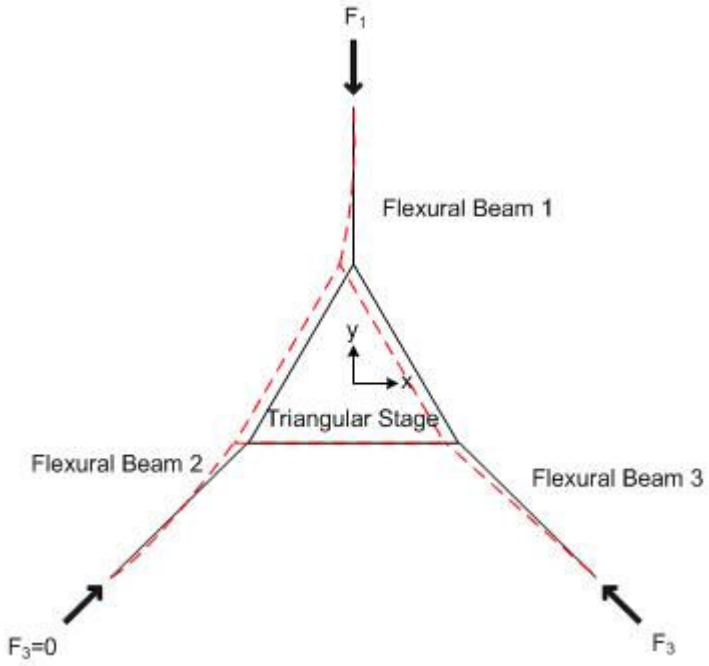

(b)

Figure 2.7 x displacements of the stage fort he given linear forces

PI's piezoelectric micrometer drives called "Piezomike" are selected for the actuation of the mechanism. The reason is that they are available in out laboratory, they

can be operated manually, and the sensivity of the micrometer is 1μm. The micrometer tip can automatically move up to 25 μm by controlling the piezo voltage. So they can also be used remotely for fine positioning. The resolution of the piezoelectric motion is in sub-nanometer range. The travel range of the micrometers that is used is 18mm which is P-854 shown in Figure 2-8. The maximum axial push force is 20N which will determine the maximum deflection of the beams.

Figure 2.8 PiezoMike P-854

2.3.2 The dimensions and final design of the compliant mechanism

The basic dimensions of the compliant mechanism that affect the performance are shown in Figure 2-9. The parameters are tuned by looking at the deflection of the stage. The material of the stage is assumed to be Aluminum (AL6061). By using these parameters shown in Table 2.1 when 20N force is given to the mechanism the material doesn't have any plastic deformation. The results will be shown in Finite Element Analysis (FEA) section.

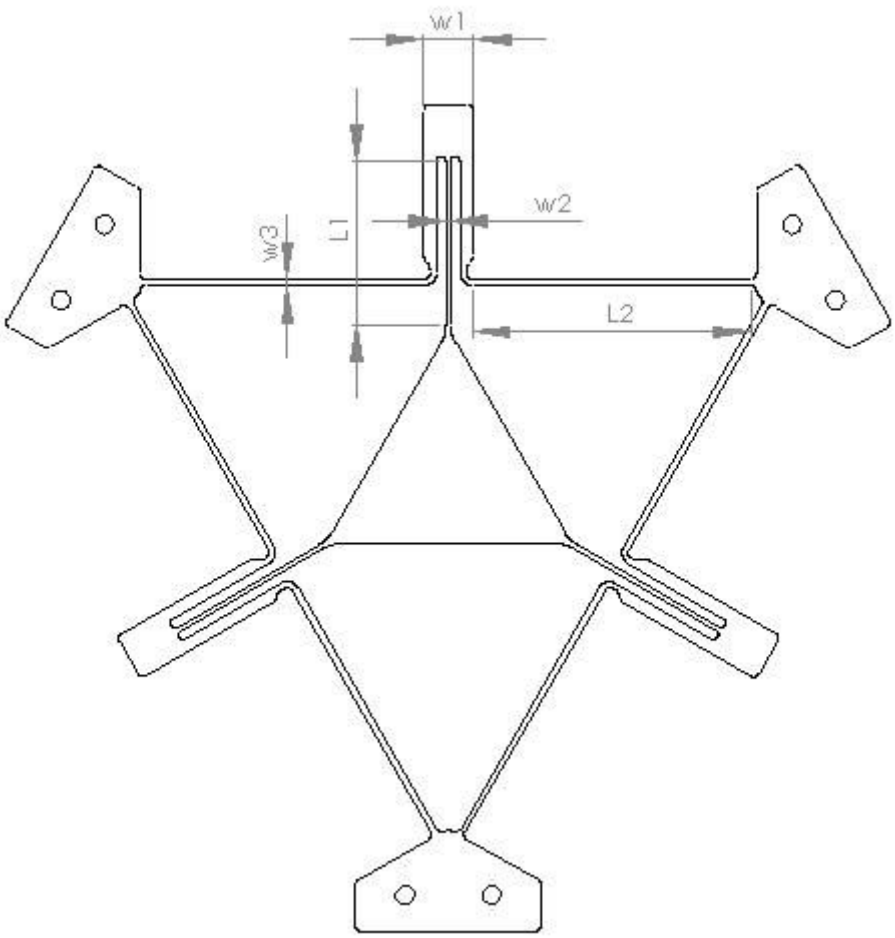

Figure 2.9 The parameters that affect the performance

Table 2-1 The parameters that are used

L_1	26.4 mm
L_2	45 mm
w_1	8 mm
w_2	0.8 mm
w_3	1 mm
t (thickness)	2 mm

2.3.3 Mounting the mechanism

A base shown in Figure 2-10 is designed for mounting the compliant mechanism and the micrometer derives. It is designed so that the micrometer drive tip axes collide with the corresponding axes of the flexural beams. It is designed as small as possible because the application of this mechanism is micro system. The base has a space of 179mm x 156 mm. The main dimensions of the base can be seen in Figure 2-11.

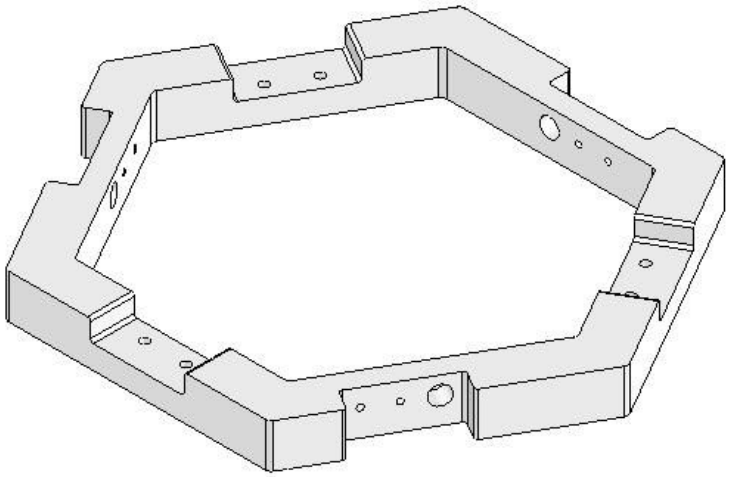

Figure 2.10 Isometric view of the base

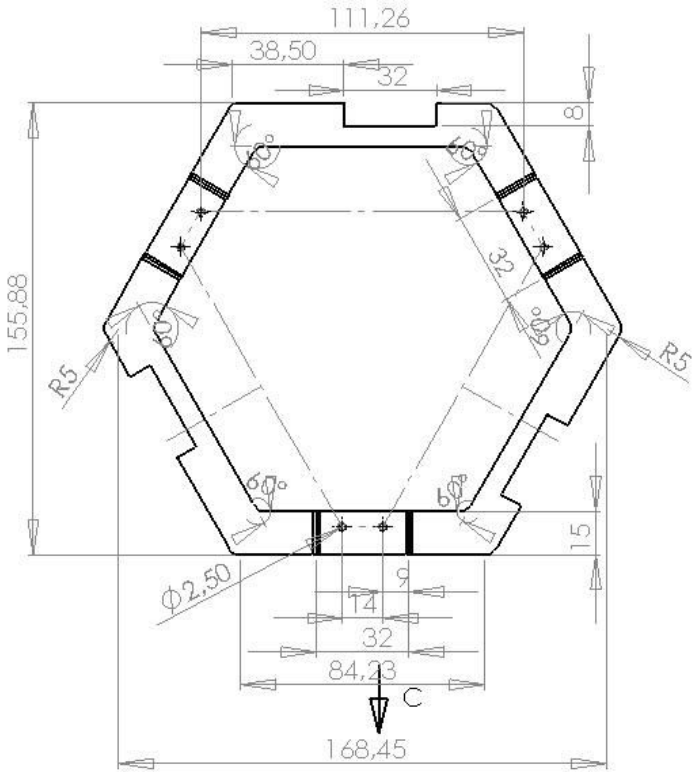

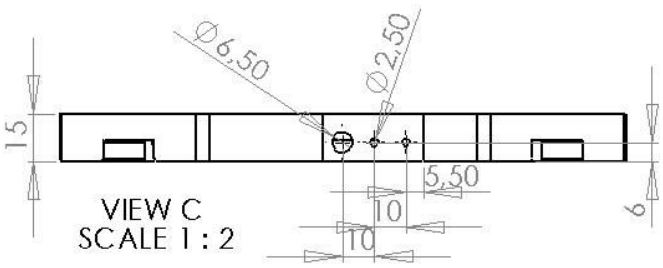

Figure 2.11 Dimensions of the base

An intermediate part is also designed for keeping the tip axes of the micrometers collide with the axes of the beams that they are actuating. This part is shown in Figure 2-12. The left circular cut will be connected to the tip of the micrometer and the right rectangular cut will be connected to the tabs of the compliant mechanism like shown in Figure 2-13 and Figure 2-14. The actuation axis will be on the axis of the center of the stage. The forces will not create any moment to the system so the triangular stage will not rotate. Also this part also helps to prevent the compliant mechanism to bend in z direction.

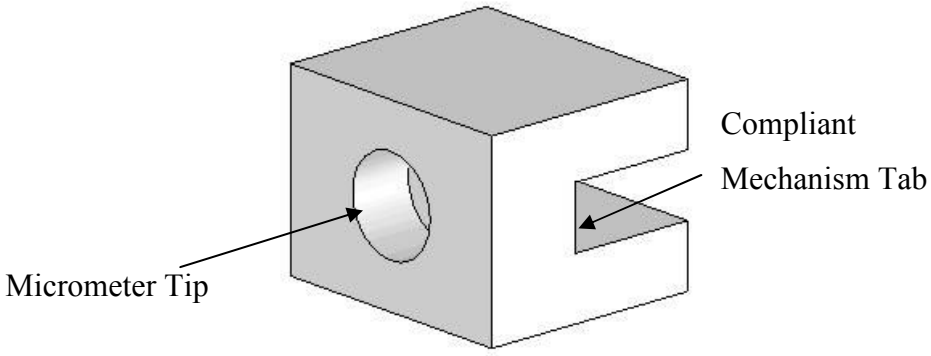

Figure 2.12 Intermediate part

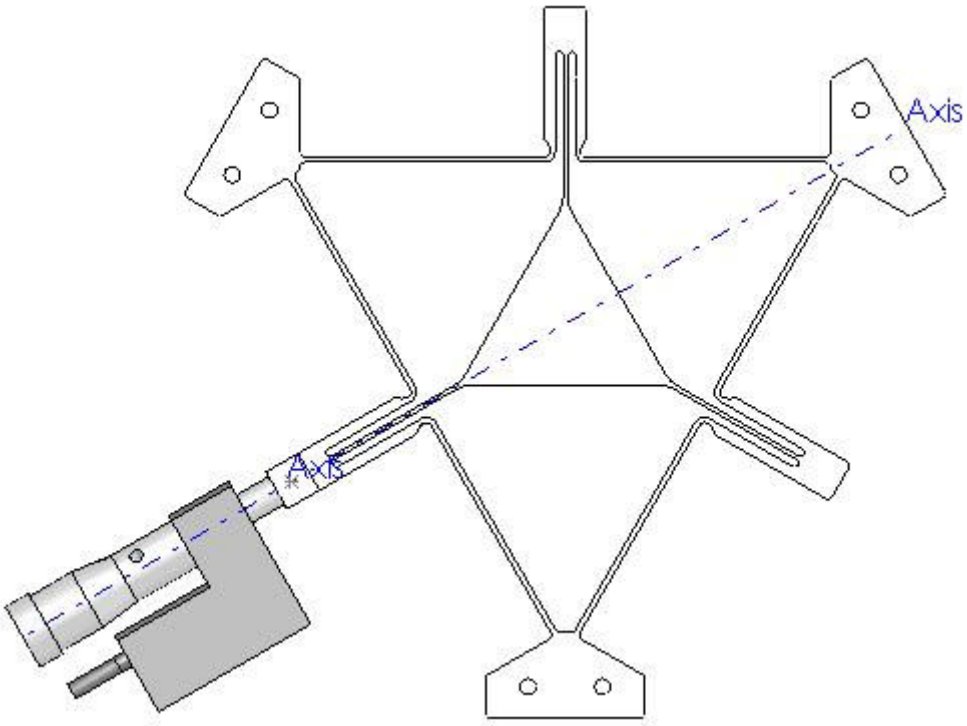

Figure 2.13 The Assembly of the micrometer drive and the compliant mechanism

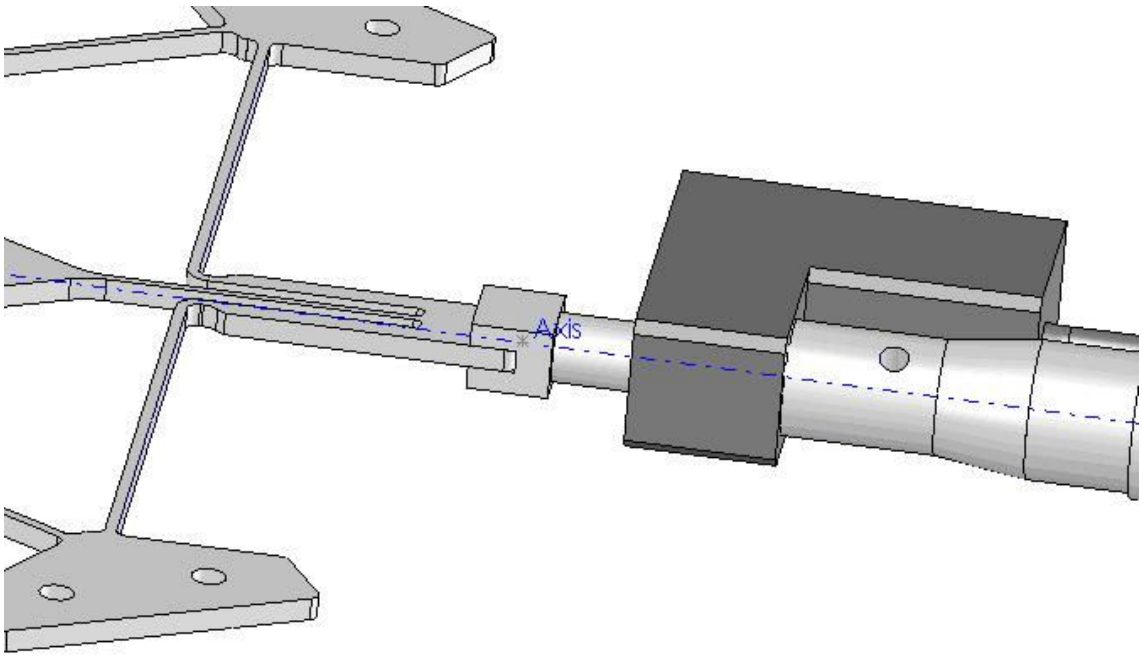

Figure 2.14 The axis of the micrometer collide with the axis of the tab of the compliant mechanism

The final isometric view of the assembly can be seen in Figure 2-15. It can be seen that the system is compact. It is also easy to assemble and carry.

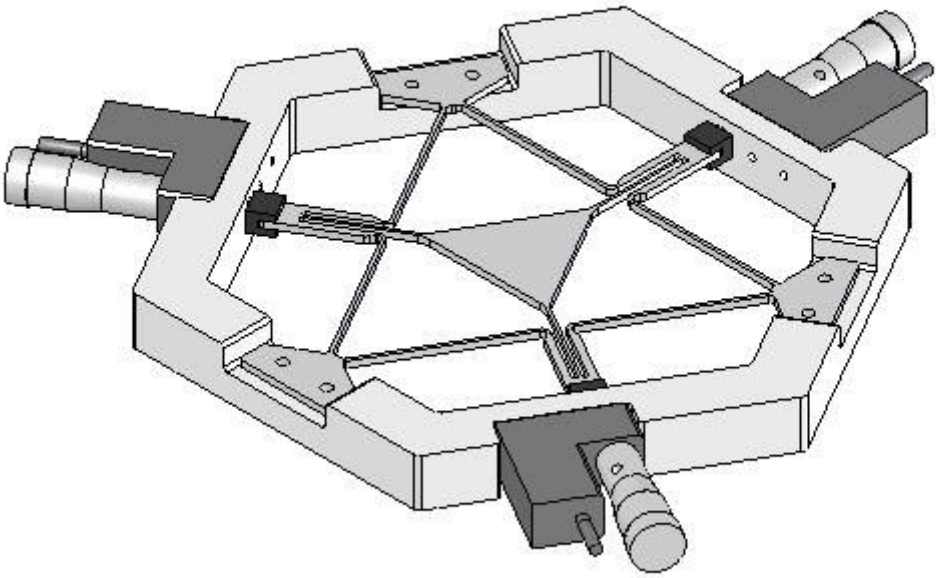

Figure 2.15 The isometric view of the Assembly

2.4 FEA Analysis

Material selection has a very important role for designing the compliant mechanism because, the material properties determine the maximum deflection of the beams that do not result plastic deformations. The application and the geometry of the mechanism have an important role to make that selection. The materials which have low elastic modulus, means have more flexibility, can be used where the application needs higher motions and the geometry of the mechanism permits the material to bend where the material is not overstressed. If the material is overstressed then the material has plastic deformation which causes damage to the mechanism. If the mechanism is subjected to heavy loads, then the material should have higher strength but then the flexibility of the material will decrease so the motion capability of the mechanism will also decrease.

Finite element analysis of the compliant mechanism by using three different types of material is done in ABAQUS. The materials that are used in the analysis are

aluminum, stainless steel and titanium. The properties of the materials that are used are given in Table 2-2.

Table 2-2 The properties of materials

Materials/Properties	Elastic Modulus (Young's Modulus) (N/m^2)	Poisson Ratio	Shear Modulus (N/m^2)	Density (kg/m^3)	Yield Strength (N/m^2)
Aluminum (AL6061)	6.9e10	0.33	2.6e10	2700	1.24e8
Stainless Steel (AISI304)	1.9e11	0.29	7.5e10	8000	2.068e8
Titanium	1.1e11	0.3	4.3e10	4600	1.4e8

Conventional shell elements are chosen to make the FEA analysis of the mechanism, because the thickness of the mechanism is 2mm. and the length of the mechanism 135mm. So the ratio between the thickness and the minimum length of the beam is 1/67,5. It is proper to use S8R shell element type which is a quadratic (second order) element type in ABAQUS. To use a quadratic element gives the advantage of producing better results than the first order elements like S4R in ABAQUS and quadratic elements needs smaller mesh densities than the linear elements and quadratic elements are more reliable than the triangular elements.

Firstly, the minimum number of elements is determined. The boundary conditions and applied load is defined in Figure 2-16. The mechanism is fixed from the fixture holes and the deformation in 2 direction and the rotations in 1, 2 and 3 directions is set to zero for all tabs to make the tabs only move in their directions. One of the tabs is pushed by using 1N concentrated force. The material is selected to be aluminum. The mesh density is increased until the displacement of the triangle in 3 direction converges to some number.

Table 2-4 shows that the displacement of the triangle in 3 direction converges to 0.1265mm. So the optimum number of elements that can be used is 5808 elements. For the FEM simulations S8R element type, 5808 number of elements and 19624 number of nodes are used. In Figure 2-17 the meshed part can be seen.

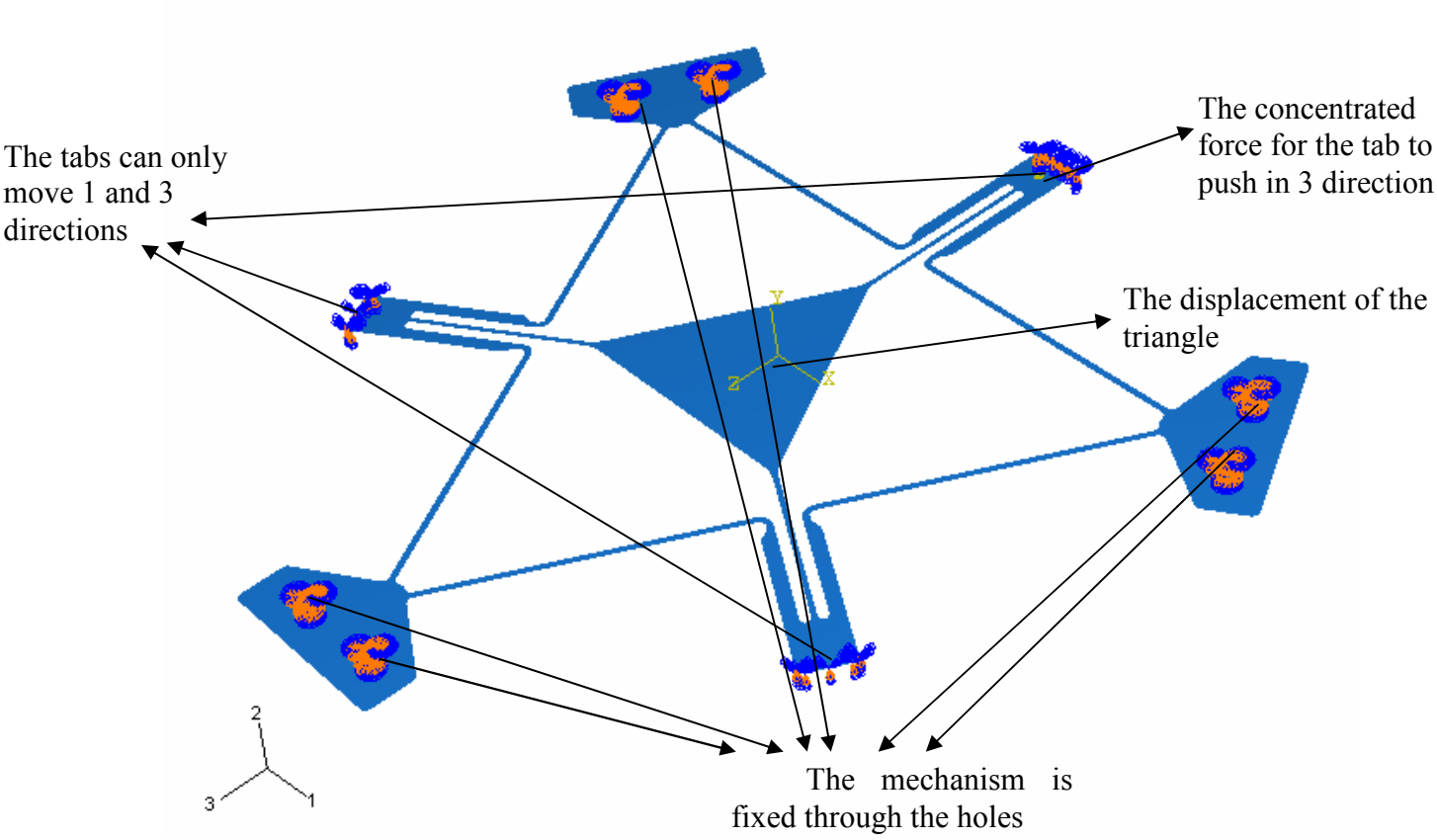

Figure 2.16 The boundary conditions and load for the mechanism

Table 2-3 The displacement results for varying number of elements

Number of elements	Displacement of the triangle in 3 direction (mm)
1744	0,1261
2066	0,1262
2331	0,1263
2932	0,1264
3612	0,1264
4035	0,1264
4704	0,1264
5087	0,1264
5808	0,1265
6678	0,1265
7452	0,1265
8005	0,1265

Number of elements	Displacement of the triangle in 3 direction (mm)
8883	0,1265
9339	0,1265
10762	0,1265

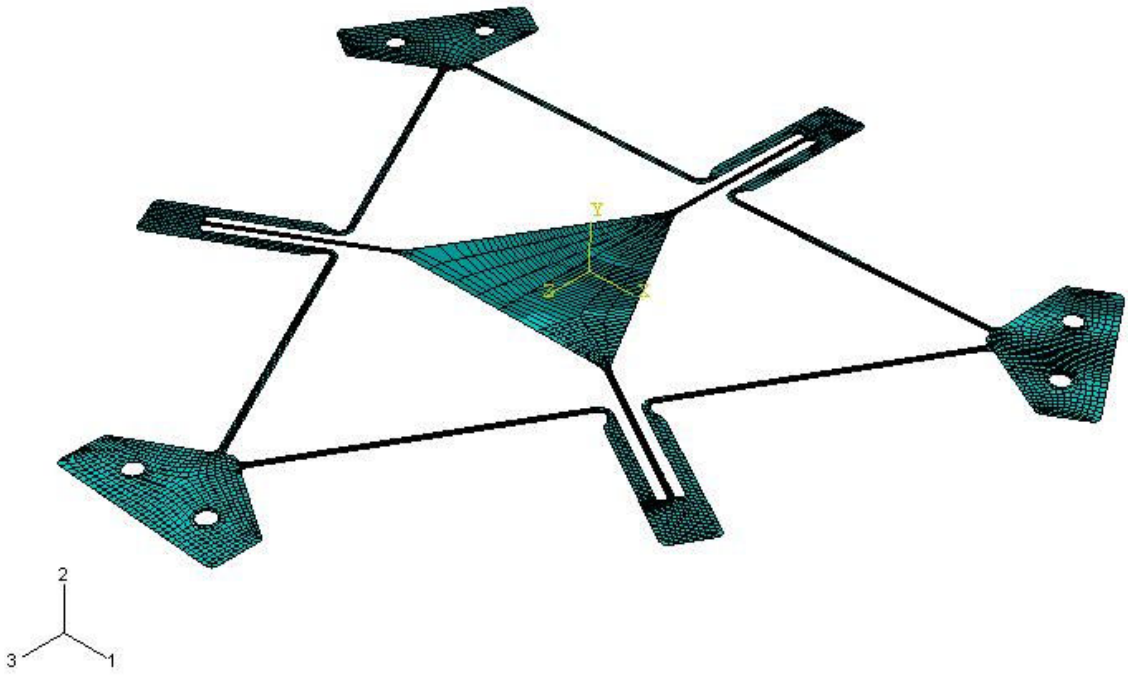

Figure 2.17 Meshed mechanism

Three types of material is used to find the maximum displacement of the triangle is founded by giving maximum concentrated forces to one of the compliant mechanisms tab that the material's yield strength can let.

When using aluminum and one of the tabs of the mechanism is pushed with 5.4 N force on the axis of the tab, the stresses can be seen in Figure 2-18. The maximum stress of the mechanism is 122 N/mm^2. The maximum stresses occur in the beams where they are fixed to the tabs as shown in Figure 2-19.The yield strength of the aluminum is 124 N/mm^2 so approximately 5.4 N force is the maximum force that the material can let. The displacement of the triangle for 5.4N force is 0.6828 mm shown in Figure 2-20.

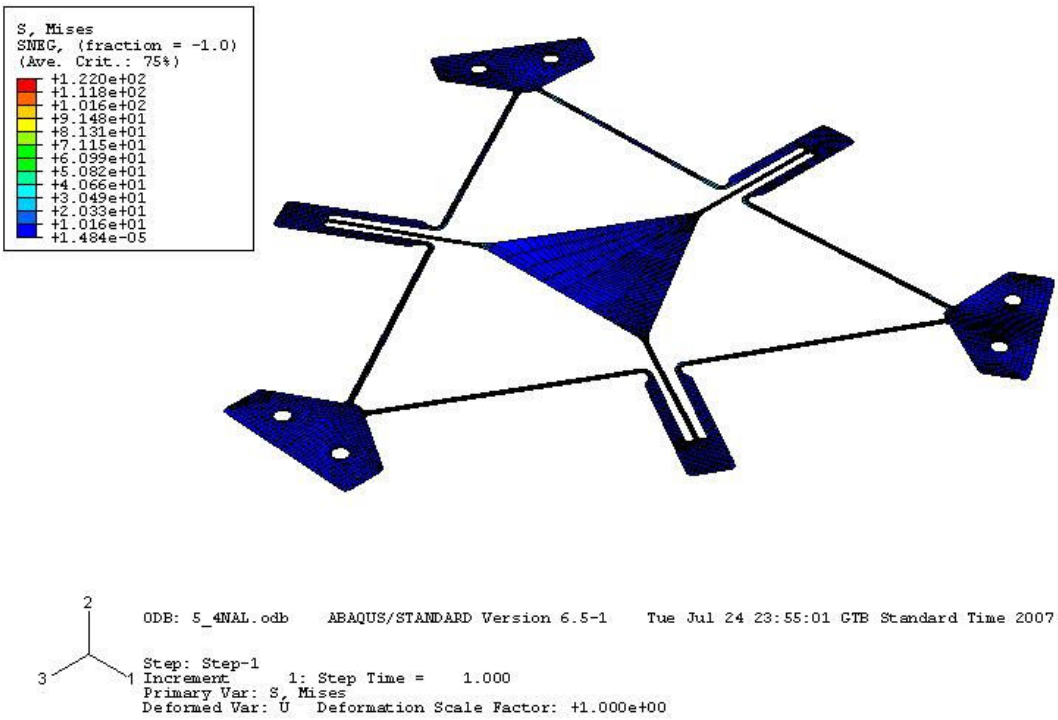

Figure 2.18 Von Mises stress analysis of Aluminum made compliant mechanism.

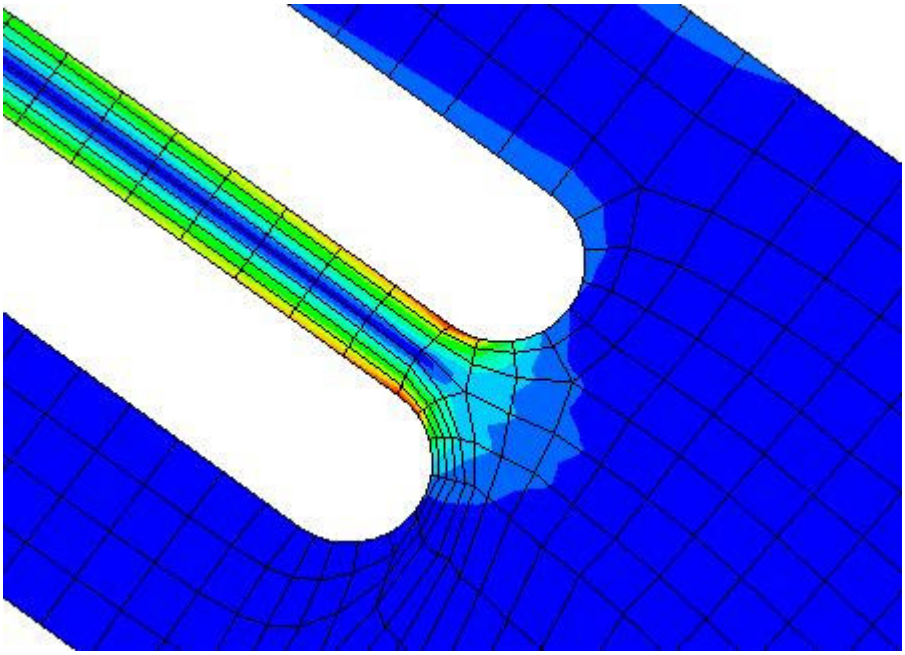

Figure 2.19 Maximum stress

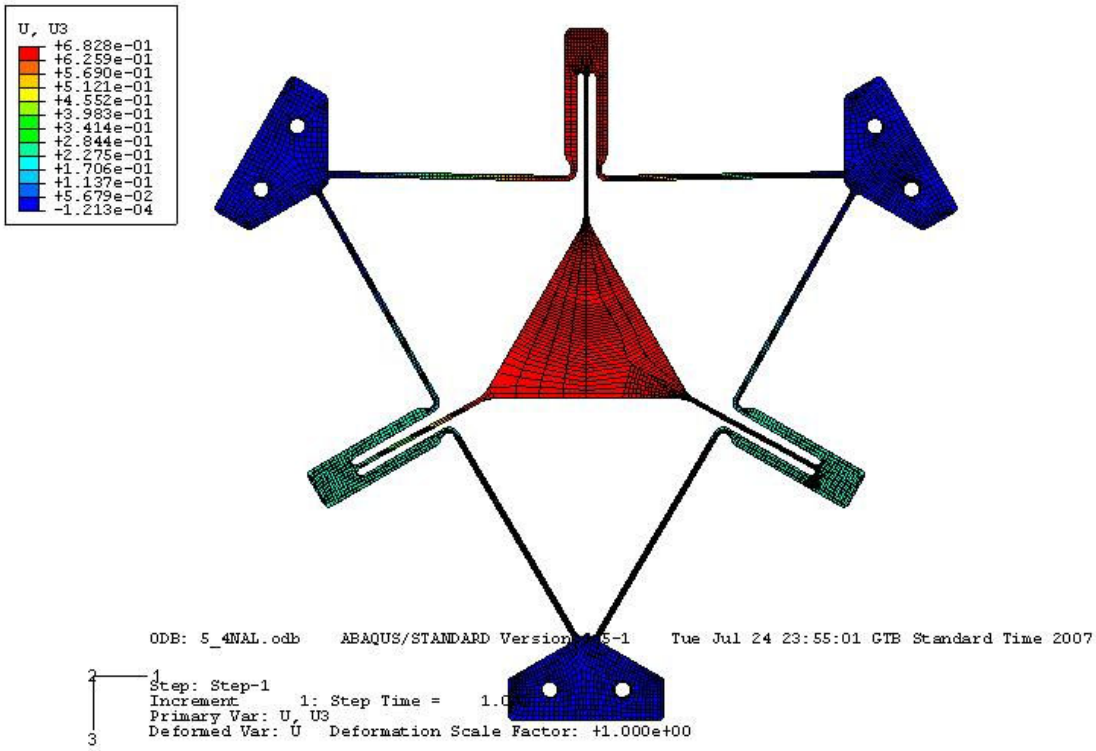

Figure 2.20 Displacement analysis of Aluminum.

If stainless steel is used, the mechanism lets higher force than the aluminum because the yield strength of the stainless steel is much greater than the aluminum. The force applied is 9N as shown in Figure 2-21, the corresponding maximum stress of the mechanism is 203.3 N/mm^2 which occur as shown in Figure 2-19. The yield strength of the aluminum is 206.8 N/mm^2 so this stainless steel mechanism can let almost 9N force when it is given to one of the tabs. On the other hand the corresponding displacement of the triangle is 0.4133 mm as shown in Figure 2-22. Stainless steel has higher strength than the aluminum but the elastic modulus is higher than the aluminum so it is not flexible as aluminum. The mechanism which is made of stainless steel has more strength but less motion capability than the aluminum.

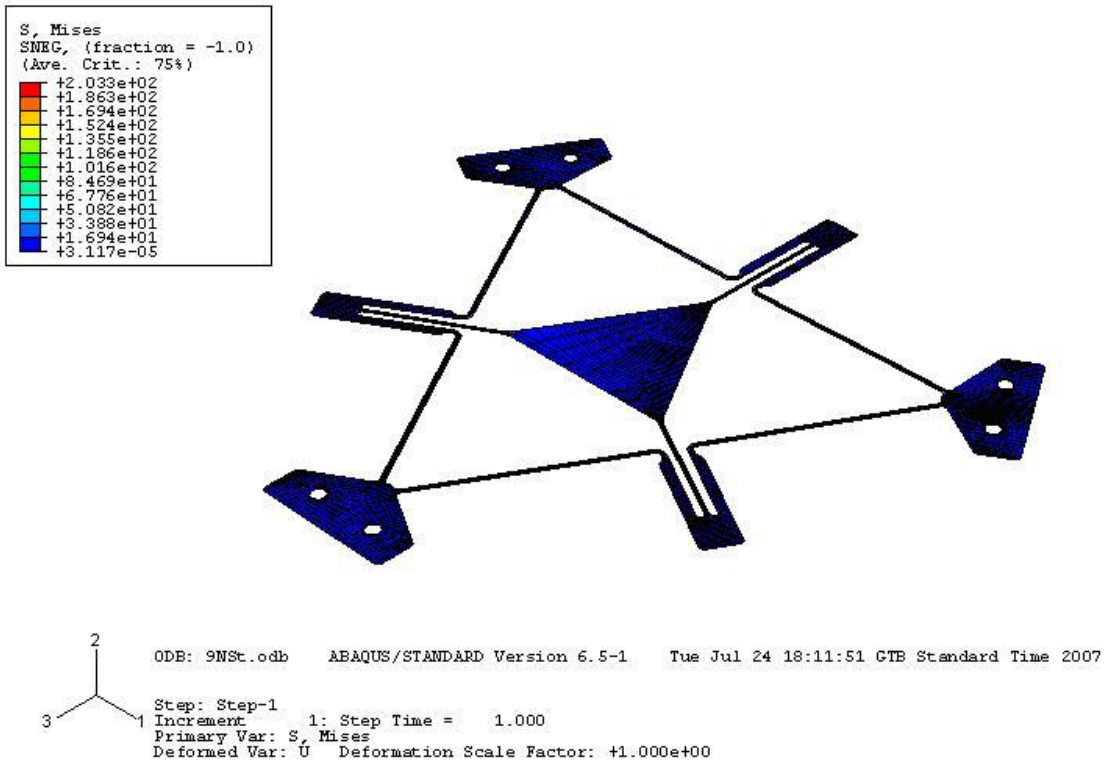

Figure 2.21 Von Mises stress analysis of Stainless Steel made compliant mechanism.

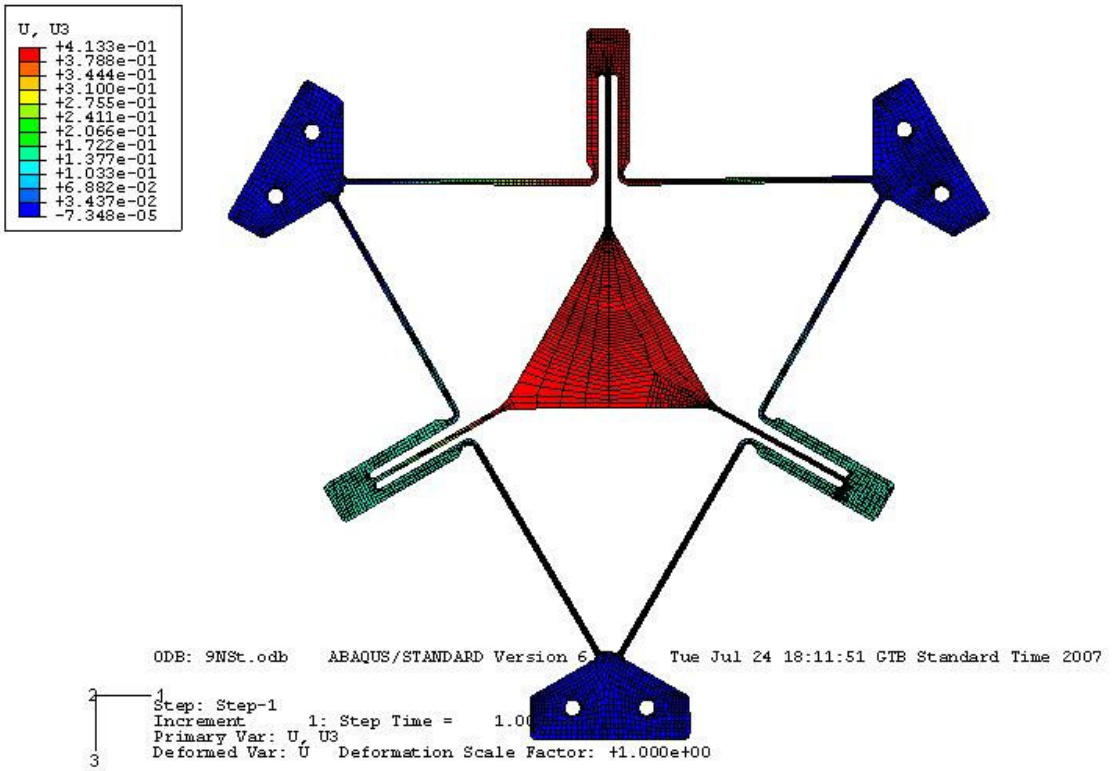

Figure 2.22 Displacement analysis of Stainless Steel.

Finally, if titanium is used, the mechanism lets higher force than the aluminum not much than the stainless steel but greater than the aluminum. In Figure 2-19 6.2N force is applied and the corresponding maximum stress is 140N/mm2. The maximum stress occurs as it said before in Figure 2-19. The yield strength of the aluminum is 140 N/mm^2 so this titanium made mechanism can let 6.2N force. The corresponding maximum deflection of the mechanism is 0.4918 mm as shown in Figure 2-20. The maximum deflection of the titanium is greater than the stainless steel because titanium has lower elastic modulus than the stainless steel so titanium made mechanism is more flexible than the stainless steel but not flexible as aluminum one.

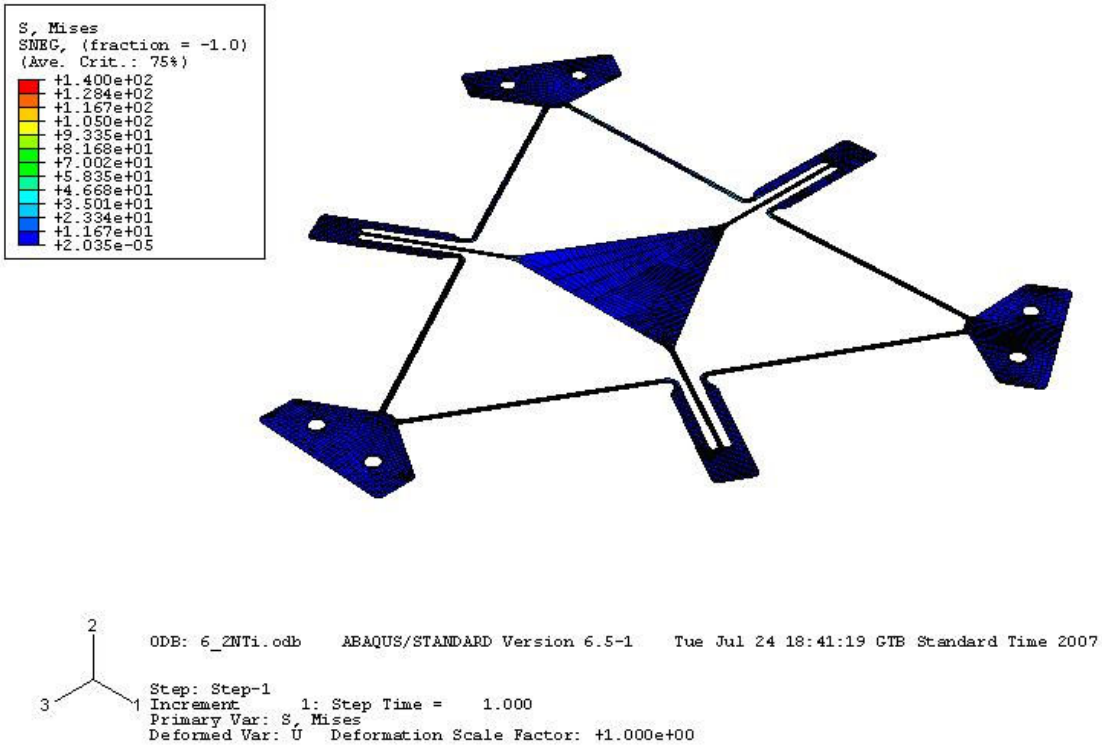

Figure 2.23 Von Mises stress analysis of Titanium made compliant mechanism.

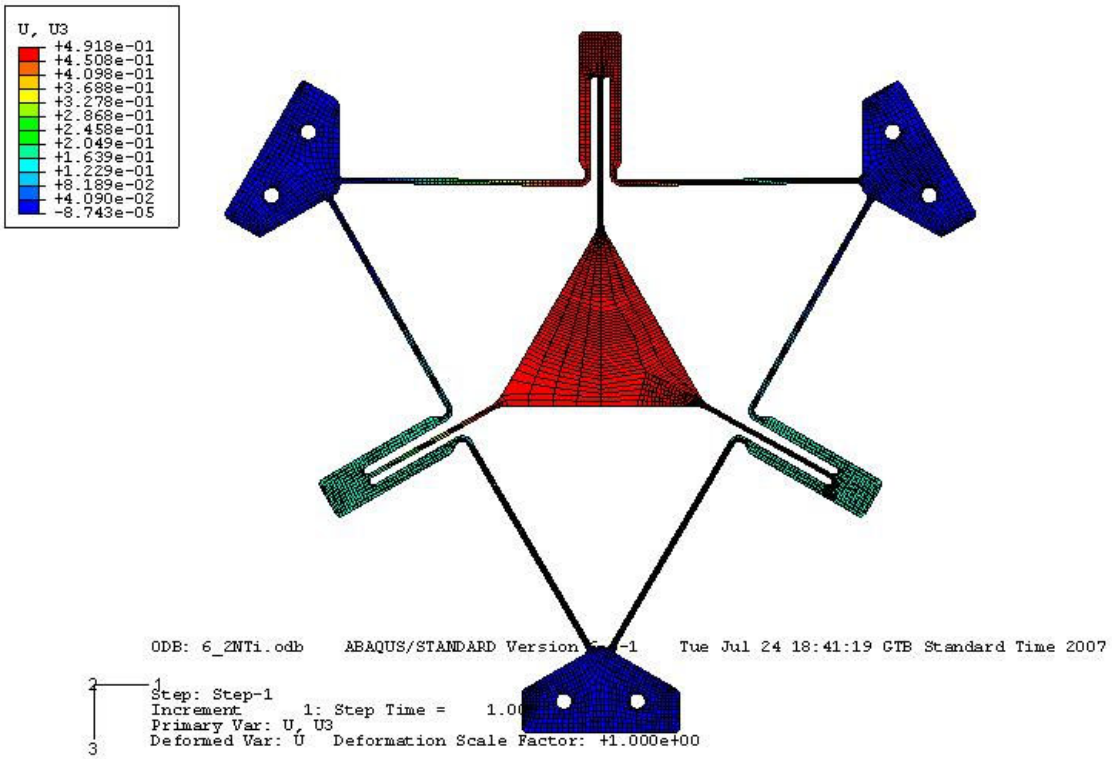

Figure 2.24 Displacement analysis of Titanium.

In conclusion, if we look at the analysis the most flexible material is aluminum but the strength of this material is not good and the machinability of this material is not so good because the minimum thickness of the compliant mechanism is 0.8mm which is very small value to be machined. Titanium is the most optimum material, because it has strength and flexible enough but the cost of this material is high. Stainless steel costs less and it has a good strength which allows to be machined more easily than the aluminum. So firstly the mechanism material is selected to be stainless steel and it is machined by using laser and water jet cutting techniques. The machining techniques will be discussed later.

3 MODELING OF COMPLIANT MECHANISM

In this section, the proposed compliant mechanism that is described in Chapter 2 will be mathematically modeled. It is assumed that we have three beams that are connected to an equilateral triangular stage's edges. The beam dynamics determine the dynamics of the stage.

3.1 Literature Review for Modeling Compliant Mechanisms

The modeling of flexure based mechanisms is a very difficult problem. Because of the nonlinearities in the dynamics of the flexures, by making assumptions and using different techniques to simplify the modeling problem of compliant mechanisms a reasonably simple model could be obtained. [26]

Flexures can be considered as beams and in order to model the bending Euler–Bernoulli equation which ignores shearing and rotary inertia effects is often used. These two effects may be incorporated by using a Timoshenko beam which is generally used if the beam is short relative to its diameter. The original dynamics of a flexible link which is described by partial differential equations and possesses an infinite dimension is not easily available to be used directly in system analysis. As a result of that dynamic equations are reduced to some finite dimensional models by using assumed modes, finite elements or lumped parameter methods.

In assumed mode model, reduced finite modal series in terms of spatial mode Eigen functions and time-varying mode amplitudes are used to represent the link flexibility. The main drawback of this method is the difficulty in finding modes for links with non-regular cross sections and multi-link manipulators. [27]

In finite element method, elastic deformations are analyzed by assuming a known rigid body motion and later superposing the elastic deformation with this motion. A huge number of boundary conditions which are uncertain in most of the

situations for flexible manipulators should be considered to solve a large set of differential equations derived by the finite element method.

In the lumped parameter model, the manipulator is modeled as spring and mass system, which may not give sufficiently accurate results. This method is the simplest one for analysis purposes. [26]

Another common method for modeling the dynamic behavior of flexure mechanisms is Pseudo-Rigid-Body model. In this modeling technique each flexure is treated as a revolute joint with a torsion spring. Using such a kind of modeling makes the analysis of mechanisms with flexures easier and faster. This model also eases to see the effects the parameters on mechanism design and significantly simplify the design process. Using this model results can be expressed in analytical forms and the effects of parameters such as link lengths, initial position etc. on the motion of the stage. [2] Pseudo rigid body models (PRBs) are generally used to accurately and efficiently model such elastic deflections. [28] formulated the PRB model of a 2-DOF mechanism with flexures. Methods based on finite element method or the elliptic integral solutions are more realistic in the analysis of flexure mechanisms. However, PRB model gives results precise enough to be used in the actual design. In [29] Bernoulli-Euler beam equation is used for deflections with elliptic integrals, and the elliptic integral solutions are used to determine when an inflection point will exist.

A substructuring dynamic modeling procedure is proposed for closed-loop flexible-link mechanisms and applied and applied to a planar parallel platform [30]. The Lagrange finite element (FE) formulation is used to model flexible linkages, in which both translational and rotary degrees of freedom exist.

3.2 Dynamics of Compliant Mechanism

A compliant mechanism is a distributed-parameter system, because the motion of these systems is provided by the deflection of the flexural elements and these elements dynamics depend on both time and the position.

The dynamics of the mechanism that it is proposed in Chapter 2 is formed by the three beams' dynamics. It is assumed that we have three fixed free beams and the tip motion of these beams will determine the motion of the triangular stage as shown in Figure 3.1. Beams are elements that are constructed possess a continuous distribution of

inertia and compliance properties. So these elements are represented by linear partial differential equations in space and time. Separation-of-Variables Solution method is used to solve these partial differential equations. This method is based on separating the partial differential equation into a position and a time function multiplication. The dynamics of these systems are composed of propagating waves that comes from the boundaries and add together to produce what is actually observed at any point and time. Mode shapes of Euler Bernoulli beams are used to define these wave shapes that create the motion of the flexible systems.

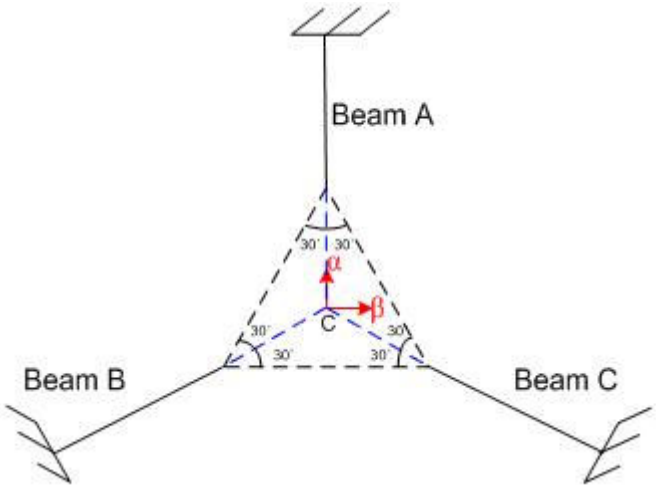

Figure 3.1 Assumed compliant mechanism

The dynamics of the mechanism is found by separating the transverse and longitudinal motions of the beams. Firstly, the forces that cause transverse and longitudinal deflection of the three beams are calculated. Second, the dynamics of the beams are calculated by using Euler-Bernoulli beam equations and finally the corresponding center deflection is calculated by using the deflection vectors of the beams.

3.2.1 Transverse Dynamics

The transverse forces that are acting on each beam can be calculated as following figures. Each force acting on the beams, F_A, F_B and F_C are shared equally by the other two beams because the directions of the actuating forces are all on the centre axes of the equilateral triangle which cause no moment on the triangular stage. The perpendicular components of these shared forces are the transverse forces for the beams.

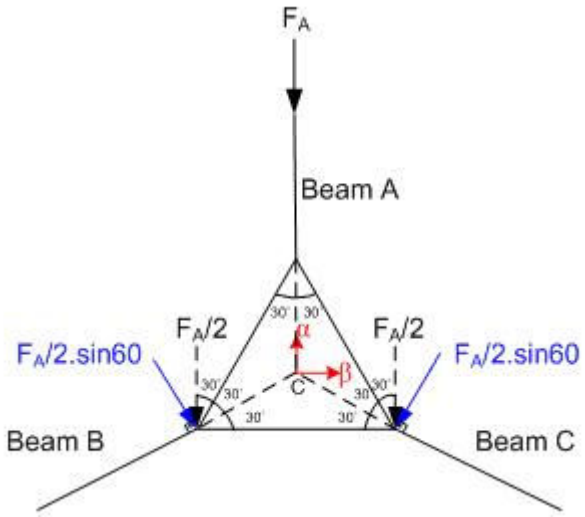

Figure 3.2 The transverse forces produced by F_A

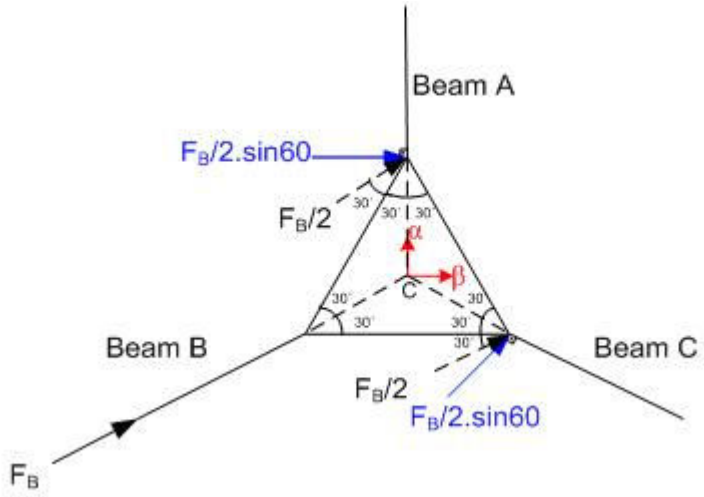

Figure 3.3 The transverse forces produced by F_B

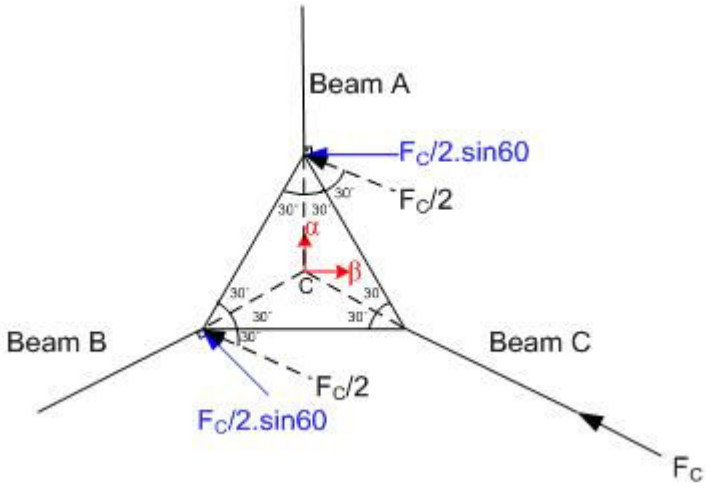

Figure 3.4 The transverse forces produced by F_C

So, we can assume that we have three separate fixed free beams shown in Figure 3-5 which are under transverse forces. The forces which lie on the clock wise direction are taken as positive forces.

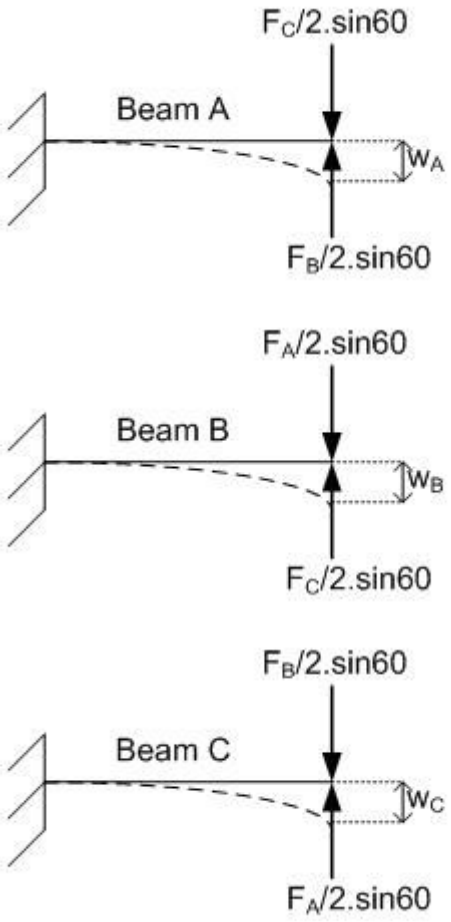

Figure 3.5 The transverse forces acting on the beams

The transformation matrix between the actuating forces and the transverse forces to the beams are;

$$\frac{1}{2}\begin{bmatrix} 0 & \sin 60 & -\sin 60 \\ -\sin 60 & 0 & \sin 60 \\ \sin 60 & -\sin 60 & 0 \end{bmatrix} \cdot \begin{bmatrix} F_A \\ F_B \\ F_C \end{bmatrix} = \begin{bmatrix} F_{1t} \\ F_{2t} \\ F_{3t} \end{bmatrix} \tag{3.1}$$

$$T_{forcetransverse=} \frac{1}{2}\begin{bmatrix} 0 & \sin 60 & -\sin 60 \\ -\sin 60 & 0 & \sin 60 \\ \sin 60 & -\sin 60 & 0 \end{bmatrix} \tag{3.2}$$

The determinant of $T_{forcetransverse}$ is 0 so the matrix is not invertible but it is not a problem for us because we don't need a transformation from transverse forces to the actuating forces.

Euler-Bernoulli Transverse Beam Dynamics:

The general Euler Bernoulli beam equation acting one external force:

$$EI\frac{\partial^4 w}{\partial x^4}+\rho A\frac{d^2 w}{dt^2}=F\delta(x-x_1) \tag{3.3}$$

The boundary conditions for the fixed-free beam are as follows:

There is no deflection at the fixed end so the boundary condition for the fixed end is:

$$w(0,t)=0 \quad ; \quad \frac{\partial w}{\partial x}(0,t)=0 \tag{3.4}$$

There is no load at the free end of the beam. There is zero moment and zero shear so the boundary condition for the free and is:

$$\frac{\partial^2 w}{\partial x^2}(L,t)=0 \quad ; \quad \frac{\partial^3 w}{\partial x^3}(L,t)=0 \tag{3.5}$$

The transverse displacement depends on the position (x) and time (t).We can define as two functions:

$$w(x,t)=Y(x)f(t) \tag{3.6}$$

If we substitute 3.6 into 3.3:

$$EI\frac{d^4 Y}{dx^4}f+\rho AY\frac{d^2 f}{dt^2}=0 \tag{3.7}$$

Dividing each term by ρAYf :

$$\frac{EI}{\rho A}\frac{1}{Y}\frac{d^4 Y}{dx^4}f+\frac{1}{f}\frac{d^2 f}{dt^2}=0 \tag{3.8}$$

In 3.8 the term which depends on x and the term which depend on t equal to the same constant. If we say the second term equal to $-\omega^2$:

$$\frac{d^2 f}{dt^2}+\omega^2 f=0 \tag{3.9}$$

$$\frac{d^4 Y}{dx^4}-\frac{\rho A}{EI}\omega^2 Y=0 \tag{3.10}$$

We can rewrite equation 3.10 as:

$$\frac{d^4 Y}{dx^4}-k^4 Y=0 \tag{3.11}$$

$$k^4=\frac{\rho A}{EI}w^2 \tag{3.12}$$

Equation 3.11 is a differential equation and if we use boundary conditions shown in equations 3.4 and 3.5, the mode shapes and associated mode frequencies will be found. If we use equation 3.6, the boundary conditions will be:

$$Y(0) = \frac{dY}{dx}(0) = \frac{d^2Y}{dx^2}(L) = \frac{d^3Y}{dx^3}(L) = 0 \tag{3.13}$$

The differential equation 3.11 has the general solution:

$$Y(x) = A\cos\beta hx + B\sinh\beta x + C\cos\beta x + D\sin\beta x \tag{3.14}$$

If we solve this differential equation we will find a frequency equation:

$$\beta_n = \frac{(2n-1)\pi}{2L} \tag{3.15}$$

And the mode shape functions:

$$Y_n(x) = \cosh\beta_n x - \cos\beta_n x - \frac{\sinh\beta_n L - \sin\beta_n L}{\cosh\beta_n L + \cos\beta_n L}\left(\sinh\beta_n x - \sin\beta_n x\right) \tag{3.16}$$

4 modes are used for defining the dynamics. The shape functions can be seen in Figure 3-6.

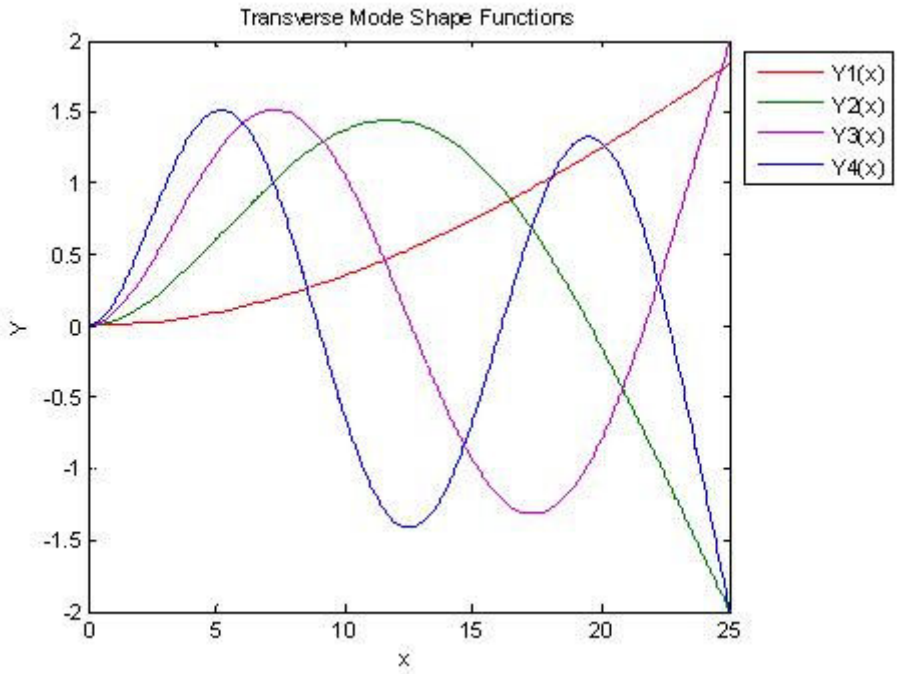

Figure 3.6 Transverse Mode Shape Functions

The shape functions are also called eigen functions, mode shapes or normal modes. The motion at any time history that the beam executes, from its initial condition, is a linear combination of the mode shapes oscillating at their respective natural frequencies. Another important fact about these mode shapes is that they are orthogonal.

$$\int_0^L Y_n(x)Y_m(x)dx = 0, \quad n \neq m \tag{3.17}$$

If we multiply by ρA :

$$\int_0^L \rho A Y_n(x)Y_m(x)dx = 0, \quad n \neq m \tag{3.18}$$

The solution has the form:

$$w(x,t) = \sum_{n=0}^{\infty} Y_n(x)\eta_n(t) \tag{3.19}$$

If equation 3.19 is substituted in equation 3.3 and by using the orthogonality property of the shape functions multiply the equation by Y_n:

$$\left(\int_0^L \rho A Y_n^2 dx\right)\ddot{\eta}_n + \left(\int_0^L Y_n EI \frac{d^4Y}{dx^4} dx\right)\eta_n = F(t)Y_n(L) \tag{3.20}$$

If we substitute equation 3.10 into 3.20:

$$\left(\int_0^L \rho A Y_n^2 dx\right)\ddot{\eta}_n + \left(\int_0^L \rho A Y_n^2 dx\right)\omega_n^2\eta_n = F(t)Y_n(L) \tag{3.21}$$

We can rewrite equation 3.21 more simply as:

$$m_n\ddot{\eta}_n + k_n\eta_n = F(t)Y_n(L) \tag{3.22}$$

m_n is the modal mass which is:

$$m_n = \int_0^L \rho A Y_n^2 dx \tag{3.23}$$

k_n is the modal stiffness which is:

$$k_n = m_n\omega_n^2 \tag{3.24}$$

We can add some damping to the system because typically structures are lightly damped [32]. So 3.22 equation can be written as:

$$m_n\ddot{\eta}_n + R_n\dot{\eta}_n + k_n\eta_n = F(t)Y_n(L) \tag{3.25}$$

R_n is the modal damp which is:

$$R_n = 2m_n\zeta\omega_n \tag{3.26}$$

ζ is the damping mode ratio and for lightly damped systems it is in the range of 0.01-0.1.

$$\left(\int_0^L \rho A Y_n^2 dx\right)\ddot{\eta}_n + 2\left(\int_0^L \rho A Y_n^2 dx\right)\zeta\omega_n\dot{\eta}_n + \left(\int_0^L \rho A Y_n^2 dx\right)\omega_n^2\eta_n = F(t)Y_n(L) \tag{3.27}$$

Kinematics for Transverse Motion of the Beams:

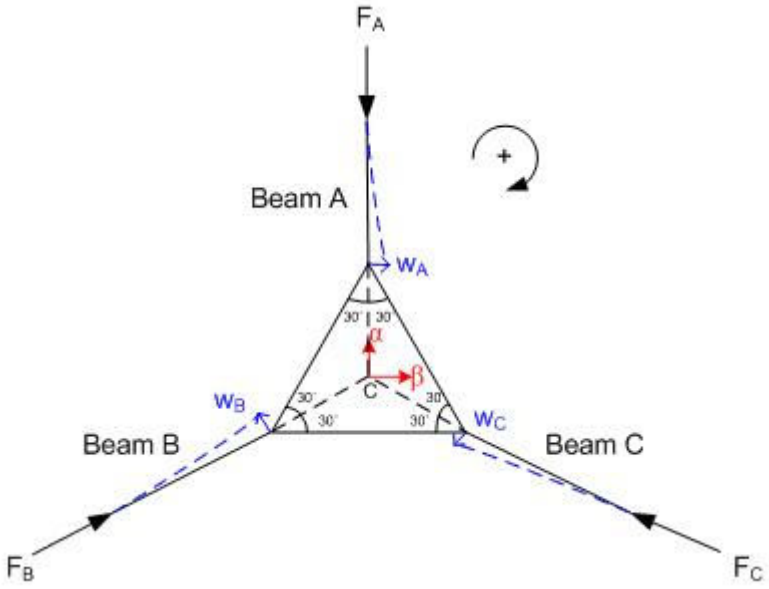

Figure 3.7 Kinematics of transverse motion

The transverse motion of the beams are showed in Figure 3-7.By looking at the figure and if the clock wise direction is set to be positive direction, the relationship between the transverse deflection of the beams and the x_α and x_β which are the coordinates of the center of the equilateral triangle can be calculated as follows:

$$x_\alpha = w_B \sin 60 - w_C \sin 60 \tag{3.28}$$

$$x_\beta = w_A - w_B \cos 60 - w_C \cos 60 \tag{3.29}$$

We can write a transformation matrix between the transverse deflections and the center coordinates by using equations 3.28 and 3.29.

$$\begin{bmatrix} 0 & \sin 60 & -\sin 60 \\ 1 & -\cos 60 & -\cos 60 \end{bmatrix} \cdot \begin{bmatrix} w_A \\ w_B \\ w_C \end{bmatrix} = \begin{bmatrix} x_\alpha \\ x_\beta \end{bmatrix} \tag{3.30}$$

$$T_T = \begin{bmatrix} 0 & \sin 60 & -\sin 60 \\ 1 & -\cos 60 & -\cos 60 \end{bmatrix} \tag{3.31}$$

3.2.2 Longitudinal Dynamics

The forces that act on the mechanism also cause longitudinal deflections. We can assume that we have three bars that have flexibility in longitudinal direction and they are connected to the edges of a triangular stage. The components of these forces that cause longitudinal motion for the bars can be seen in Figures 3-8, 3-9 and 3-10.

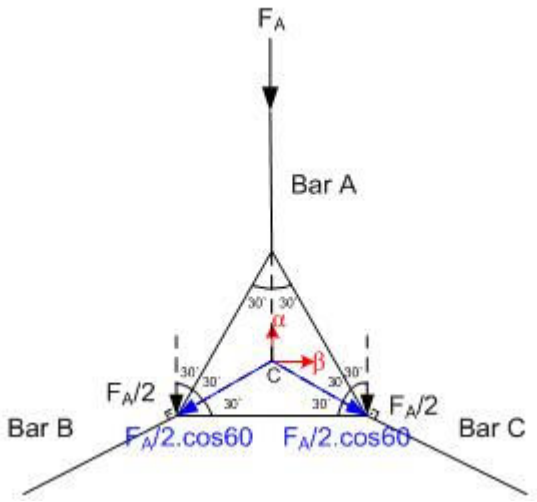

Figure 3.8 The Longitudinal forces produced by F_A

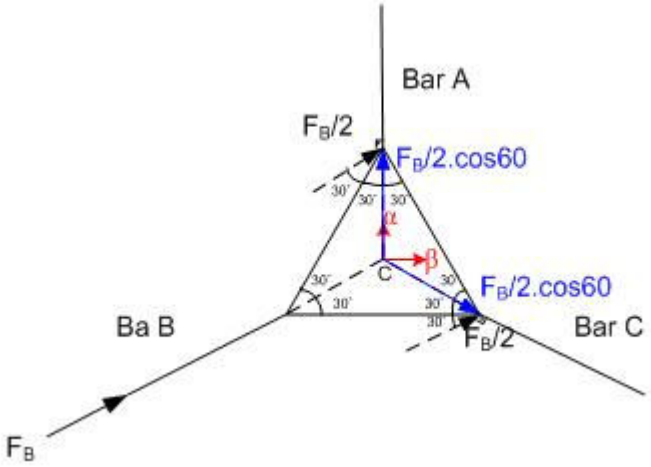

Figure 3.9 The Longitudinal forces produced by F_B

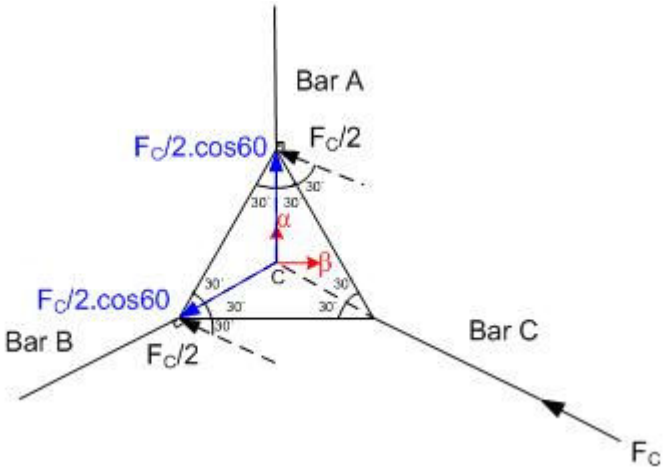

Figure 3.10 The Longitudinal forces produced by F_C

We can also assume as the transverse dynamics that we have three separate fixed free bars shown in Figure 3-11 which are under longitudinal forces.

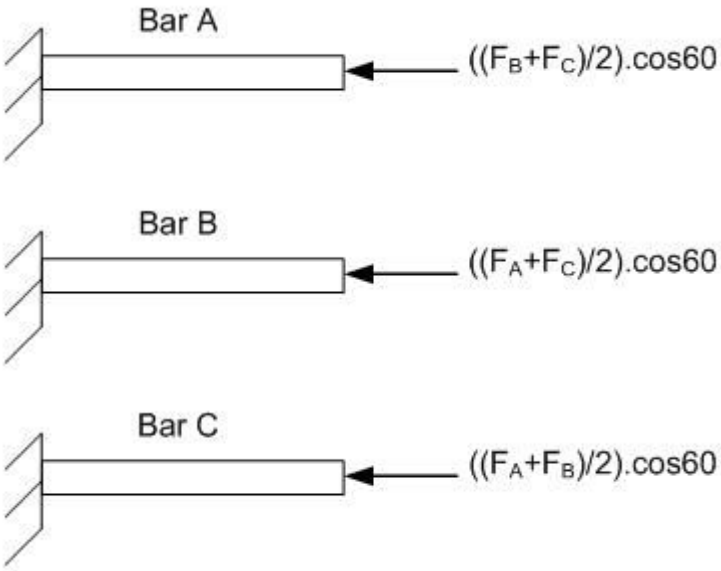

Figure 3.11 The longitudinal forces acting on the beams

The transformation matrix between the actuating forces and the longitudinal forces to the beams are;

$$\frac{1}{2}\begin{bmatrix} 0 & \cos 60 & \cos 60 \\ \cos 60 & 0 & \cos 60 \\ \cos 60 & \cos 60 & 0 \end{bmatrix} \cdot \begin{bmatrix} F_A \\ F_B \\ F_C \end{bmatrix} = \begin{bmatrix} F_{1l} \\ F_{2l} \\ F_{3l} \end{bmatrix} \tag{3.32}$$

$$T_{forcelongitudinal=}\frac{1}{2}\begin{bmatrix} 0 & \cos 60 & \cos 60 \\ \cos 60 & 0 & \cos 60 \\ \cos 60 & \cos 60 & 0 \end{bmatrix} \tag{3.33}$$

The dynamic equation for longitudinal forced bar is in equation 3.34

$$\rho\frac{\partial^2\xi}{\partial t^2}-E\frac{\partial^2\xi}{\partial x^2}=\frac{F(t)}{A}\delta\left(x-L\right) \tag{3.34}$$

$\xi(x,t)$ is the longitudinal motion of the bar which is depend on both the displacement and time. It can be separated into a product of a function of x only Y(x) and a function of time only f(t) that we have done in transverse dynamics.

$$\xi(x,t)=Y(x)\cdot f(t) \tag{3.35}$$

If we substitute equation 3.35 into 3.34 we will get:

$$\rho Y\frac{d^2f}{dt^2}-Ef\frac{d^2Y}{dx^2}=0 \tag{3.36}$$

If we divide equation 3.38 by ρYf :

$$\frac{1}{f}\frac{d^2f}{dt^2}=\frac{E}{\rho}\frac{1}{Y}\frac{d^2Y}{dx^2} \tag{3.37}$$

In equation 3.37 the terms on the left depends on only time and the terms on the right depends on only displacement x. These two terms must be equal to the same constant. So if we say:

$$\frac{1}{f}\frac{d^2f}{dt^2}=-\omega^2 \tag{3.38}$$

$$\frac{d^2f}{dt^2}+\omega^2f=0 \tag{3.49}$$

$$\frac{d^2Y}{dx^2}+\frac{\rho}{E}\omega^2Y=0 \tag{3.40}$$

We can rewrite equation 3.40 as:

$$\frac{d^2Y}{dx^2}+k^2Y=0 \tag{3.41}$$

$$k^2=\frac{\rho}{E}\omega^2 \tag{3.42}$$

If we solve the differential equation 3.41 the general solution is:

$$Y(x)=A\cos kx+B\sin kx \tag{3.43}$$

The boundary conditions for the fixed-free bar are:

The displacement at x=0 is zero because it is fixed so;

$$\begin{aligned} &\xi(0,t) = Y(0) f(t) = 0 \\ &Y(0) = 0 \end{aligned} \tag{3.44}$$

The force is applied at a small distance upstream of the free end so there must be no stress on the free end;

$$\sigma(L,t) = E\frac{\partial \xi}{\partial x}(L,t) = 0 \tag{3.45}$$

$$\begin{aligned} &\frac{\partial \xi}{\partial x}(L,t) = \frac{dY}{dx}(L)\cdot f(t) = 0 \\ &\frac{dY}{dx}(L) = 0 \end{aligned} \tag{3.46}$$

If we use the boundary conditions for the solution of the general solution 3.43 we will find;

$$A = 0 \tag{3.47}$$

$$Bk\cos kL = 0 \tag{3.48}$$

If B or k is zero then Y(x)=0 and ξ(x,t)=0 which is not possible so;

$$\cos kL = 0 \tag{3.49}$$

3.49 is possible when;

$$k_n L = (2n-1)\frac{\pi}{2}, \quad n = 1,2,3,... \tag{3.50}$$

From Eq. 3.42;

$$\omega_n^2 = \frac{E}{\rho}k_n^2 = \frac{E}{\rho}\frac{(k_n L)^2}{L^2} \tag{3.51}$$

$$\omega_n = \sqrt{\frac{E}{\rho}}\frac{(2n-1)}{L}\frac{\pi}{2}, \quad n = 1,2,3,... \tag{3.52}$$

Each ω_n creates a special shape function by using Eq.3.51

$$Y_n(x) = B_n \sin\left(k_n L\frac{x}{L}\right) = B_n \sin\left((2n-1)\frac{\pi}{2}\frac{x}{L}\right), \quad n = 1,2,3,... \tag{3.53}$$

B_n is an arbitrary constant and it is convenient to take them as 1. In Figure 3-12 the longitudinal shape functions is shown for 4 modes.

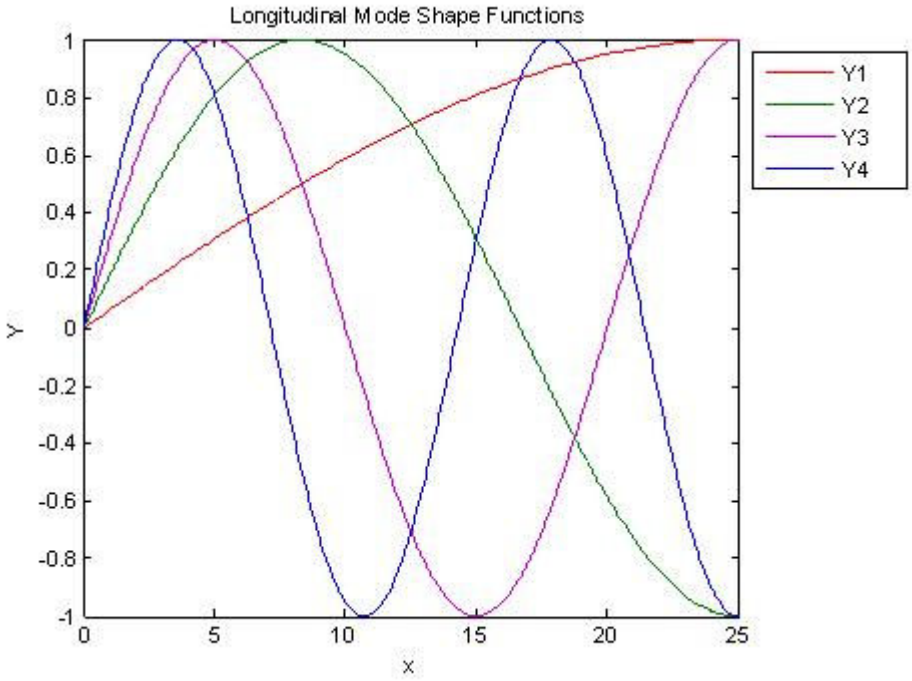

Figure 3.12 Longitudinal Mode Shape Functions

If we use the being orthogonal of the shape functions with each other as we have used before in transverse dynamics, we will get the combination of mode shapes as:

$$\int_0^L Y_n(x)Y_m(x)dx = 0, \quad n \neq m \tag{3.54}$$

The response of the bar can be expressed as linear combinations of mode shapes. So, if we use eq.3.34 and add each mode shapes to another we can express the longitudinal motion.

$$\xi(x,t) = \sum_{n=1}^{\infty} Y_n(x)\mu_n(t) \tag{3.55}$$

We can use eq. 3.54 in eq.3.34

$$\sum_{n=1}^{\infty} \rho A Y_n \ddot{\mu}_n - \sum_{n=1}^{\infty} AE \frac{d^2 Y_n}{dx^2} \mu_n = F(t)\delta(x-L) \tag{3.56}$$

By multiplying each term by the mth mode shape and integrate term by term over the bar length, we get;

$$\sum_{n=1}^{\infty} \left(\int_0^L \rho A Y_n Y_m \right) \ddot{\mu}_n - \sum_{n=1}^{\infty} \left(\int_0^L AE \frac{d^2 Y_n}{dx^2} Y_m \right) \mu_n = \int_0^L F(t)\delta(x-L)Y_m dx \tag{3.57}$$

If we rearrange equation 3.40;

$$\frac{d^2Y_n}{dx^2} = -\frac{\rho}{E}\omega_n^2 Y_n \tag{3.58}$$

If we substitute 3.58 into 3.67

$$\sum_{n=1}^{\infty}\left(\int_0^L \rho A Y_n Y_m\right)\ddot{\mu}_n - \sum_{n=1}^{\infty}\left(\int_0^L \rho A Y_n Y_m\right)\omega_n^2\mu_n = \int_0^L F(t)\delta(x-L)Y_m dx \tag{3.59}$$

The mode shapes are orthogonal to each other so the multiplication of the mode shapes is zero except n=m, shown as in equation 3.56 we will find the general longitudinal bar dynamic equation as:

$$\left(\int_0^L \rho A Y_m^2 dx\right)\ddot{\mu}_m + \left(\int_0^L \rho A Y_m^2 dx\right)\omega_m^2\mu_m = \int_0^L F(t)\delta(x-L)Y_m dx \tag{3.60}$$

At x=L the right side of the equation 3.60 will be simplified as:

$$\int_0^L F(t)\delta(x-L)Y_m(x)dx = F(t)Y_m(L)\int_0^L \delta(x-L)dx = F(t)Y_m(L) \tag{3.61}$$

We can write the dynamic equation with a simpler way:

$$m_m\ddot{\mu}_m + k_m\mu_m = F(t)Y_m(L) \tag{3.62}$$

m_m is the modal mass:

$$m_m = \int_0^L \rho A Y_m^2 dx \tag{3.63}$$

k_m is the modal stiffness:

$$k_m = m_m\omega_m^2 \tag{3.64}$$

We can add damping affect as we did in transverse dynamics:

$$m_m\ddot{\mu}_m + R_m\dot{\mu}_m + k_m\mu_m = F(t)Y_m(L) \tag{3.65}$$

R_m is the modal damp which equals:

$$R_m = 2m_m\zeta\omega_m \tag{3.66}$$

ζ is the damping mode ratio in the range of 0.01-0.1 for lightly damped systems. [31]

Kinematics for Longitudinal Motion of the Beams:

The longitudinal motion of the bars are showed in Figure 3-13

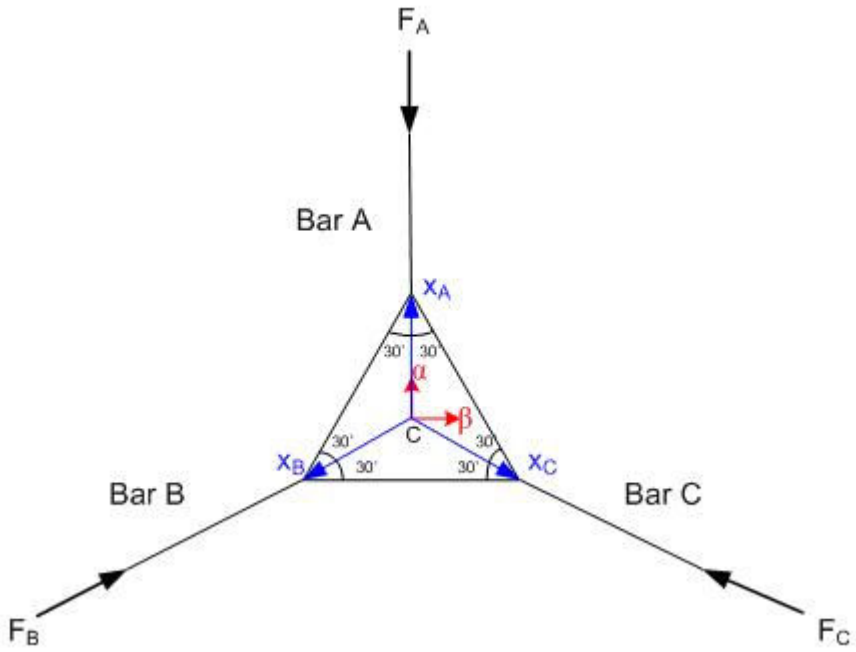

Figure 3.13 Knematics of Longitudinal motion

The center coordinates of the equilateral triangle x_α and x_β can be written in terms of the longitudinal deflections as follows:

$$x_\alpha = x_A - x_B \sin 30 - x_C \sin 30 \tag{3.67}$$

$$x_\beta = -x_B \cos 30 + x_C \cos 30 \tag{3.68}$$

We can write a transformation matrix between the longitudinal deflections and the center coordinates by using equations 3.67 and 3.68

$$\begin{bmatrix} 1 & -\sin 30 & -\sin 30 \\ 0 & -\cos 30 & \cos 30 \end{bmatrix} \cdot \begin{bmatrix} x_A \\ x_B \\ x_C \end{bmatrix} = \begin{bmatrix} x_\alpha \\ x_\beta \end{bmatrix} \tag{3.69}$$

$$T_L = \begin{bmatrix} 1 & -\sin 30 & -\sin 30 \\ 0 & -\cos 30 & \cos 30 \end{bmatrix} \tag{3.70}$$

3.3 Open Loop Simulation

The open loop simulation purpose is to calculate the central positions x_α and x_β for the given F_A, F_B and F_C forces. Firstly, by using transformation matrices F_A, F_B and F_C forces are converted to transverse and longitudinal forces for the beams and bars that are assumed to be as we have explained before. Secondly, the transverse and longitudinal deflections are calculated by using the beams and bars dynamics. Finally, these deflections are converted to x_α and x_β by using the necessary transformation matrices that are calculated before. In Figure 3.14 the schematic representation of the open loop simulation is presented.

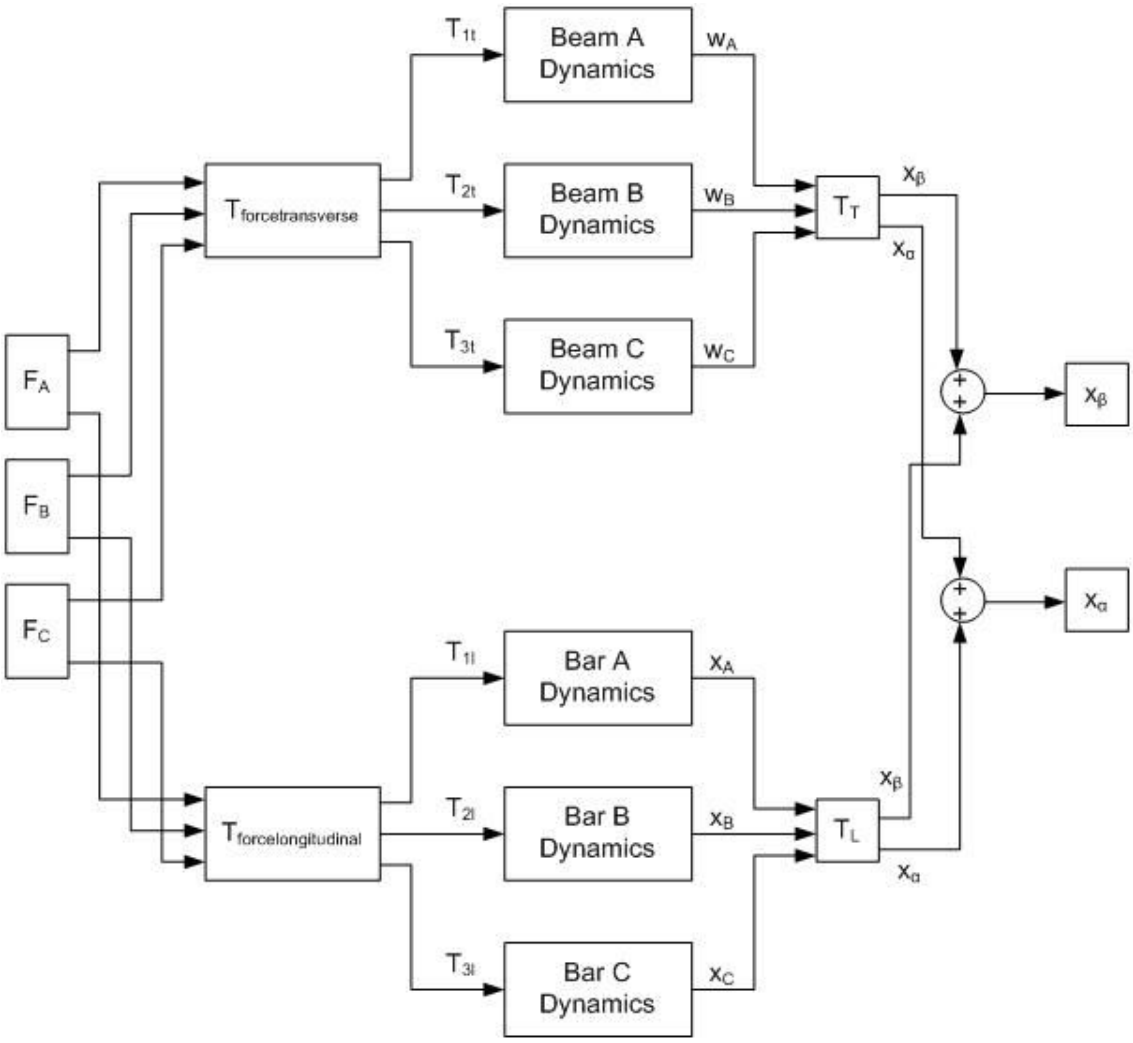

Figure 3.14 Open Loop Block Diagram

3.3.1 State Space Representation

The state space representation of the transverse and longitudinal dynamics is calculated as follows:

The transverse dynamics is derived as;

$$m_n\ddot{\eta}_n + R_n\dot{\eta}_n + k_n\eta_n = F(t)Y_n(L) \tag{3.72}$$

n is the mode number, if 4 modes is selected, then we will have 4 second order differential equations and the transverse deflection will be the sum of the multiplication of η_n and the nth shape function as shown:

$$w(x,t) = \sum_{n=0}^{\infty} Y_n(x)\eta_n(t) \tag{3.73}$$

The states are selected as η_n and $\dot{\eta}_n$. If we say:

$$\dot{\eta}_{1n} = \eta_{2n} \tag{3.74}$$

$$\dot{\eta}_{2n} = \frac{Y_n(L)}{m_n}F(t) - \frac{R_n}{m_n}\eta_{2n} - \frac{k_n}{m_n}\eta_{1n} \tag{3.75}$$

The output will be the deflection at the tip of the beam so;

$$w = Y_n(L)\eta_{1n} \tag{3.76}$$

In the state space form:

$$\begin{bmatrix}\dot{\eta}_{1n}\\ \dot{\eta}_{2n}\end{bmatrix} = \begin{bmatrix}0 & 1\\ -\frac{k_n}{m_n} & -\frac{R_n}{m_n}\end{bmatrix}\cdot\begin{bmatrix}\eta_{1n}\\ \eta_{2n}\end{bmatrix} + \begin{bmatrix}0\\ \frac{Y_n(L)}{m_n}\end{bmatrix}\cdot F(t) \tag{3.77}$$

$$w = \begin{bmatrix}Y_n(L) & 0\end{bmatrix}\cdot\begin{bmatrix}\eta_{1n}\\ \eta_{2n}\end{bmatrix} + 0\cdot F(t) \tag{3.78}$$

So we have the state space equation of the transverse beam dynamics in the form:

$$\dot{x} = Ax + Bu \tag{3.79}$$

$$y = Cx + Du \tag{3.80}$$

We have said that we will use 4 modes for the simulation so the matrices will be:

$$A=\begin{bmatrix} 0 & 1 & 0 & 0 & 0 & 0 & 0 & 0 \\ -k_1/m_1 & -b_1/m_1 & 0 & 0 & 0 & 0 & 0 & 0 \\ 0 & 0 & 0 & 1 & 0 & 0 & 0 & 0 \\ 0 & 0 & -k_2/m_2 & -b_2/m_2 & 0 & 0 & 0 & 0 \\ 0 & 0 & 0 & 0 & 0 & 1 & 0 & 0 \\ 0 & 0 & 0 & 0 & -k_3/m_3 & -b_3/m_3 & 0 & 0 \\ 0 & 0 & 0 & 0 & 0 & 0 & 0 & 1 \\ 0 & 0 & 0 & 0 & 0 & 0 & -k_4/m_4 & -b_4/m_4 \end{bmatrix} \tag{3.81}$$

$$B=\begin{bmatrix} 0 \\ Y_1(L)/m_1 \\ 0 \\ Y_2(L)/m_2 \\ 0 \\ Y_3(L)/m_3 \\ 0 \\ Y_4(L)/m_4 \end{bmatrix} \tag{3.82}$$

$$C=\begin{bmatrix} Y_1(L) & 0 & Y_2(L) & 0 & Y_3(L) & 0 & Y_4(L) & 0 \end{bmatrix} \tag{3.83}$$

$$D=0 \tag{3.84}$$

The same procedure is done for the longitudinal dynamics. 4 modes are selected for the simulation. So, by using the longitudinal dynamics that we have calculated before, we have again 4 second order differential equation and the longitudinal deflection is the sum of the multiplication of μ_m and the mth shape function.

3.3.2 The Parameters of the Mechanism

The geometric parameters:

The cross-sectional area dimensions of our beams are:

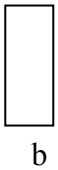

b = 0.8 mm

h = 2 mm

The length of the beams are 25 mm.

The cross sectional areas are A=bh=1.6mm^2

The inertias are: $I=bh^3/12=0.5333\ mm^4$

The material properties:

The compliant mechanism's material is selected as Aluminum which has properties as:

Elasticity modulus $E = 69000\ N/mm^2$

Density $\rho = 0.0027\ g/mm^3$

3.3.3 The Results

In Figure 3-15 there is the assumed mechanism which is simulated.

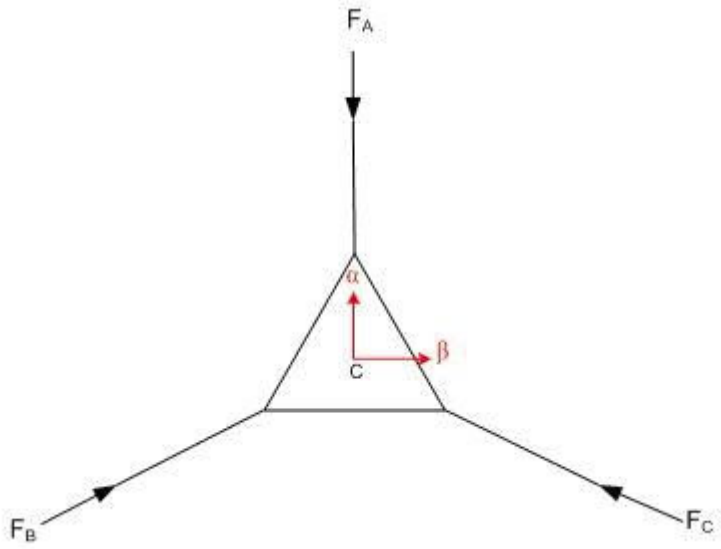

Figure 3.15 The Mechanism

Firstly only transverse and only longitudinal mathematical models are simulated. The results are shown in Table 3-1.It is seen that longitudinal dynamics have less affect on the mathematical model for the system.

Table 3-1 The displacement results of only transverse and only longitudinal modeling

Actuation	Transverse		Longitudinal	
	α	β	α	β
F_A=1N	-0.2388	0	-0.0002741	0
F_A=1N and F_B=1N	-0.1194	0.2068	-0.000137	0.0002373
F_B=1N and F_C=2N	0.3582	-0.2068	0.0004111	-0.0002373

The results for the mathematical model that have both transverse and longitudinal dynamics are shown as follows:

If F_A is given as 1N the center coordinates is expected to be changed only in $-\alpha$ direction. The result of the mathematical model is:

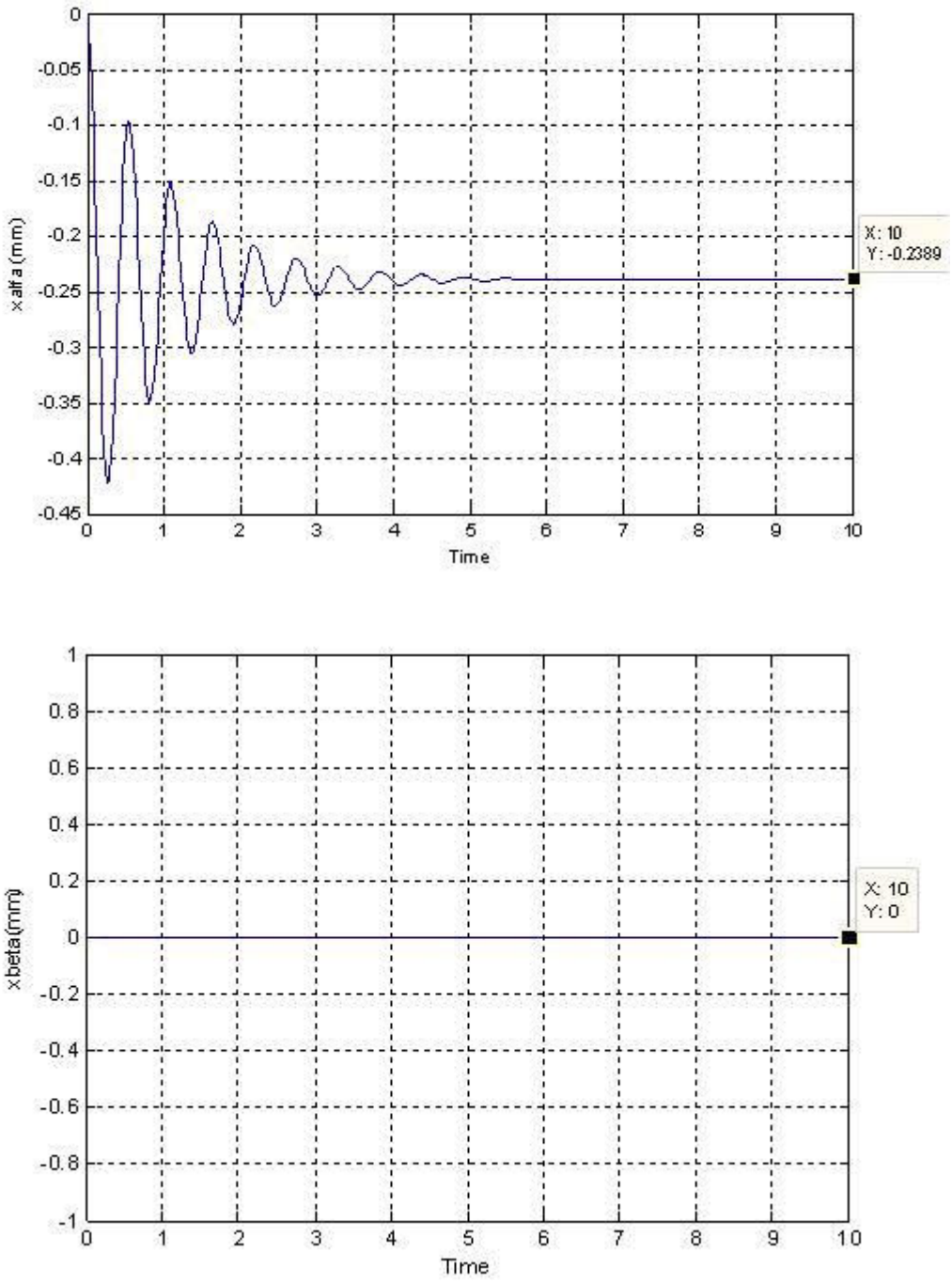

Figure 3.16 Results for F_A is 1N

As it is expected, the center coordinates have only changed in –α direction which is 0.2389mm.If F_B is given as 1N the center coordinates is expected to be changed in +α and +β direction. The result of the mathematical model is:

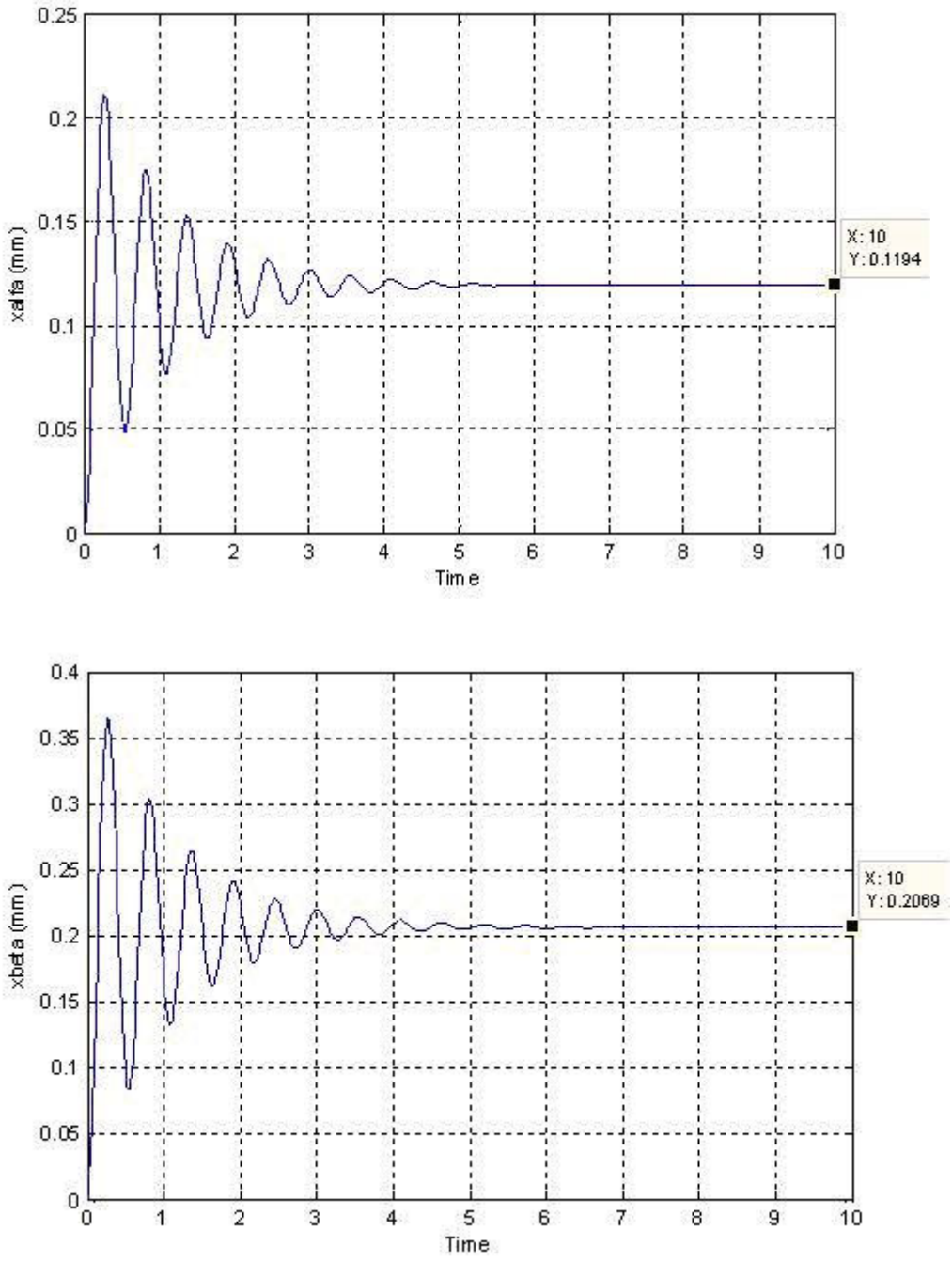

Figure 3.17 Results for F_B is 1N

As it is expected, the center coordinates have changed in +α direction which is 0.1194mm and in +β direction which is 0.2069mm.

If F_C is given as 1N the center coordinates is expected to be changed in +α and -β direction. The result of the mathematical model is:

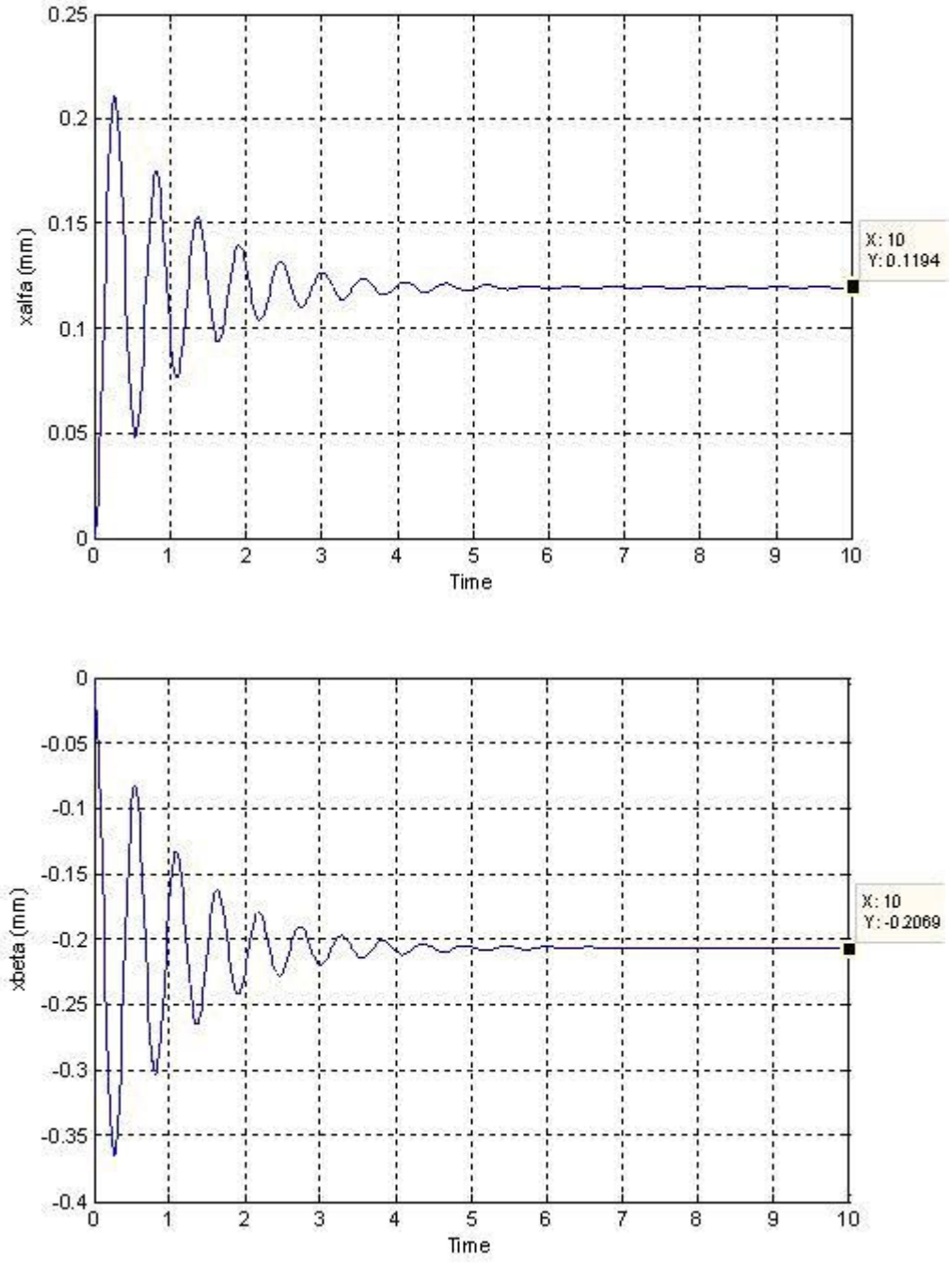

Figure 3.18 Results for F_C is 1N

As it is expected, the result is the sign change in β direction of the result of F_B is 1N. The center coordinates have changed in +α direction which is 0.1194mm and in -β direction which is 0.2069mm.

By using the geometric property of the forces the stage can also move only in –β or in + β direction. If F_B is given as 2N and F_A is given as 1N, it is expected that the triangular stage will move only in +β direction. Because α component of F_B is 1N and it will cancel F_A which is also 1N but in the opposite direction, only β component of F_B will remain. So the center coordinates is expected to be changed only in +β direction. The result of the mathematical model is:

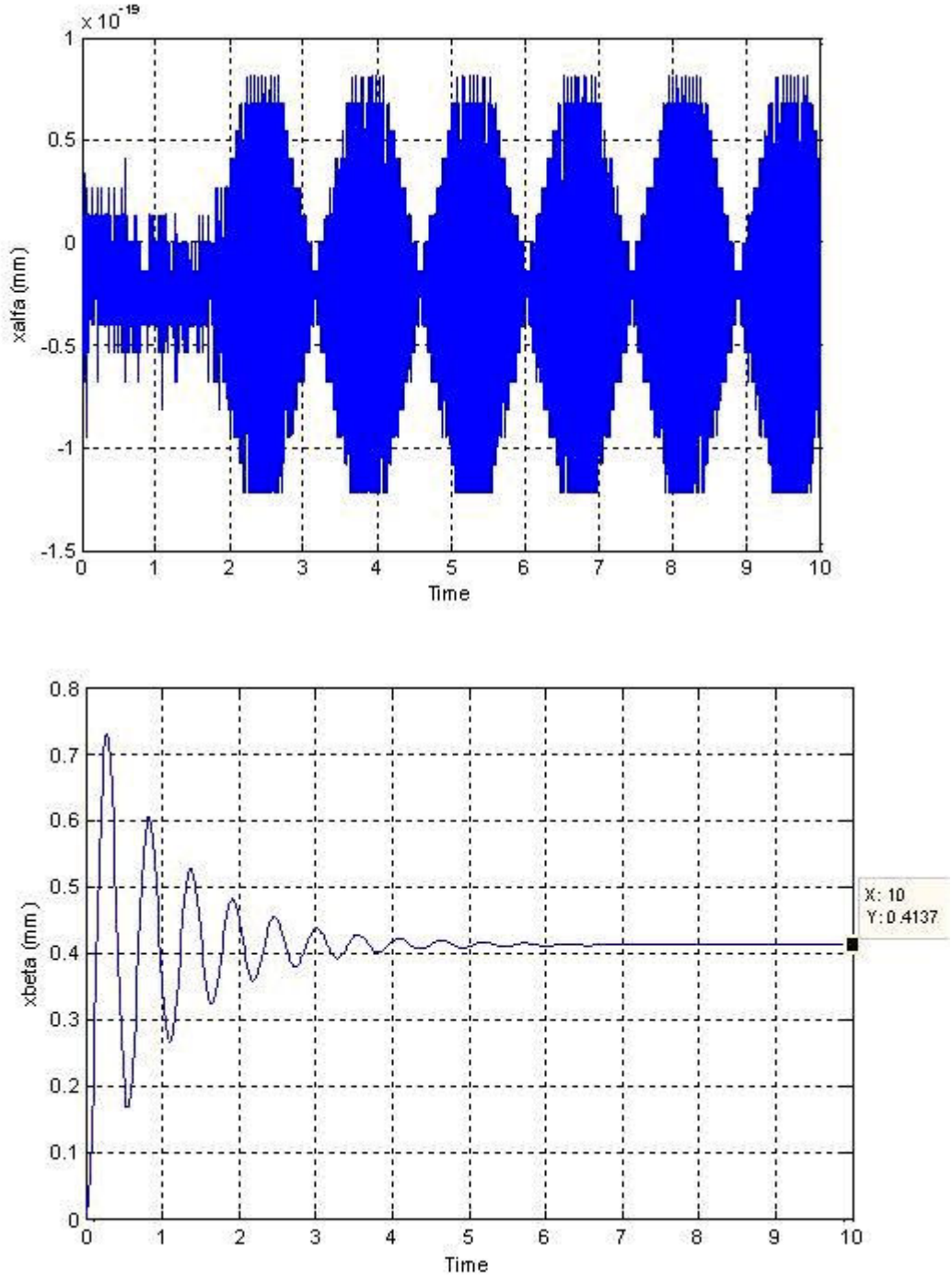

Figure 3.19 Results for F_A is 1N and F_B is 2N

The center coordinates have changed in +β direction which is 0.4137mm and there is a little error in α but it is in 10^{-19}mm range so it can be assumed that the stage does not move in α direction as it is expected.

If F_C is given as 2N and F_A is given as 1N, it is expected that the triangular stage will move only in -β direction. Because α component of F_C is 1N and it will cancel F_A which is also 1N but in the opposite direction, only β component of F_B will remain. So the center coordinates is expected to be changed only in -β direction. The result of the mathematical model is:

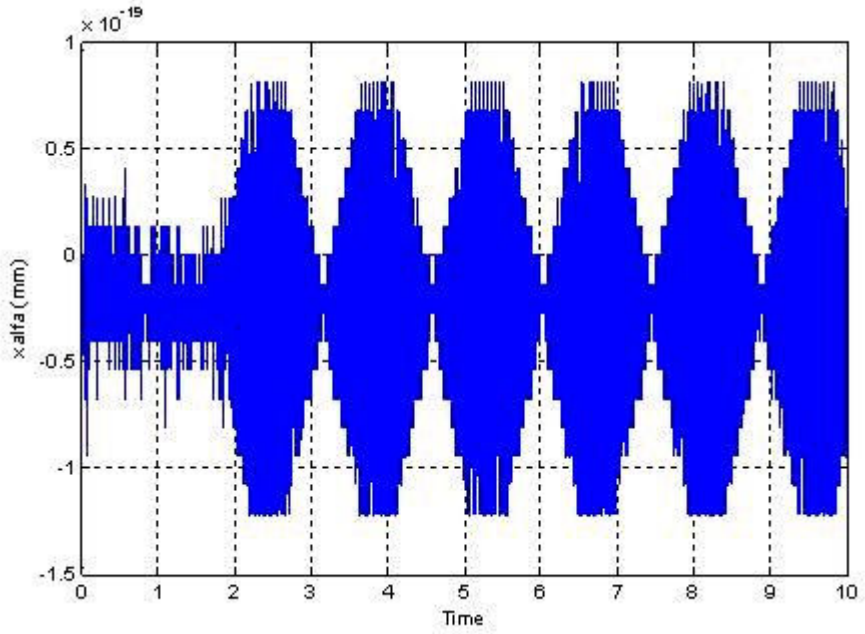

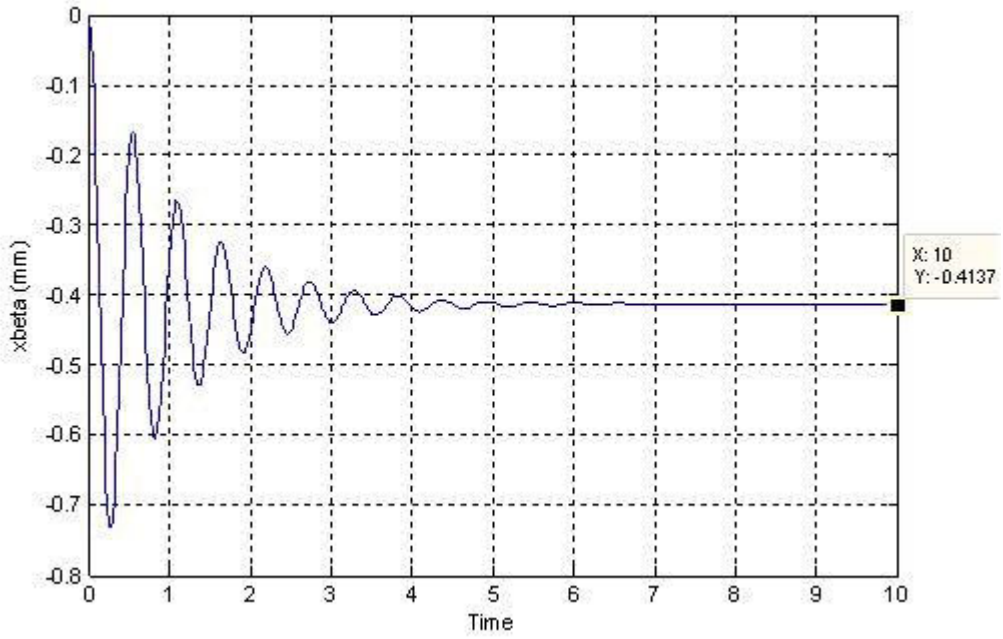

Figure 3.20 Results for F_A is 1N and F_C is 2N

The center coordinates have changed in -β direction which is -0.4137mm and there is a little error in α but it is in 10^{-19}mm range so it can be assumed that the stage does not move in α direction as it is expected.

3.3.4 Comparing the Results

The results of the dynamic simulation that are simulated in MATLAB is compared with COMET software which is developed by MIT laboratory for mapping the actuator-displacement behavior [32-33]. In Figure 3-21 the sketched mechanism in COMET is shown. The corresponding A, B and C beams of the mathematical model are also shown in the figure.

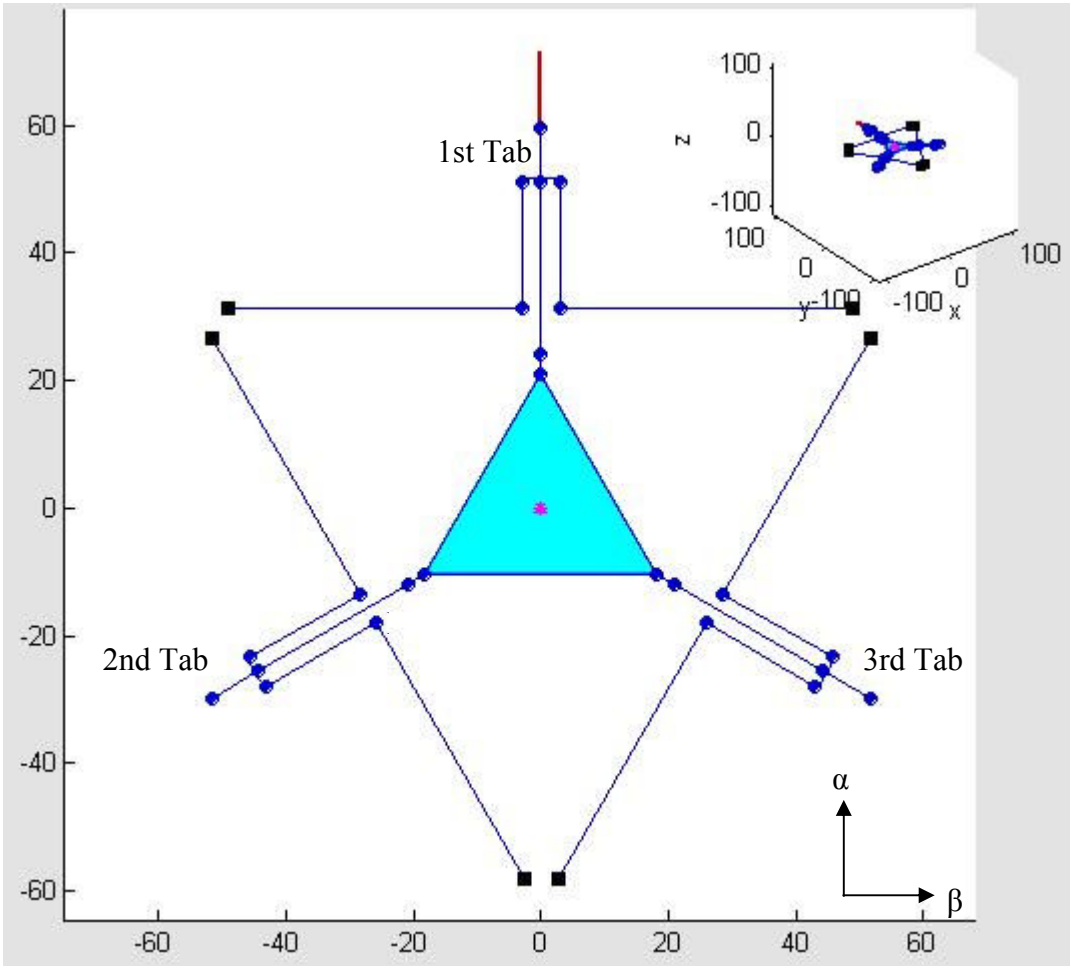

Figure 3.21Compliant mechanism drawn in COMET

Firstly the corresponding force in the mathematical model simulation that is done is found by giving 1N in –α direction to the 1st tab where beam A is connected. The transverse forces on the beams B and C are found as 0.315N in –direction so F_A should be 0.630N for the simulation that we have done. So we can say that if we apply force to any of the tabs of the mechanism, the corresponding F_A, F_B and F_C forces in the simulation that we have done will be 0.630 times of the force applied.

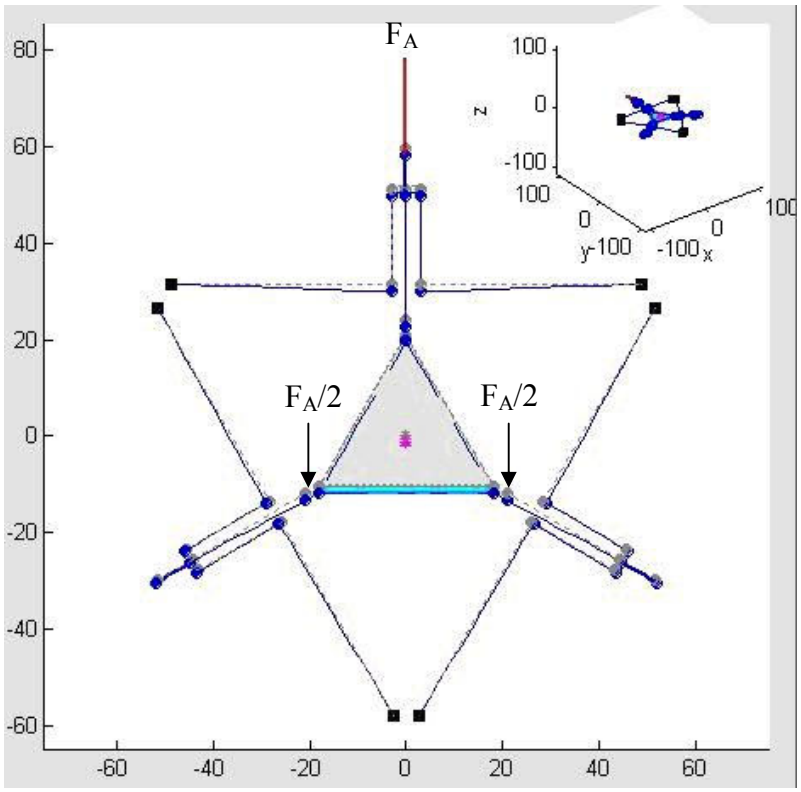

Figure 3.22 The Forces

The compared results of some forces that is applied to the mechanism is shown in Table 3-2. x_α and x_β are the displacements of the center of the mechanism.

Table 3-2 Comparing Matlab simulation and COMET

Actuation	Matlab Simulation		COMET		Error %	
	x_α (mm)	x_β (mm)	x_α (mm)	x_β (mm)	%ex $_\alpha$	%ex $_\beta$
1st Tab - 1N	-0.1505	0	-0.134	-1.156e-006	%12.31	-
2nd Tab - 1N	0.07525	0.1303	0.06678	0.14	%12.68	%6.928
1st Tab - 2N 3rd Tab - 2N	-0.1505	-0.2607	-0.133	-0.28	%13.157	%6.89
1st Tab - 3N 2nd Tab - 1N	-0.301	0.2607	-0.267	0.28	%12.73	%6.89
2nd Tab - 1N 3rd Tab - 2N	0.2257	-0.1303	0.2	-0.14	%12.85	%6.928
1st Tab - 1N 2nd Tab - 1N 3rd Tab - 2N	-0.07425	-0.1303	0.06682	-0.14	%11.119	%6.928

By looking at Table 3-2 we can say that our mathematical model has % 12.8 error in α position and %6.9 error in β position. The mathematical model can be used for simulating the dynamics of the mechanism.

4 CONTROL OF COMPLIANT MECHANISM

In this section, the position control of Hexflex mechanism is simulated by using the mathematical model of the mechanism which is done in the previous section. The main purpose of the control is shown in Figure 4-1. Simple PID control is used to give the desired forces which correspond to the desired center coordinates of the stage.

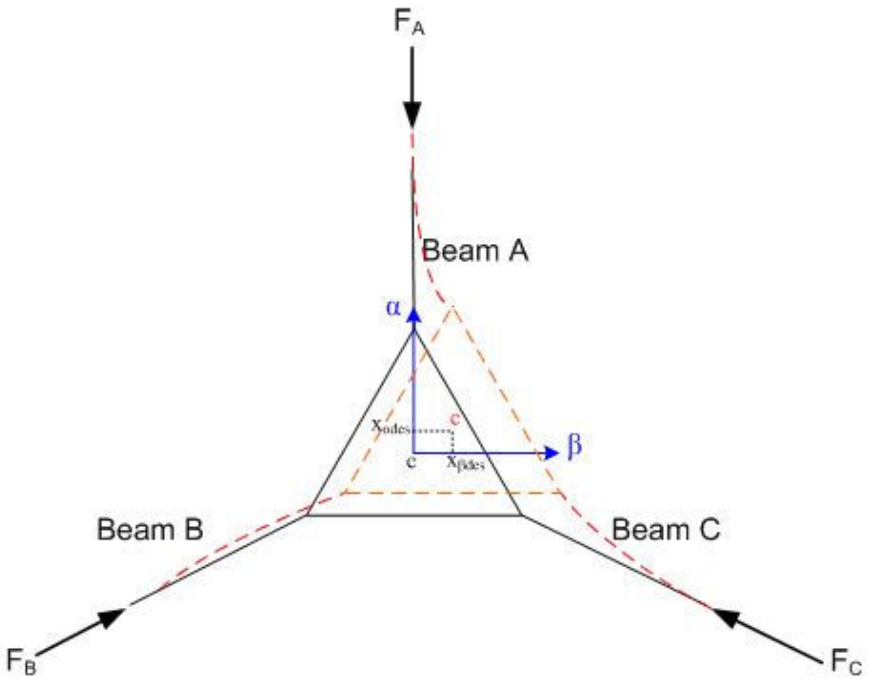

Figure 4.1 The desired displacements of the triangular stage

4.1 The Control Model

Basically, the position control model of the mechanism can be represented as the Figure 4-2.

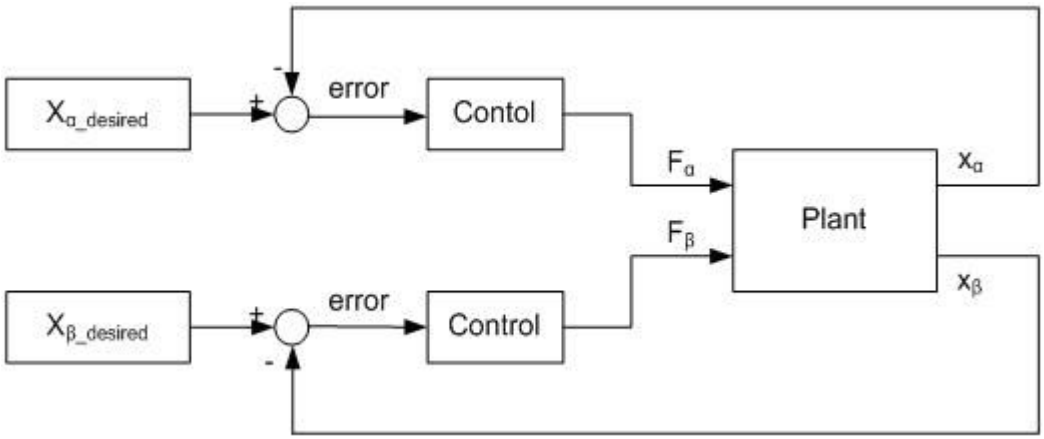

Figure 4.2 The main control block diagram

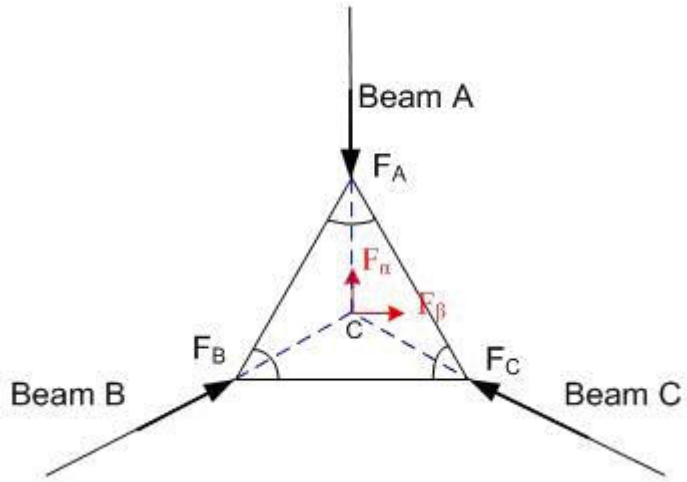

Figure 4.3 The Forces acting on the mechanism

The control inputs are the errors of the positions and the outputs of the controls are the forces. The plant is composed of the dynamics of the beams that we have calculated in Chapter 3. But the model has F_A, F_B and F_C as inputs and x_α and x_β as outputs. For simplicity of the simulation the plant is reduced to two input and two output plant. The inputs of the plant are written in α and β coordinates of the mechanism. By looking at Figure 4-2 F_α , F_β can be written in terms of F_A, F_B and F_C as:

$$F_\alpha = -F_A + \sin 30 F_B + \sin 30 F_C \tag{4.1}$$

$$F_\beta = \cos 30 F_B - \cos 30 F_C \tag{4.2}$$

The transformation matrix between F_α , F_β and F_A, F_B , F_C will be a 2x3 matrix so the matrix is not invertible. F_0 force is added to F_α , F_β forces and the matrix is turned into 3x3 matrix and the transfer matrix transpose should be equal to the inverse of the transfer matrix. F_0 is taken as 0. The transfer matrix is found in the following equations:

$$K\begin{bmatrix} -1 & \sin 30 & \sin 30 \\ 0 & \cos 30 & -\cos 30 \\ b & b & b \end{bmatrix} \cdot \begin{bmatrix} F_A \\ F_B \\ F_C \end{bmatrix} = \begin{bmatrix} F_\alpha \\ F_\beta \\ F_0 \end{bmatrix} \tag{4.3}$$

$$\text{Transformation matrix } A_{\alpha\beta 0}^{ABC} = K\begin{bmatrix} -1 & \sin 30 & \sin 30 \\ 0 & \cos 30 & -\cos 30 \\ b & b & b \end{bmatrix} \tag{4.4}$$

$$A_{\alpha\beta 0}^{ABC} \cdot A_{\alpha\beta 0}^{ABC^T} = \mathrm{I} \tag{4.5}$$

If we use equations 4.3 and 4.5 we can find the constants K and b as:

$\mathrm{K} = \sqrt{3}/2, \quad \mathrm{b} = \sqrt{2}/2$

By using the inverse of the transformation matrix, $A_{\alpha\beta 0}^{ABC}$, F_α and F_β forces can be converted into F_A, F_B and F_C forces so the beam dynamics that is calculated in Chapter 3 can be used easily.

4.2 Simulation and Results

The position control of the mechanism is simulated in MATLAB Simulink. The plant is turned into 2 input 2 output block by using the transformation matrix $A_{\alpha\beta 0}^{ABC}$. Firstly, a desired position of the center of the mechanism is given by using step block. Secondly, a circular path is generated for the desired motion of the center of the mechanism. The parameters that are used in simulation is the same as the parameters of the open loop simulation that is presented in Chapter 3.

The desired position of center coordinates of the mechanism is given as 10μm in –α coordinate and 20μm in β coordinate. PID control is used for control. The parameters of the PID control are taken as K_P: 1200, K_I: 46 and K_D: 100. The results are:

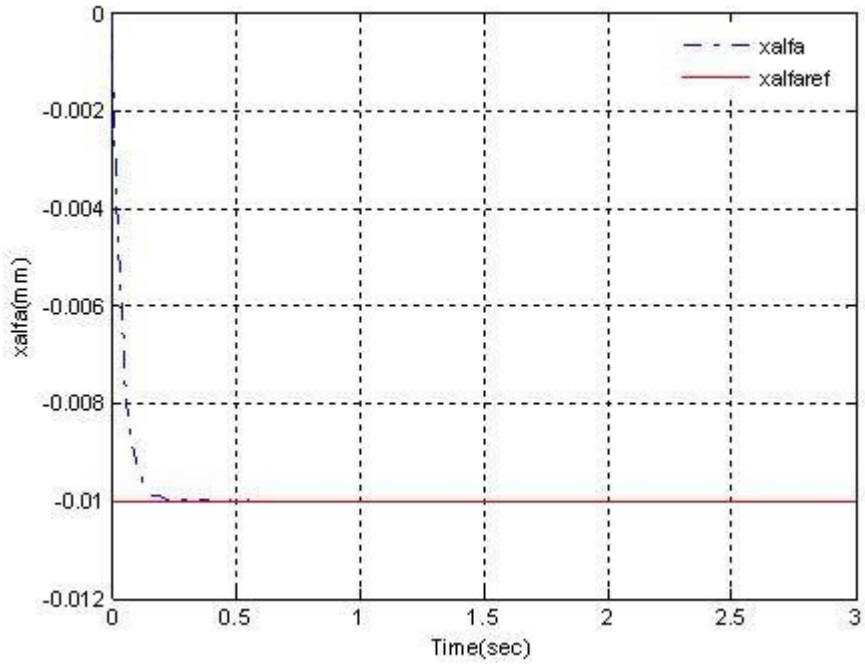

Figure 4.4 The plot of x_{α} and $x_{\alpha ref}$

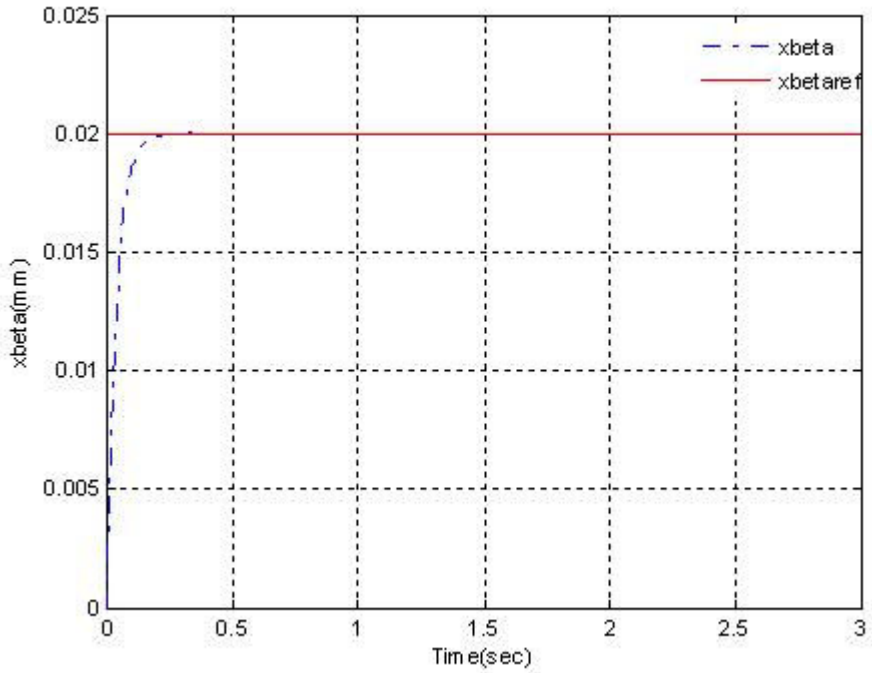

Figure 4.5 The plot of x_{β} and $x_{\beta ref}$

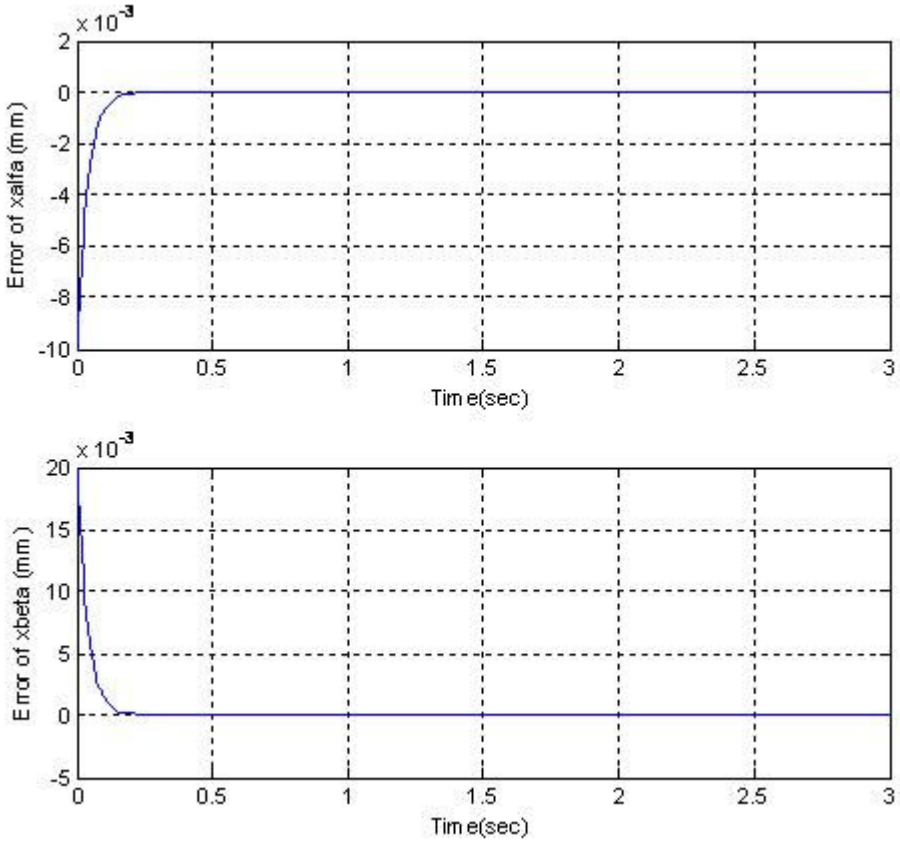

Figure 4.6 The plot of errors of x_α and x_β

As seen from the results, the center of the mechanism is coming to the desired position by using PID control.

Secondly, a circular path having 100μm diameter is generated by giving the desired positions as $x_{\alpha ref} = 0.1\sin(\pi t)$ and $x_{\beta ref} = 0.1\sin(\pi t + \pi/2) = 0.1\cos(\pi t)$. PD control is used and the parameters of the control are set as K_P: 2000 and K_D: 20. As seen from the results the center of the mechanism tracks the circular path. The results are:

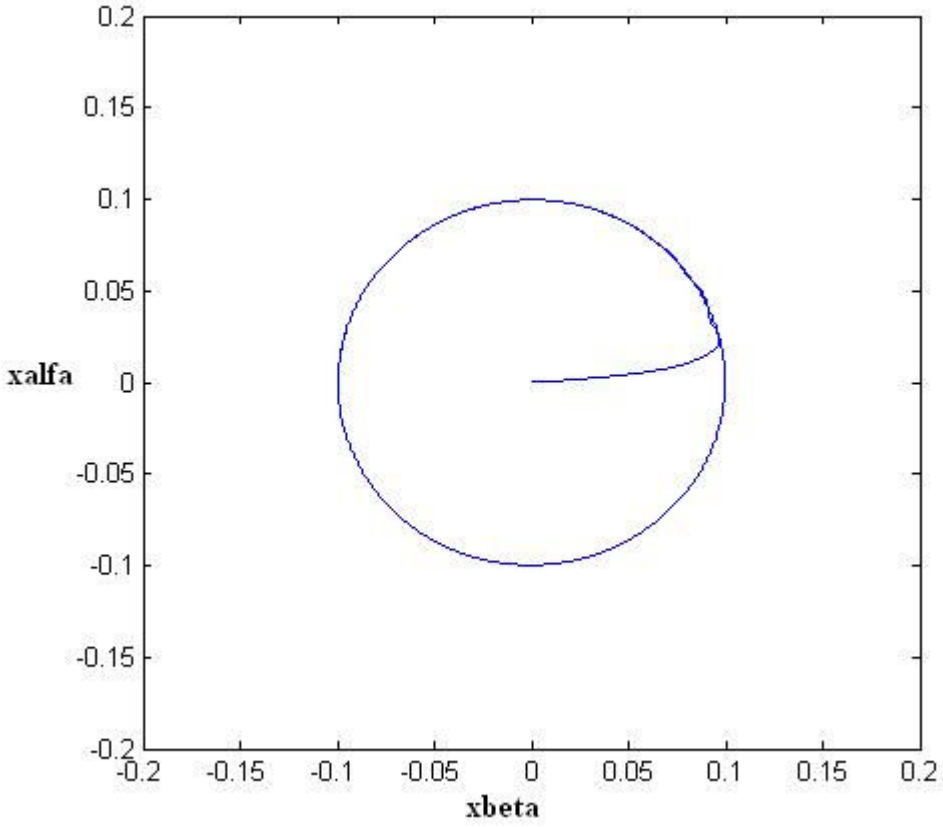

Figure 4.7 The center motion

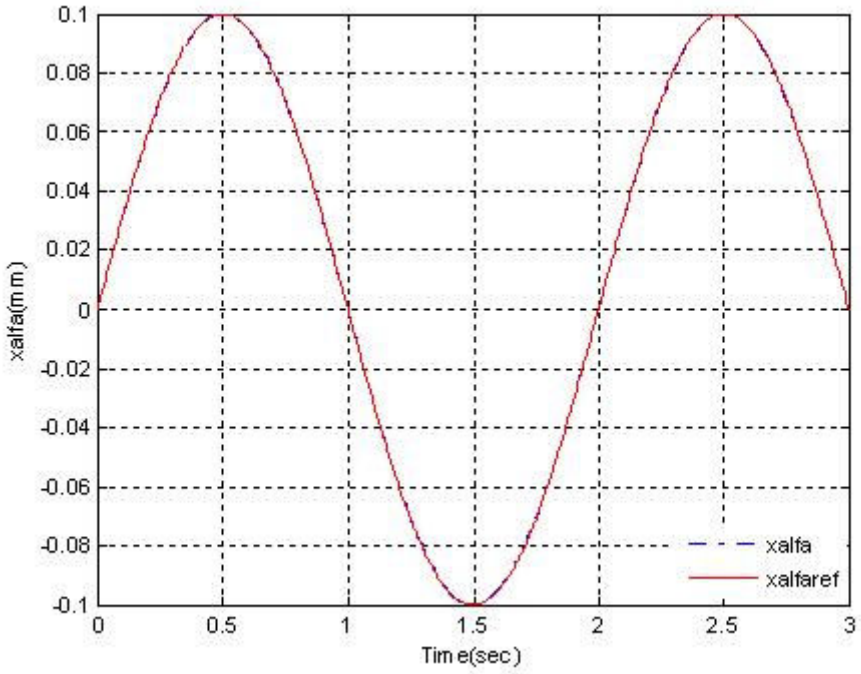

Figure 4.8 The plot of x_{α} and $x_{\alpha ref}$

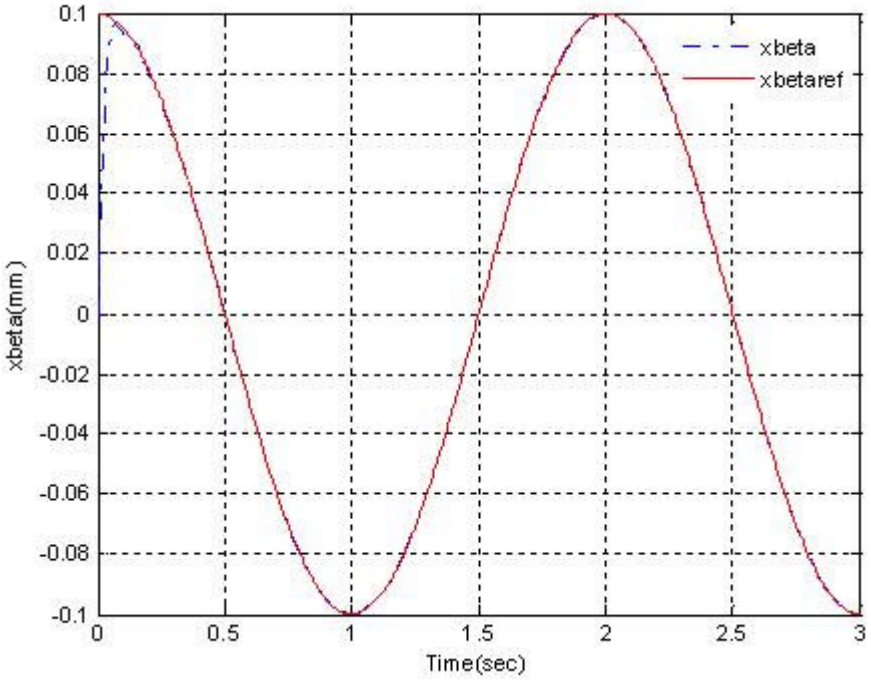

Figure 4.9 The plot of x_{β} and $x_{\beta ref}$

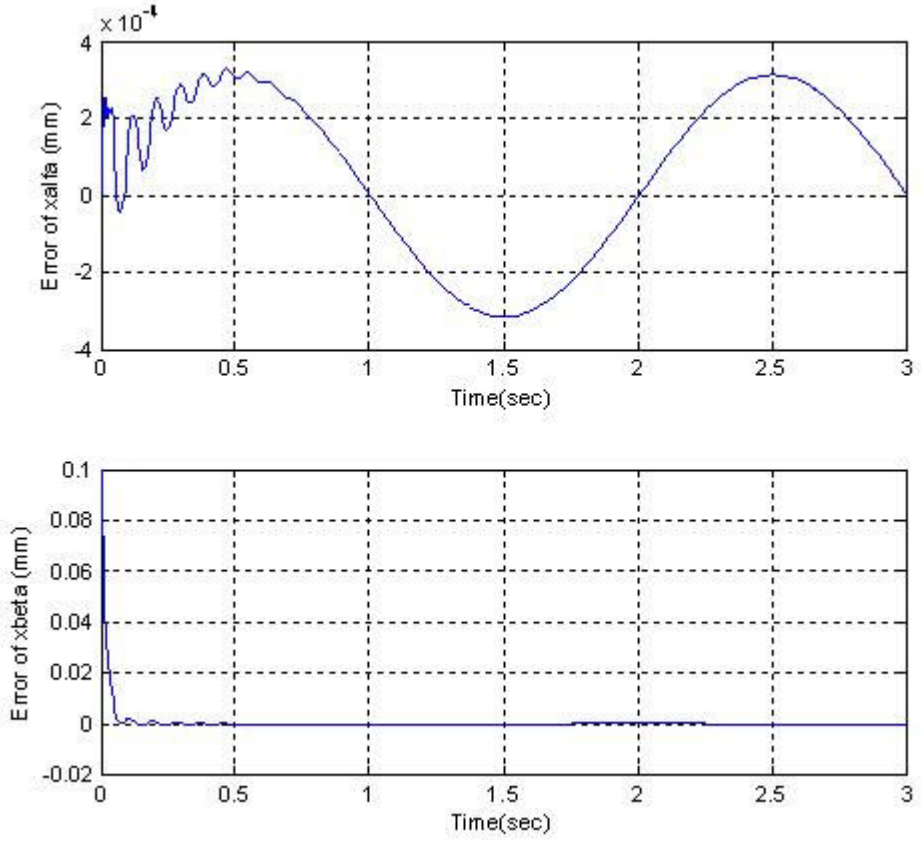

Figure 4.10 The plot of errors of x_{α} and x_{β}

5 MANUFACTURING AND EXPERIMENTS

In this chapter the manufacturing processes of the compliant mechanism that is designed in Chapter 2 are discussed. Water jet cutting (WJC) and laser cutting (LC) methods are explained. The hexflex mechanism is produced both by using WJC and LC. The comparison between these methods is also discussed in this section.

After manufacturing the compliant mechanism and the other supporting parts that is used for actuation and fixing, the experiments are done under the microscope. Static performance tests are done by actuating the motors both manually and automatically.

5.1 Manufacturing Methods

5.1.1 Laser Cutting

Laser cutting is the manufacturing process that cuts material by using laser. The cutting process is done by concentrating high power laser beam into small, well defined spot on the material which is to be cut. Typically the laser beam has 0.003in -0.005in. diameter [34]. The heat energy on the material is created by the laser and it melts or vaporizes the materials in the small defined area and these vaporized or melted materials are blown by a gas such as oxygen, CO_2, nitrogen or helium etc. as seen in Figure 5-1. The energy of the laser beam is directly applied where it is needed and minimizes the heat affected zone surrounding the area being cut.

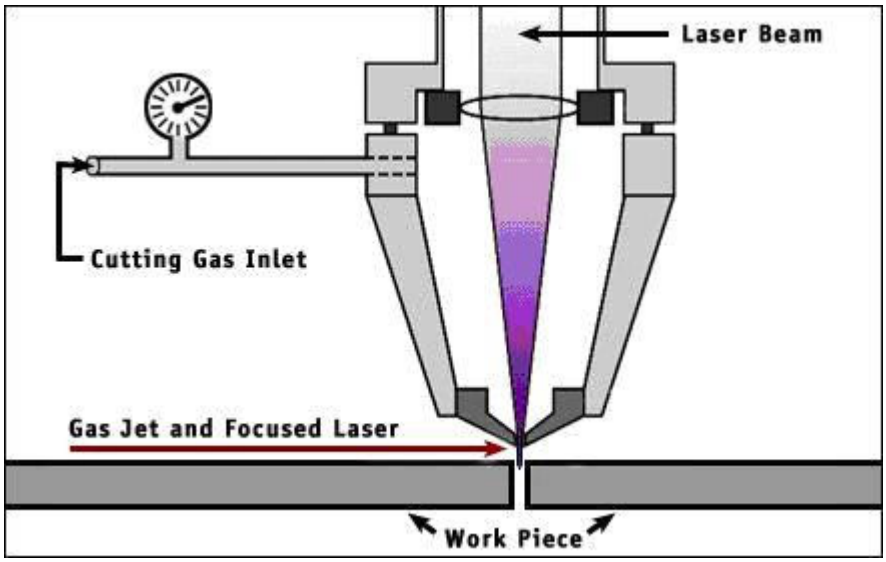

Figure 5.1Laser Cutting [35]

The main advantages of laser cutting are:

- They have no limit to the cutting path. The laser beam can move in any direction.
- Small diameter holes can quickly be made by using laser cutting.
- Fragile or flimsy parts can be cut a little or without support because the process is forceless. It allows the part to keep its original shape from start to finish.
- Materials that lack of conductivity, abrasiveness or hardness can usually be cut using laser.
- It reduces the part distortion as a result of heat affected zones.
- The focused laser beam, as small as 0.003", can produce complicated parts.

Because of the advantages of laser cutting the compliant mechanism is cut by using laser cutting technique. Firstly, the material is chosen to be 7075 Aluminum because the yield strength to young's modulus ratio is high which means it allows a larger deflection before failure [2]. But the manufacturing was not good so the material is distorted everywhere because the areas where laser beam cut melted or burned the surrounding areas. So the mechanism can only be done by using two kinds steel types, one is black steel which is the steel with much carbon in it and the other is stainless steel.

5.1.2 Water Jet Cutting

Water jet cutting is the cutting process that cuts the materials by using a jet of water at high velocity or pressure. The material remove process is a kind of erosion process that is generated by high pressure water flows usually forces of 2 Ib. Abrasive powders are added to water for cutting hard metals such as metals, stone, composites and ceramics. Abrasive power jets are much more powerful the pure water jets. [36]

The main advantages of water jet cutting are:

- They perform high precision cutting, beveling, piercing, etching, and slotting up to accuracies of ± 0.005".
- Wide range of materials can be cut by using this technique.
- They eliminate the distortions due to heat or burning as laser cutting does.
- The parts edges can be produced smooth.
- They can cut all kinds of materials up to 8" thick.

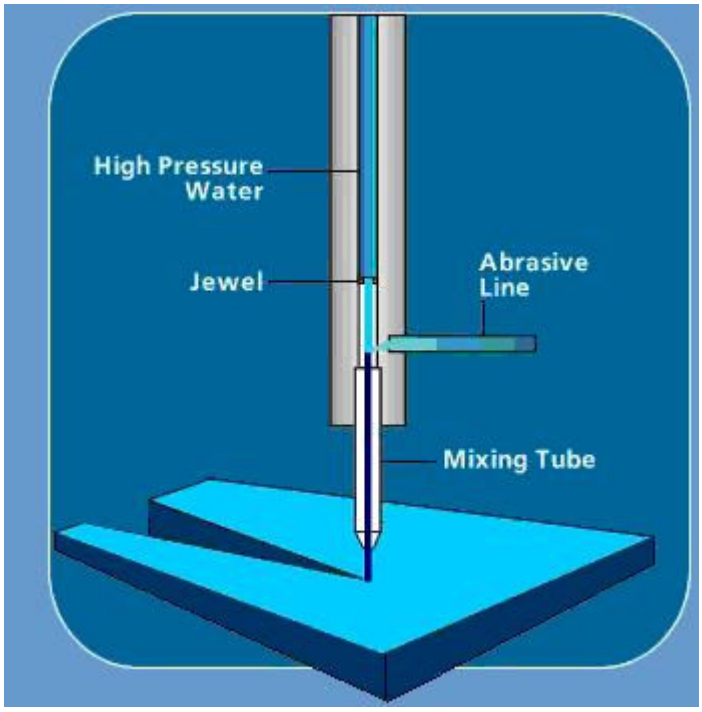

Figure 5.2 Abrasive water jet cutting [37]

Because of these advantages water jet cutting technique is also selected for manufacturing the compliant mechanism. Steel and Black steel materials are used for manufacturing.

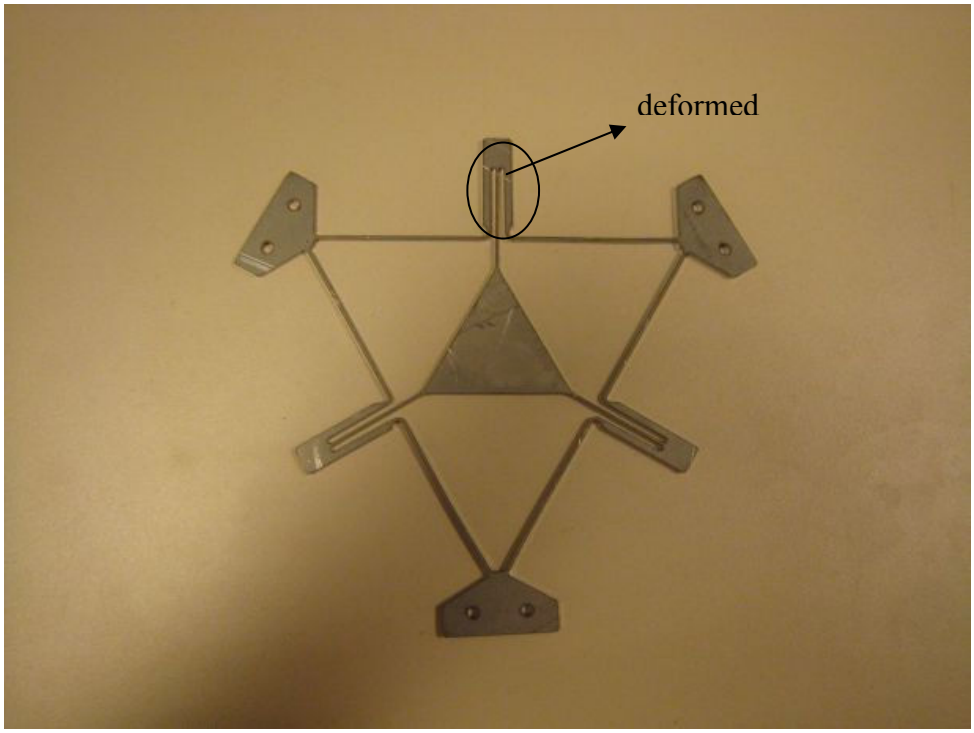

Figure 5.3 Stainless steel laser cutting manufactured compliant mechanism

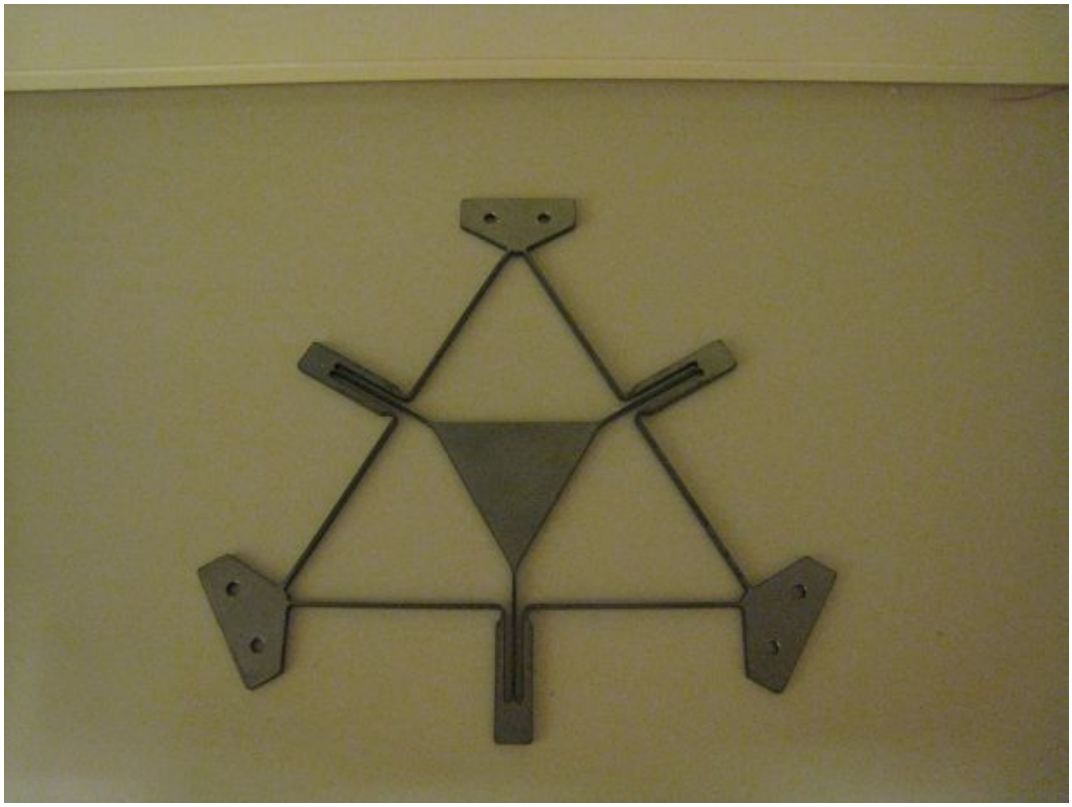

Figure 5.4 Black steel water jet cutting manufactured compliant mechanism

When it is compared the compliant mechanisms that are manufactured from laser cutting and water jet cutting, it is understood that for manufacturing compliant mechanisms abrasive water jet cutting is more suitable than laser jet cutting. Because there are burnings in laser jet cutting and the beams that are connected to the triangle are distorted by the heat of the laser cutting. In Figure 5-3 you can see that the upper beam connected to the triangular stage is not straight, it is deformed. The mechanism that is made by water jet cutting shown in Figure 5-4 is better than the laser jet because the beams are straight and not distorted.

5.2 Experiments

The full experimental setup is shown in Figure 5-5. In Chapter 2 the compliant mechanism, the base which is used to fix the mechanism and holds the actuators and piezo mike actuators are explained. After manufacturing the parts and assembling the setup, the open loop experiments are done under the microscope as seen in Figure 5-6 whether to see how the mechanism behaves when the actuators work. The piezo mike actuators can be used both manually and automatically by giving voltage to the piezos. So the open loop experiments are done firstly by turning the shafts of the actuators manually, then voltage signals are given to the actuators. The measurement of the displacement of the triangular stage is done by using cameras. A small dot is put on the triangular stage as seen in Figure 5-7 and by using the images from the camera that is mounted on the microscope, the pixel coordinates of the point is calculated then it is converted to world coordinates.

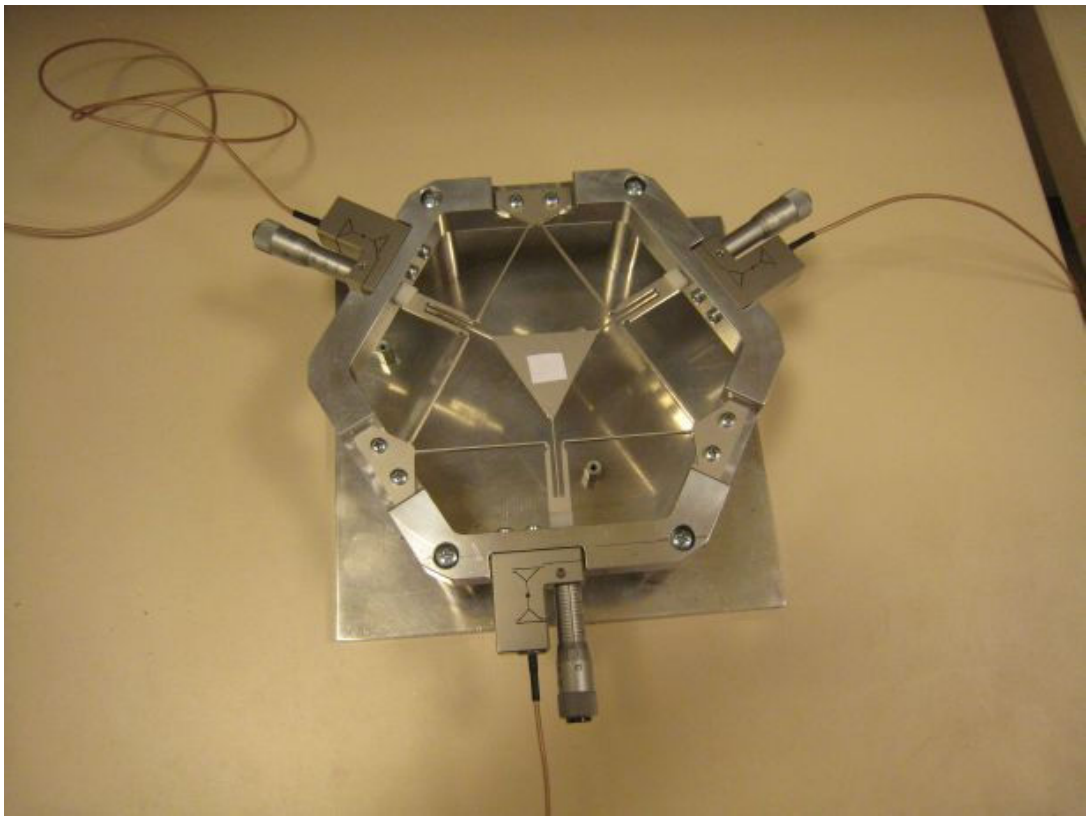

Figure 5.5 The full assembled system

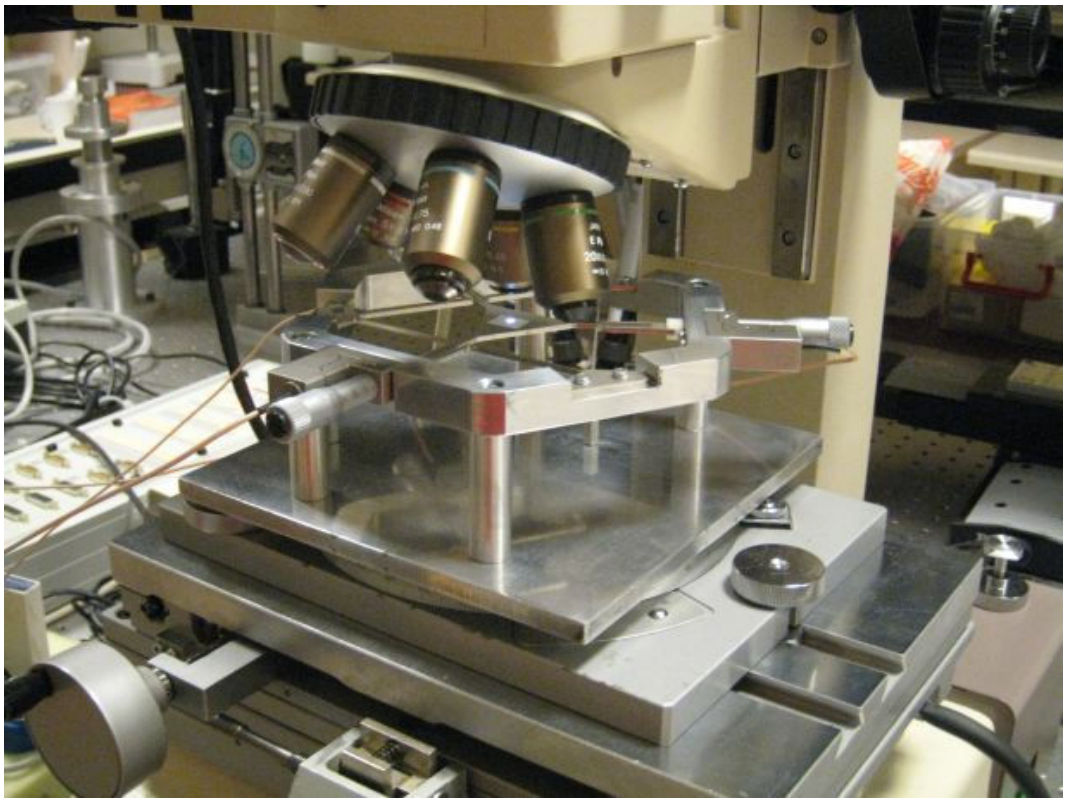

Figure 5.6 The setup under the microscope

Figure 5.7 The actuator mounting and the dot on the triangular stage

5.2.1 Results of Manually Actuating

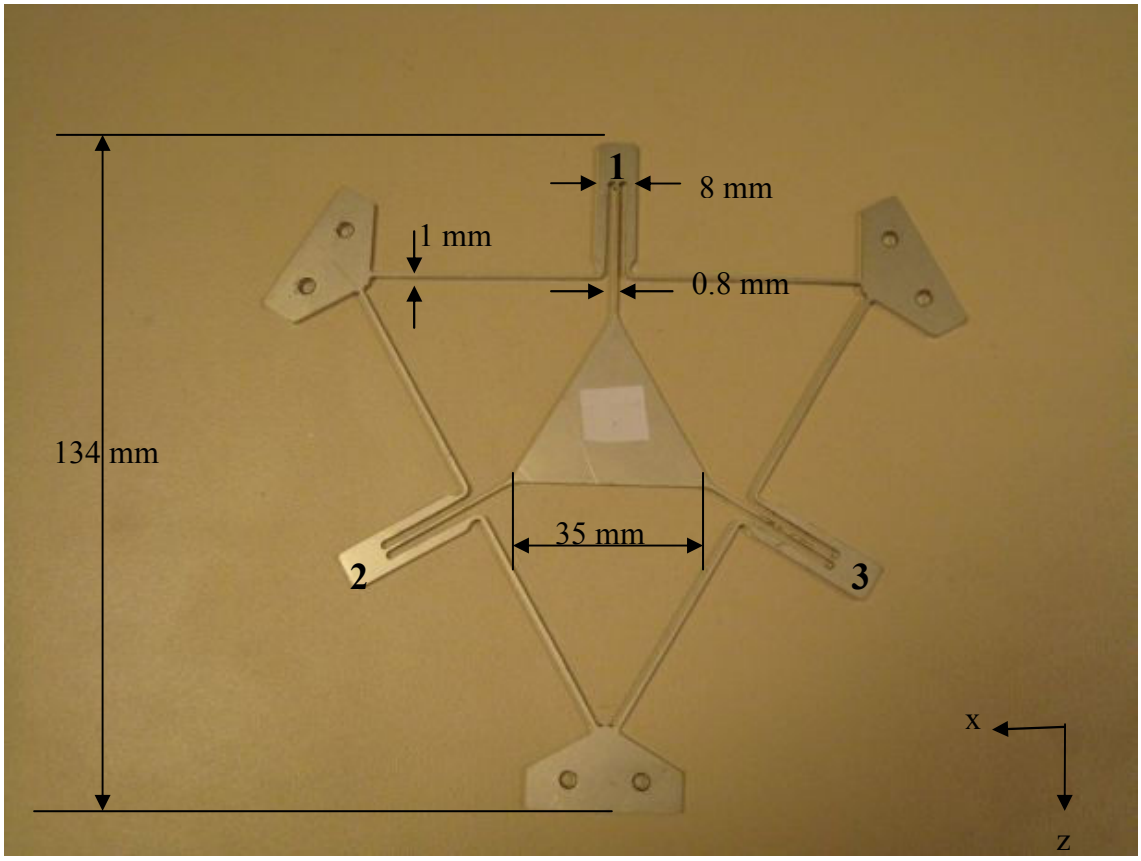

Figure 5.8 The mechanism with some dimensions and numbered tabs

The tabs are numbered as in Figure 5-8. The coordinate system is also can be shown in the figure. A dot is put on the triangular stage and the dot is watched at 5x magnification under the microscope. Firstly the mechanism is positioned under the mechanism so that the coordinate of the mechanism collide with the coordinate of the mechanism. This is done by giving motion to tab 1 and orienting until the less pixel coordinate change is determined in x direction. Then the piezo mike actuators that are connected to tabs are first set to 50 μm then 100 μm. The results are in Table 5-1.

Table 5-1 Experimental Results

Actuation (Displacement)	X	Z	Angle of the motion	Expected Angles	Error of the Angles
1st Tab – 50µm	-2.695µm	21.9µm	82.98°	90°	%7.8
1st Tab – 100µm	-1.6793µm	59.1161µm	88.37°	90°	%1.81
2nd Tab – 50µm	-31.5912µm	-21.8343µm	34.65°	30°	%15.5
2nd Tab –100µm	-55.9261µm	-47.5011µm	40.34°	30°	%34.46
3rd Tab – 50µm	24.4687µm	-24.1630µm	44.63°	30°	%48.76
3rd Tab –100µm	57.6299µm	-51.7526µm	41.92°	30°	%39.73

As seen from Table 5-1, the tabs motions are not as expected values. The worst tab motion is the third tab. This situation can be because of the distortions in the compliant mechanism while manufacturing and the base part which holds the actuators should hold the actuators in the direction of the beams so that the forces intersect at the center of the stage. If the forces are not intersect at the center, then the stage will start to rotate and the rotation will give wrong results.

ADAMS simulation of the mechanism is done for comparing the results that we have got from the experiments. The mechanism is meshed in ADAMS Auto Flex, fixed from its holes and translational joint is added to tab 1. 50 µm and 100 µm step displacement is given to the translational joint. The simulation model can be seen in Figure 5-9. The coordinate axes of the mechanism are in the center of mass of the mechanism.

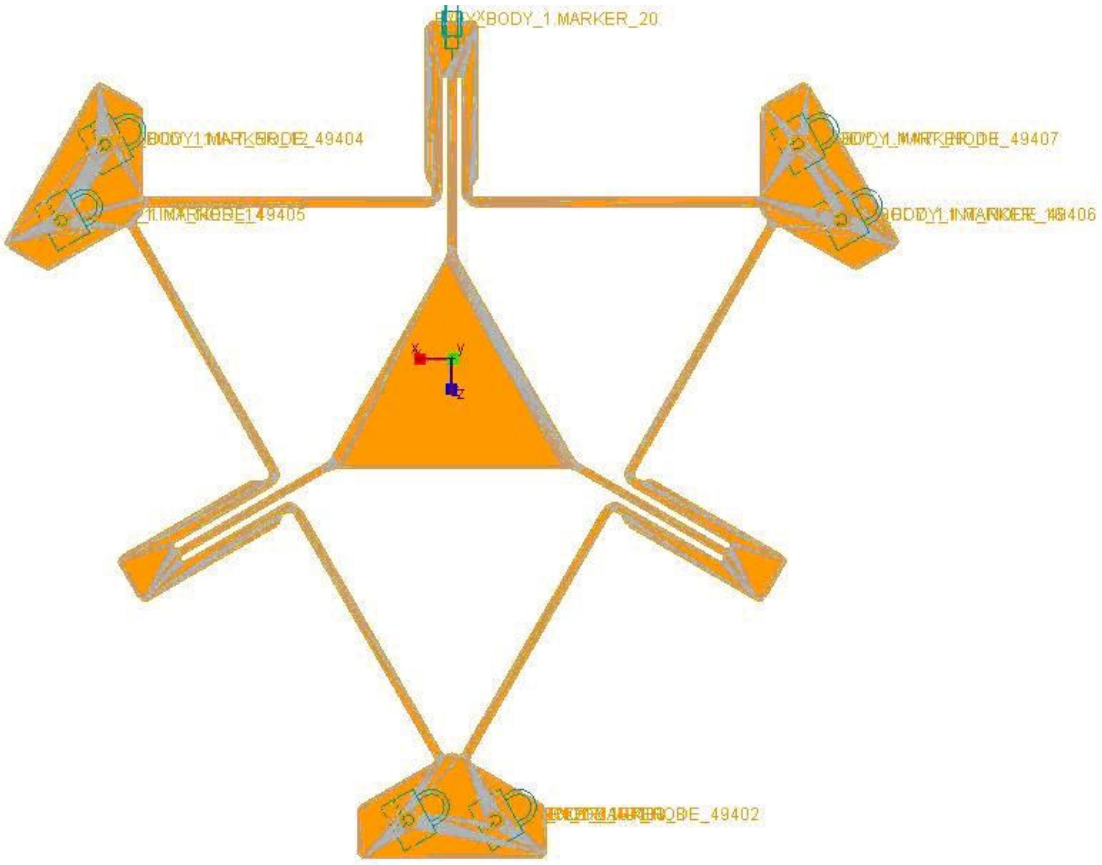

Figure 5.9 Mechanism in ADAMS

In Figure 5-10,11 and 12 the center of mass of the mechanism motions are presented when 50 μm step motion is given to the translational joint.

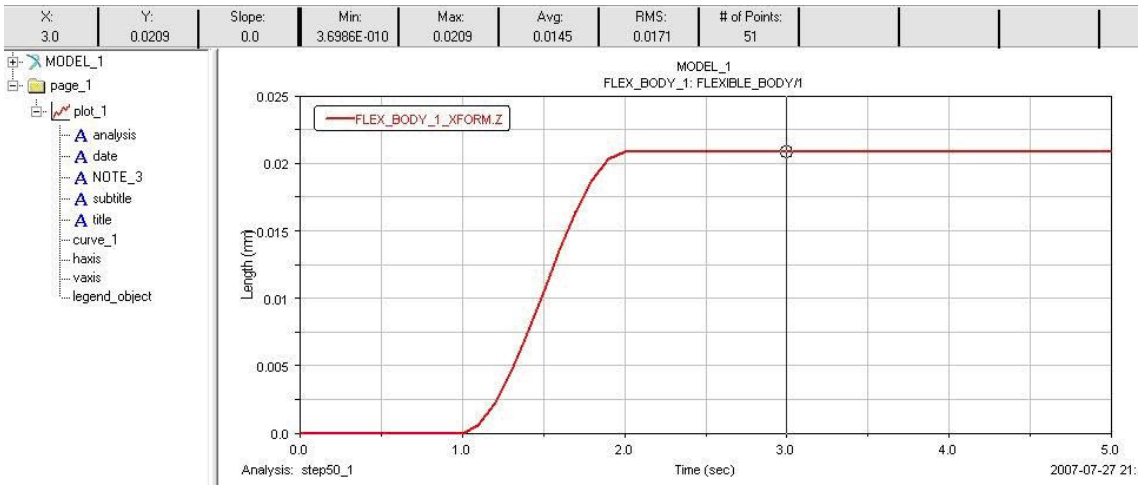

Figure 5.10 The result in Z direction

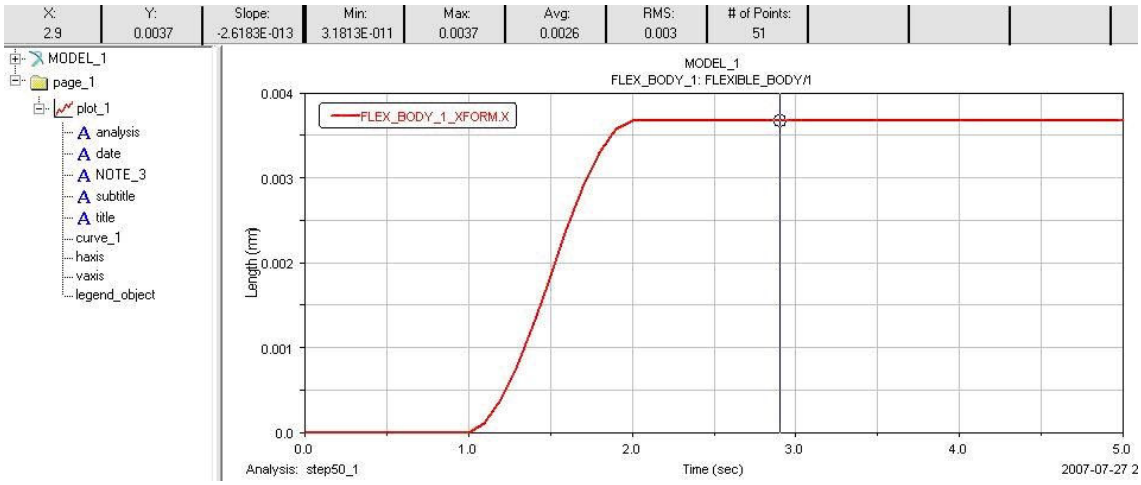

Figure 5.11 The result in X direction

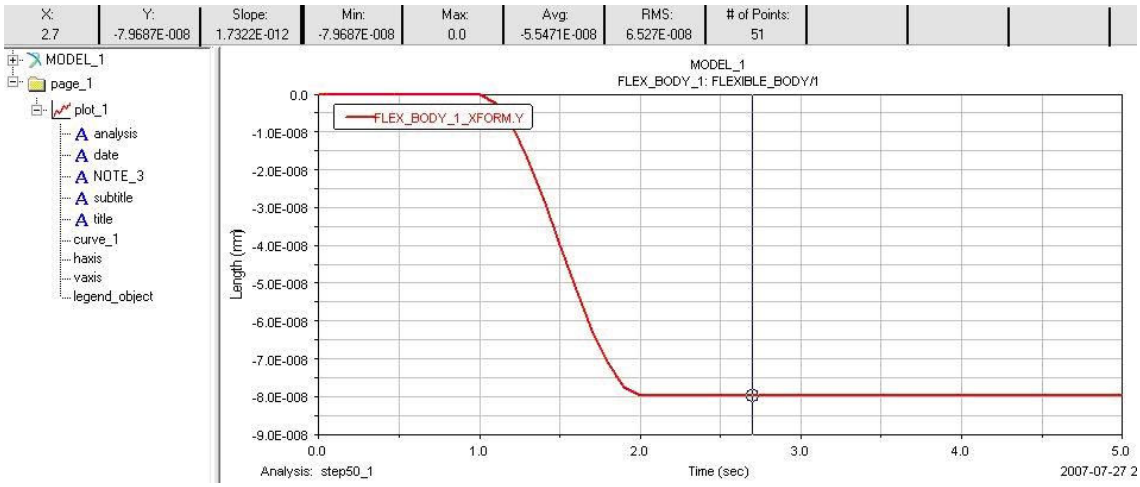

Figure 5.12 The result in Y direction

In Figure 5-13,14 and 15 the center of mass of the mechanism motions are presented when 100 μm step motion is given to the translational joint.

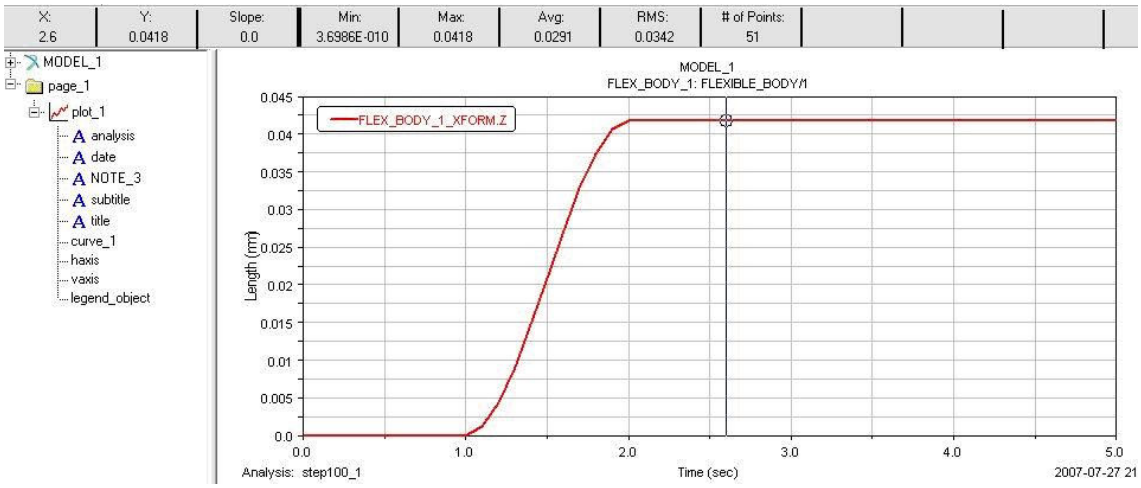

Figure 5.13 The result in Z direction

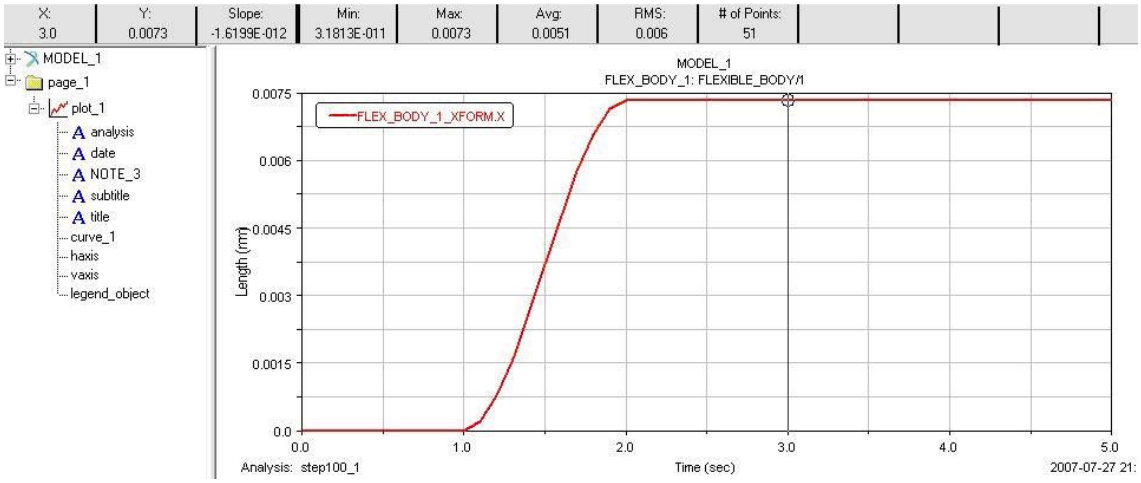

Figure 5.14 The result in X direction

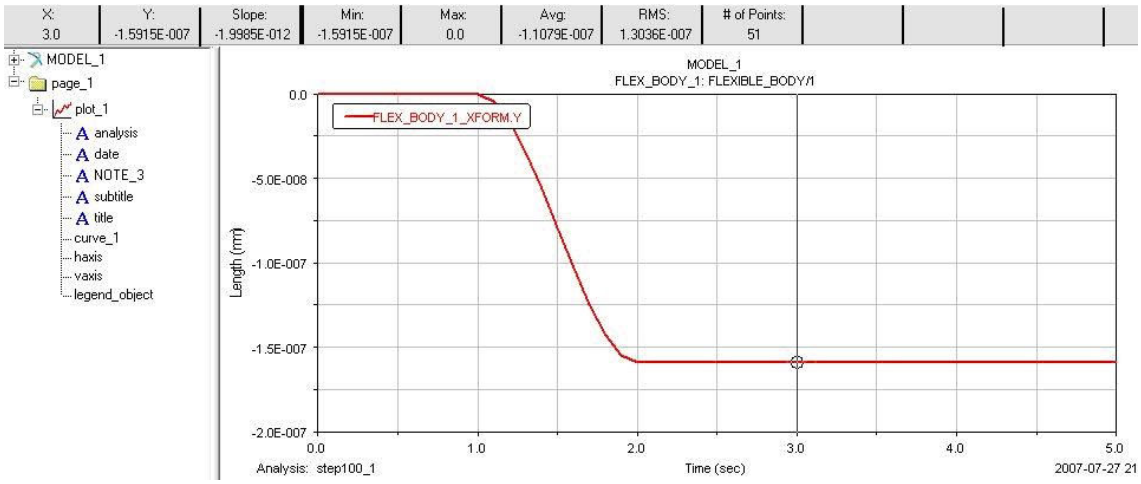

Figure 5.15 The result in Y direction

The resultant Z and X displacements comparison between the simulation and the experiment can be seen in Table 5.2. The Z displacements are close but the X displacements have a sign change. We were expecting that there will be no displacement in X direction but we can see that in the simulation and experiments we have. The reason of the simulation is the displacement joint can not be put directly in the middle of the 2nd tab because of the meshed elements on the mechanism. The reason of the error in the experiment can be because the mechanism is distorted or the force we are applying is not on the direction of the center of the mechanism so the mechanism is rotating or beams are twist bending.

Table 5-2 Comparison of experiment and simulation

Actuation	Experiment		ADAMS	
	Z	X	Z	X
50 µm	21.9 µm	-2.695 µm	20.9 µm	3.7 µm
100 µm	59.1161 µm	-1.6793 µm	41.8 µm	7.3 µm

The comparison in Y direction can't be made because in experiment Y direction can not be measured. But if we look at the simulation results in Figure 5-12 and 5-15 the motion in Y direction is not so much.

5.2.2 Results of Voltage Actuating

The piezo mike actuators are connected to their amplifiers and by using DSPACE 1103 the desired sinusoidal or step signals are given to the amplifiers and the piezos are moved automatically by the given voltage signals.

The control desk layout is in Figure 5-16

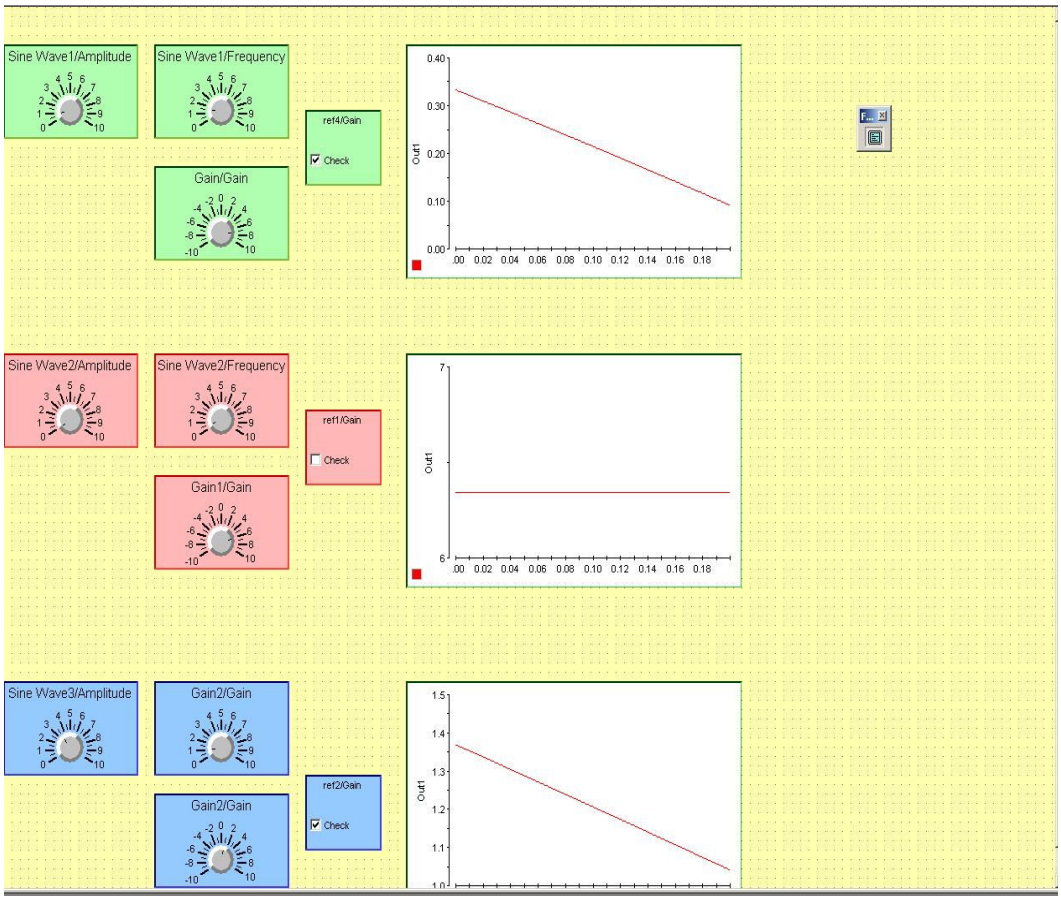

Figure 5.16 Controldesk Layout

The experiment is made by giving sinusoidal signals to the piezo mike actuator that is connected to tab 2. Tab 2 can be seen in Figure 5-17. The coordinate system is taken as shown in Figure 5-17 for understanding the motion of the stage easily.

Through vision the position of the triangular stage where a dot is put, is measured in pixel coordinates. Then the first pixel coordinate is taken as (0,0) point and subtracted from the other measured pixel coordinates. Finally, the pixel coordinates is converted to world coordinates. So the displacement of the triangular stage is found in X and Z coordinates and they are plotted.

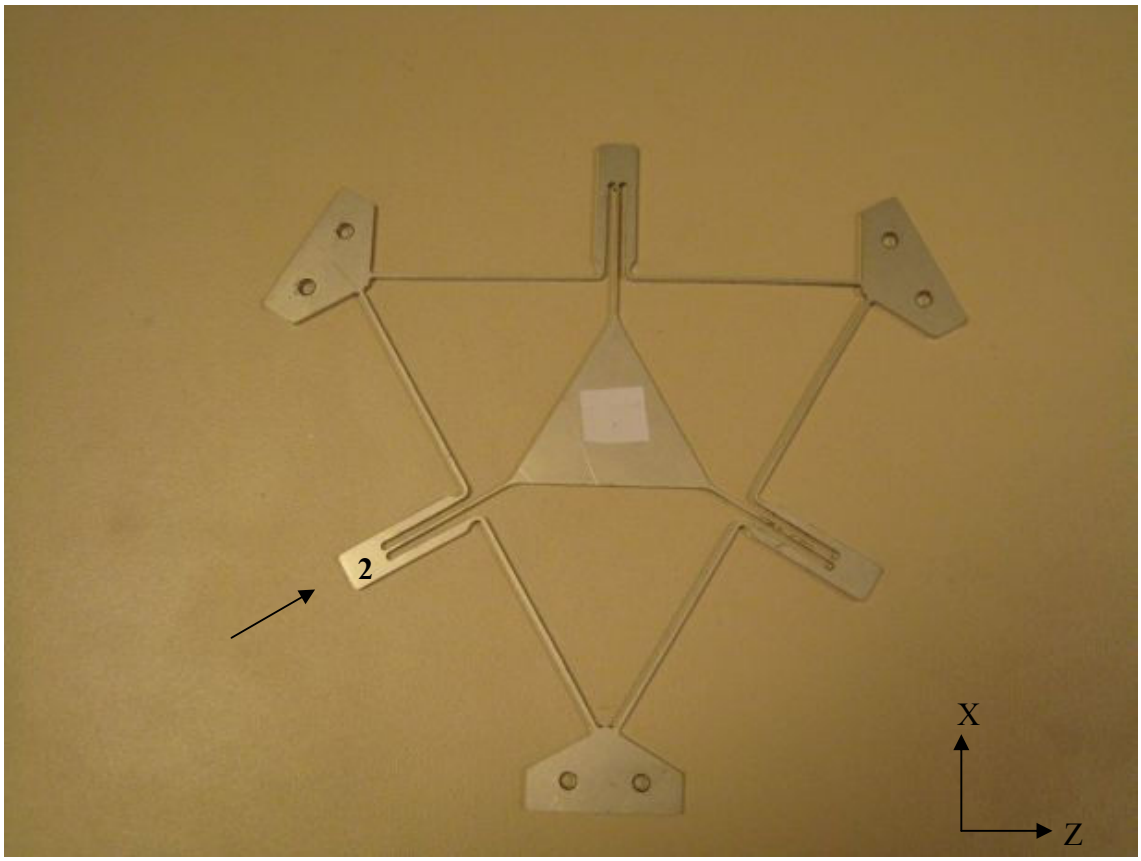

Figure 5.17 Actuated tab of the mechanism and the coordinate system.

First experiment is done by giving 20sin0.02t with shifted 20 volts is given to the piezo motor. The results are in Figure 5-18 and 5-19. The frequency of the motion in X and Z is $0.02sec^{-1}$. The motion of the dot is also plotted in Figure 5-20. The angle between X and Z motion is approximately 24°.

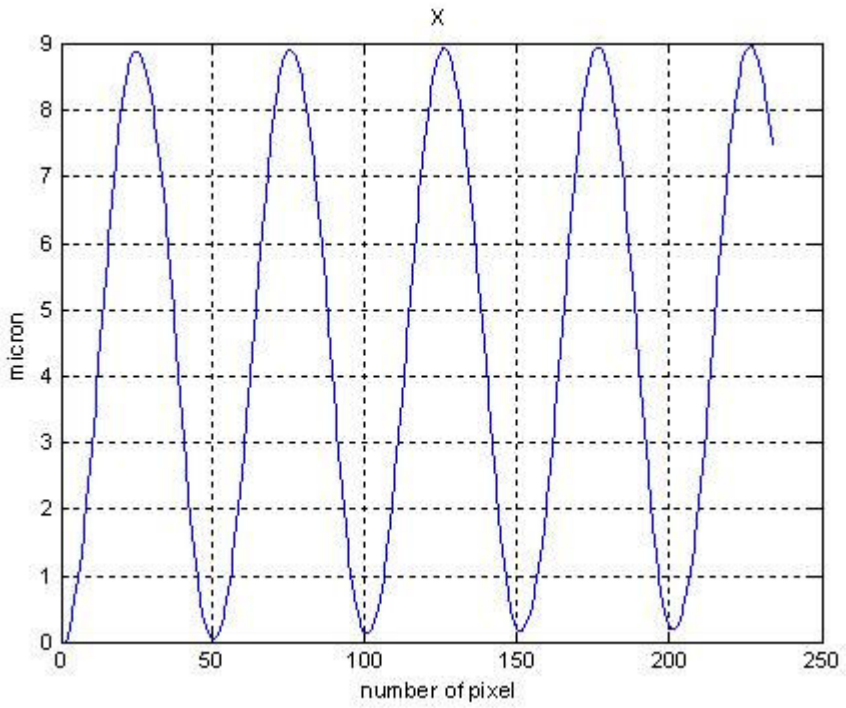

Figure 5.18 Motion in X

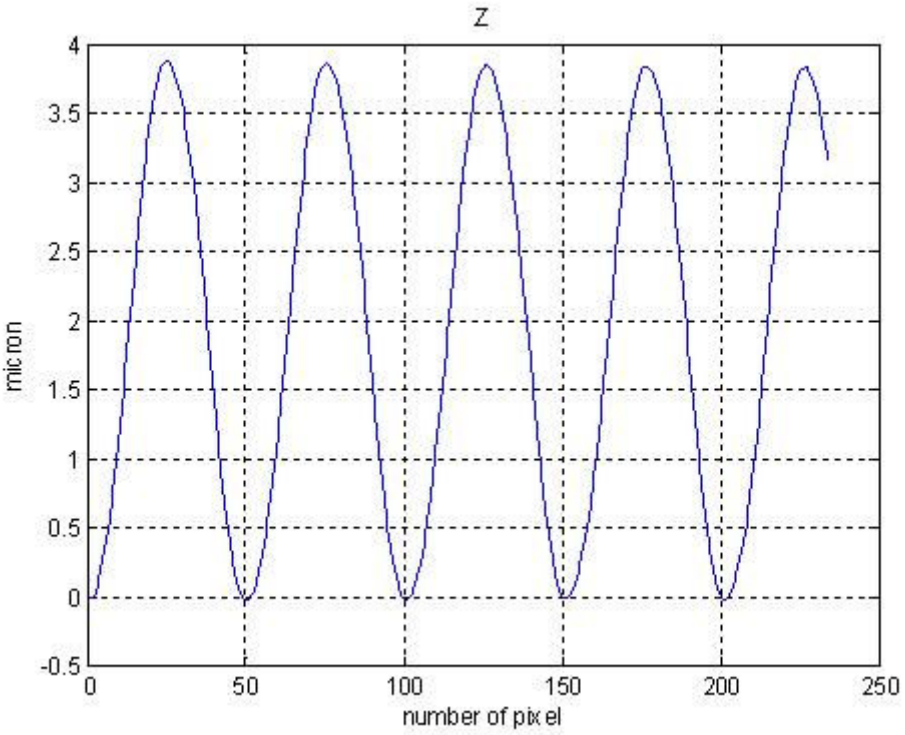

Figure 5.19 Motion in Z

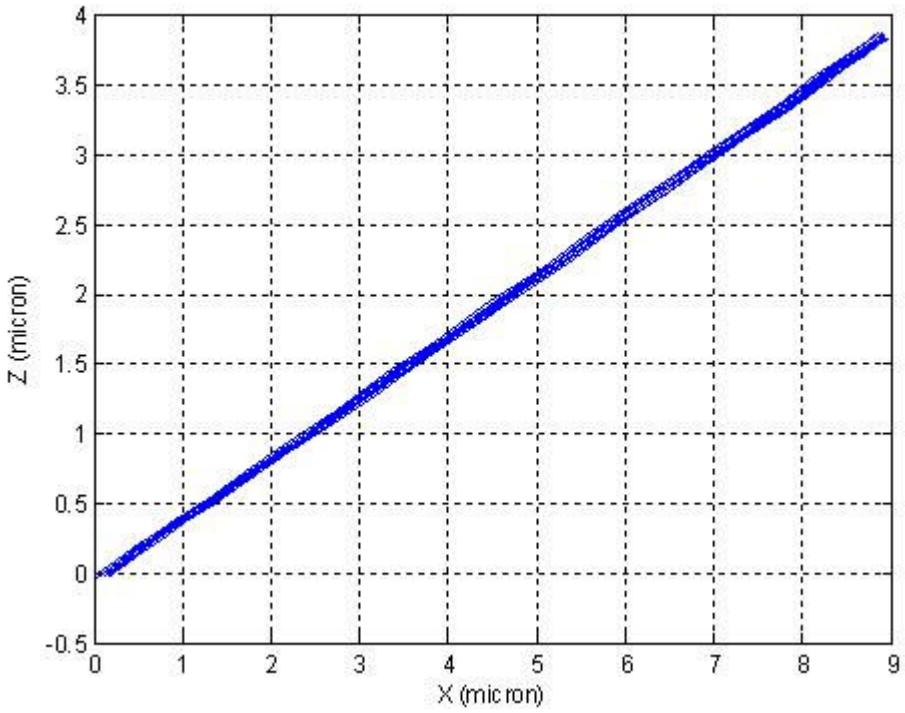

Figure 5.20 The motion of the dot

Secondly, the frequency of the signal is increased to 0.04sec^{-1}. The results are in Figure 5-21 and 22. The motion is showed in Figure 5-23. We can see that the frequency of the motion in X and Z is also increased to 0.04sec^{-1}.

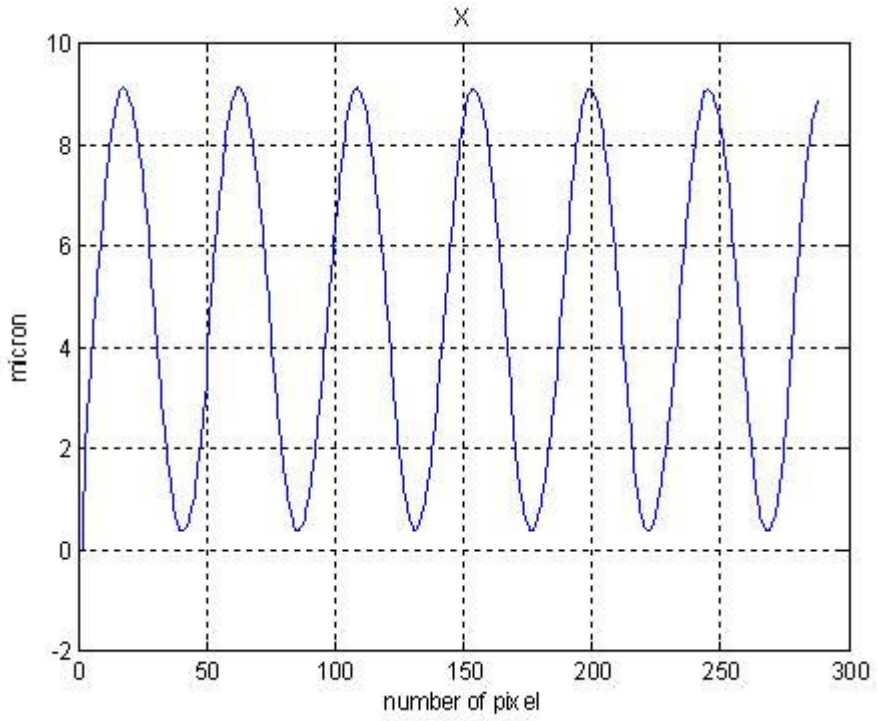

Figure 5.21 Motion in X for higher frequency

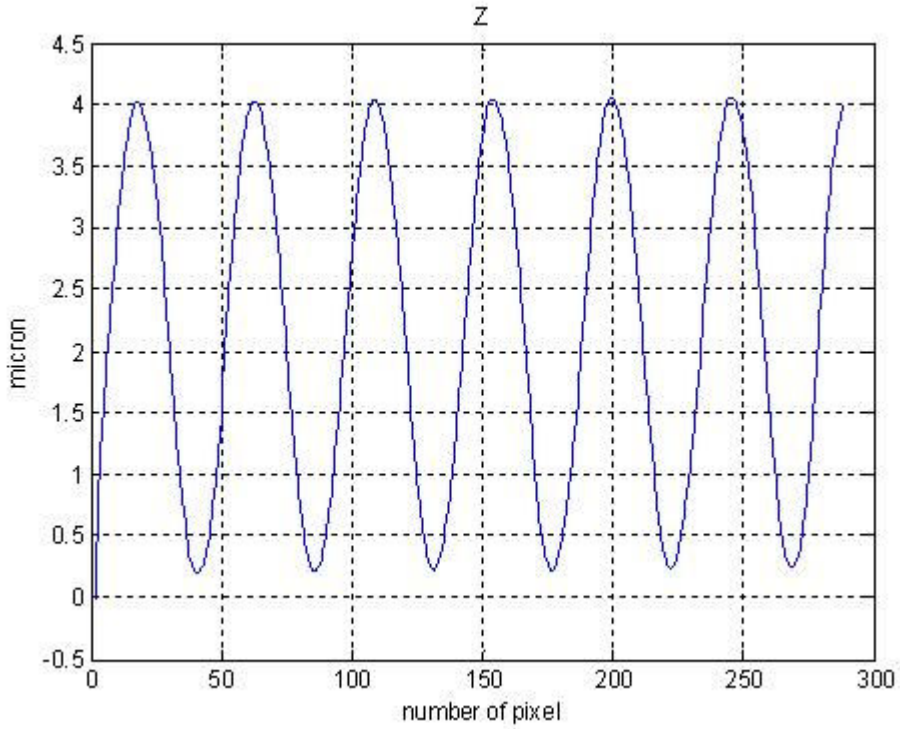

Figure 5.22 Motion in Z for higher frequency

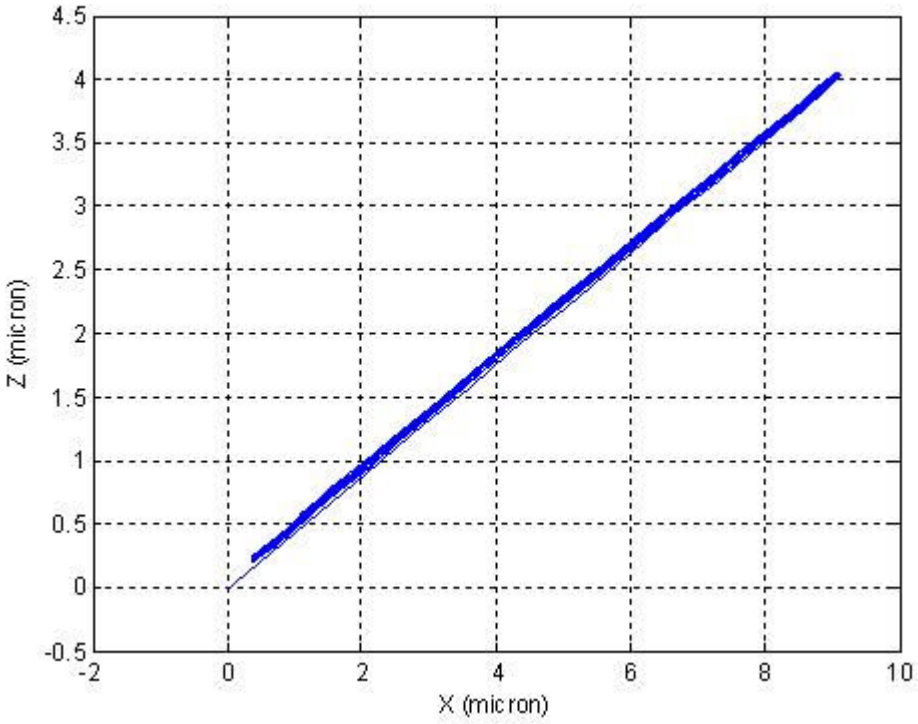

Figure 5.23 Motion of the dot

6 CONCLUSION

In this thesis, design and modeling of a compliant mechanism is presented. The mechanism is a parallel planar compliant mechanism which is thought to be used as a positioning stage in microassembly. The main idea of this type of mechanism is using the deflections of the flexible elements to generate the motion of the stage. The mechanism is designed so that the actuation forces do not create any rotation; only two translational motions are created. Thus the stage is designed as a two degree of freedom mechanism. The material type for this kind of mechanism is important because the material properties determine the deflections. Finite element analysis (FEA) is done for the mechanism to see the behavior of the mechanism for different types of materials that can be used.

The mathematical modeling is done for simulating the dynamic behavior of the system so that any kind of control method can be applied and simulated. The system is a distributed parameter system because the deflections of the beams depend on both position and time. Necessary kinematic calculations are done for defining the center of the stage position in terms of the deflection of the flexible elements. Then Euler Bernoulli beam equations are used for defining these flexible elements dynamics. Separation of variables method is used to represent the motion for distributed systems in terms of time and position separately. The mathematical model is written in state-space form to be easily simulated. The position results of open loop simulated model is compared with software called COMET and it is seen that the mathematical model can be used for the mechanism. The open loop model is closed by using simple PID control and position control for the system is simulated.

The prototypes of the mechanism are manufactured by using both laser cutting and water jet cutting. The base part is manufactured in CNC. The mechanism is assembled on the base part and the piezo mike actuators are also mounted. After assembly the experimental setup is put under the microscope to see the motion of the stage. The actuators that are used for the mechanism can be driven both manually and

automatically. Firstly, the motors are driven manually and the position of the stage is calculated by using a vision tracking algorithm. One of the actuated tab result is compared with the simulation in ADAMS. The results are a little different because there are some distorted parts on the mechanism due to the manufacturing errors. Secondly, one of the tabs of the mechanism is actuated by giving sinusoidal voltage to connected piezo mike motor. The results show us that the motion of the mechanism is compatible with the given sinusoidal input. The motion of the mechanism has the same frequency as the given sinusoidal input so this means that the mechanism can be actuated by these kinds of motors.

7 FUTURE WORK

Since the compliant mechanism is designed for macro scale motion, the next main goal for the future is to redesign the mechanism and make it as small as possible that the manufacturing can let to do.

The control of the mechanism will also be verified with the experiments when accurate measurement of the position of the stage can be taken as input for the system. Another suggestion for the future work is to change the piezomike micro motors to piezo motors that we know a relationship between the given voltage and the force so a comparison can be made between the assumed mathematical model that we have derived and the experiments. Then by looking at the results of the comparison the assumed mathematical model can be changed and other beam affects on the mechanism can be added to the model for making the model more reliable.

8 REFERENCES

[1] Lobontiu N., "Compliant Mechanisms design of flexure hinges", *CRC Press*, 2003.

[2] Howell L. L., "Compliant Mechanisms", John *Wiley & Sons*, 2001.

[3] Speich J., Goldfarb M.,"A compliant mechanism based three degree of freedom manipulator for small scale manipulation", *Robotica*, Vol. 18, pp 95-104, 1999.

[4] Shorya A., "Synthesis and Analysis of Parallel Kinematic XY Flexure Mechanisms", Ph.D. Thesis, Massachusetts Institute of Technology, *Cambridge MA*, 2003.

[5] Smith S. T. and Chetwynd D. G., "Foundations of Ultraprecision mechanism design", *Gordon and Breach Science*, 1992.

[6] Baker M. S, Howell L. L., **"**On-Chip Actuation of an In-Plane Compliant Bistable Micromechanism", *IEEE Micro Electro Mechanical Systems (MEMS),* 2002.

[7] B. D. Jensen, L. L. Howell, and L. G. Salmon, "Design of two-link in-plane, bistable compliant micro-mechanisms," *ASME J. Mechan. Design*, vol. 121, pp. 416–423, Sept. 1999.

[8] Clements D., Howell L. L.,Masters N. and Weight B. L. "Floating Pin Joints Fabricated From Two Layers of Polysilicon at the Micro Level"

[9] Nielson A. J., "Demonstration of the Pseudo-Rigid-Body Model for Macro and Micro Compliant Pantographs"

[10] Blideran M.M., Bertsche G.,Henschel W. and Kern D. P., "A mechanically actuated silicon microgripper for handling micro- and nanoparticles", *Elsevier*, February 2006

[11] Nah S. K. and Zhong Z. W., "A microgripper using piezoelectric actuation for micro-object manipulation", *Elsevier*, February 2006.

[12] Hohl M., Krevet B. and Just E., “SMA microgripper system”, *Elsevier*, October 2001.

[13] Belfiore N.P., Scaccia M., Di Vasta A., Ianniello F., “Dynamic Performance of Micro-Compliant Platforms: Experimental Analysis”,*Robotics in Alpe-Adria-Danube Region (RAAD)*, 2006.

[14] Bergna S., Gorman J.J., Dagalakis N.G.,November, ” Design and modeling thermally actuated mems nano positioners”, *ASME*, 2005.

[15] Attoh-Okine, N., “Uncertainty Analysis in Surface Micromachined Force Gauges: Convex Model Approach”, *ASCE*, 2004.

[16] Compliant Mechanisms, 2000, Retrieved May 2007 from http://techtransfer.byu.edu/techabstracts/compliantmech.htm

[17] Compliant Mechanisms at BYU, 2004, Retrieved May 2007 from http://research.et.byu.edu/llhwww/

[18] Yao Q., Dong J., Ferreira P. M., “Design, analysis, fabrication and testing of a parallel-kinematic micropositioning XY stage”, 2006.

[19] Lu T.,Handley D.C.,Yong Y.K.,Eales C., “A three-DOF compliant micromotion stage with flexure hinges”., 2004.

[20] Shorya A., ”Synthesis and Analysis of Parallel Kinematic XY Flexure Mechanisms”, 2003.

[21] Ryu J. W., Gweon D., Monnt K. S., “Optimal Design of a flexure hinge based XYθ wafer stage”, 1997.

[22] Kang B.H., Wen J. T.,Dagalakis N.G.,Gorman J.J.,“Analysis and Design of Parallel Mechanisms with Flexure Joints” ,2005.

[23] Culpepper M.L.,Anderson G., “Design of a low-cost nano-manipulator which utilizes a monolithic, spatial compliant mechanism”, 2003.

[24] Slocum A. H., “Presicion Machine Design”, *Prentice Hall*, 1992.

[25] Culpepper M.L.,Anderson G., Petri P., “HexFlex: a planar mechanism for six axis manipulation and alignment”, *ASPE,* November 2002.

[26] Dwivedy S. K., Eberhard P., “Dynamic analysis of flexible manipulators, a literature review”, *Mechanism and Machine Theory*, 2006.

[27] R.J. Theodore, A. Ghosal, “Modeling of flexible-link manipulators with prismatic joints”, *IEEE*, (1997) 296–305. Transactions on Systems, Man, and Cybernetics, Part B: Cybernetics 27 (2).

[28] Pham H.H.,Chen I. , “Optimal Synthesis for Workspace and Manipulability of Parallel Flexure Mechanism”, *Mechanism and Machine Science*, 2003.

[29] Kimball C.,Wen-Tsai L., “Modeling of Flexural Beams Subjected to Arbitrary End Loads”, *Journal of Mechanical Design*, Volume 124, Issue 2, pp. 223-235, 2002.

[30] Xiaoyun Wang, James K. Mills, “Dynamic modeling of a flexible-link planar parallel platform using a substructuring approach ”, *Mechanism and Machine Theory*, Issue 6, pages 671-687, June 2006.

[31] C. Karnopp, Donald L. Margolis, Ronald C. Rosenberg.,2006,” System dynamics : modeling and simulation of mechatronic systems”, *John Wiley & Sons,* pages 426-433.

[32] Culpepper, ML, Kim, S, “CoMeT: Compliant Mechanism Tool Users Guide 1.0,” *MIT Precision Systems Design and Manufacturing Laboratory Publications*, 2003. Available for download at psdam.mit.edu/tools/index.html.

[33] Petri, P, “A continuum mechanic design aid for non-planar compliant mechanisms”, MS Thesis, MIT, 2002.

[34] Laser Cutting Manufacturing Process, 2003, Retrieved July 2007 from http://www.bgpeck.com/laser.html

[35] Metal Cutting and Laser Cutting Tips, 2005, Retrieved July 2007, http://www.teskolaser.com/tips.html

[36] Water Jet Cutting, Abrasive Machining and Industrial Cleaning, Retrieved July 2007 from http://www.flowcorp.com

[37] Water Jet Cutting, Retrieved July 2007 from http://www.newaterjet.com/